University of Southern Queensland

Faculty of Engineering and Surveying

Investigation into the Limitation of Measuring to 360 Degree Prisms using Automatic Target Recognition Technology

A dissertation submitted by

Mr Matthew McDonald

In fulfilment of the requirements of

Course ENG4111 and ENG4112 Research Project

towards the degree of

Bachelor of Spatial Science (Surveying)

Submitted: October, 2011

Abstract

This dissertation outlines the limitations of reading to a 360 degree prism using Automatic Target Recognition (ATR) technology, covering the 360 degree prism attributes that affect the accuracy of the readings obtained and possible ways to reduce these effects to obtain more precise readings.

The methods designed to measure these effects are outlined along with the design considerations and reasons behind the selection of these methods. The designed methods were tested on three selected instruments with their accompanying 360 degree prism.

The instruments selected for testing had different manufacturers and their date of release was spread over the years which ATR evolved. This provided various 360 degree prism designs, the use of different ATR technology and different electronic distance measurement devices for testing.

Using the field testing data gathered from the three instruments, software formulae for each instrument were calculated to predict the vertical height and horizontal distance corrections. These formulas could be applied in the reduction process of the observation to reduce these effects.

By understanding the causes of these errors and how they occur, recommendations for ways to minimise these effects on accuracy of the readings were outlined. The measured limitations for each instrument was determined and presented with the discussion of their accuracy and possible effects that may have hindered the results.

The benefits of identifying the significance of these errors and their causes means that when new technology is developed, they can be considered and reduced through prism design or reduction, which will improve the accuracy of this method of survey used by machine guidance and instrument operators.

University of Southern Queensland

Faculty of Engineering and Surveying

ENG4111 & ENG 4112 Research Project

Limitations of Use

Prof Frank Bullen
Dean
Faculty of Engineering and Surveying

Certification

I certify that the ideas, designs and experimental work, results, analyses and conclusions set out in this dissertation are entirely my own effort, except where otherwise indicated and acknowledged.

I further certify that the work is original and has not been previously submitted for assessment in any other course or institution, except where specifically stated.

Matthew McDonald

Student Number: 0050023688

Signature

26/10/11

Date

Acknowledgements

This research was carried out under the principal supervision of Kevin McDougall. Appreciation is also due to Dave Fredriksen for his guidance and support throughout the course of this research project.

Special thanks must also be made to Fredriksen Maclean and Associates for the use of their robotic equipment, to Jordan Johnsen and Jason McDonald for their endless hours of assistance during field testing, to my lovely mother for proofreading and to my loving wife for her continued patience and understanding throughout this research project.

Table of Contents

Contents **Page**

Chapter 3 – Method

List of Figures

List of Tables

List of Appendices

Chapter 1 – Introduction

1.1 Project Background

Surveying robotics has become more and more a part of the general practice of surveying, reducing costs for the client and overheads in the surveying practice. This is possible because an assistant is no longer required to hold and align the prism while the surveyor observes readings from behind the instrument. Now the surveyor is able to hold the prism and instruct the instrument to measure to that point at the same time. This has been made possible through a number of technological advancements including the automatic target recognition system that enables the instrument to follow/track and align the instrument to a reflective target (prism).

The Automatic Target Recognition (ATR) system is of some concern as little is known about the workings of the system with limited published research on the accuracy or operations of ATR. This has made investigating the accuracy and understanding the methodology of the system difficult. Surveying firms are trying to remain competitive through reduced costs and advanced technology. Inadvertently firms have turned to purchasing and using technology such as ATR to remain competitive. However, by not completely understanding the limitations of the equipment, it can lead to costly corrections when used inappropriately.

Surveying has always been a profession that has prided itself with the quality of its work by reducing or eliminating all measurement errors by performing appropriate checks and calculations. However, surveying instruments are very user friendly and can perform many reduction calculations for the operator. This has allowed many unqualified operators to perform survey tasks, assuming that the displayed information is correct, unaware of the appropriate checks required to confirm that no errors have been introduced.

1.2 Statement of Problem

Automatic Target Recognition has been around since 1992 and during this time a number of concerns with the system have been investigated. Kirschner & Stempfhuber (2008) among other researchers have performed investigations, however most focused on the reading ability in dynamic mode, which impacts on machine guidance. Mao and Nindl (2009) have investigated the effects of using a poorly constructed prism, identifying that if the target/prism is not correctly pointed at the instrument it causes errors with the vertical and distance readings. Horizontal angle errors were not an issue during this research as the instrument was always manually aligned, as ATR was not utilised. During the previous research completed by Kirschner and Stempfhuber (2008) on the dynamic tracking ability of ATR, it was noted that there were errors reading to the 360 degree prism that would need to be eliminated to achieve their desired outcome. This was performed by not using a 360 degree prism and reading to a standard round prism, which was always aligned with the instrument.

The impact of the design for the various 360 degree prisms used by ATR systems is not well understood and hence their impact on the horizontal and vertical pointing accuracies is not clearly quantified.

1.3 Justification for the Project

This project is important to understand the type of measurement accuracies that are achieved with this method of survey. Identifying the causes of these errors and knowing their impacts on the measurements, will not only make surveyors aware of the limitations for this method of survey but also lead to possible ways of reducing them.

This information will enable prism designers and software programmers to consider these effects when designing or creating new equipment and software releases that will reduce these reading errors, further improving the measurement accuracies achieved with this method of survey.

These improvements will benefit not only surveyors but also machine control guidance systems which are well on the way to becoming the normal methods of practice on earthwork construction projects.

Machine control guidance systems are now being relied upon quite heavily and with the diverse range of applications increasing, the requirement for greater trimming accuracy is even more essential.

1.4 Project Aim

The aim of this project is to investigate how automatic target recognition aligns the instrument to the centre of the target and thereby determine the impacts on the accuracy of reading to a 360 degree prism using ATR.

1.5 Objectives

The objectives of this project are to:

- Research the operations and mechanics of the ATR system centres, including the calibration process and centring accuracies of ATR.
- Design an appropriate testing regime to test the accuracy of 360 degree prisms under various ATR situations.
- Undertake field testing using a range of robotic instruments with their accompanying 360 degree prism measuring:
    - Horizontal centring errors.
    - Distance centring errors.
    - Vertical centring errors.
- Analyse the test results of the varying instruments and derive solutions to reduce the centring errors, including the modelling of the physical attributes of the 360 degree prism.
- Document the outcomes including findings and recommendations for use.

1.6 Structure of the Dissertation

This section provides a brief overview of each chapter within the dissertation.

Chapter 1 outlines the scope of the project. Providing a background understanding into the implication of ATR, the concerns about the measuring accuracies achieved, the productive ability and reduced costs of the technology, along with the unqualified operators using the equipment due to the advanced user friendly automative software.

The specific area of investigation has been identified along with previous research which determined ATR measuring errors when reading to a 360 degree prism during their project. The importance of determining the causes of these measuring errors has been examined and their implications on the measuring accuracy obtained.

The implications of this research were also noted in this chapter. With the research results possibly leading to future equipment designs, that would eliminate or reduce the determined error causing factors and improve the measurement accuracy and reliability.

Furthermore chapter 1 sets out the objectives of the project which the remainder of the dissertation discusses in depth.

Chapter 2 is a review of literature. Providing an understanding of the individual components that make up the automatic target recognition system, and how each individual component contributes to the overall accuracy of the measurement achieved. The chapter allowed a closer look at what could be causing the ATR measuring errors and other contributing measuring factors that required eliminating in order to clearly measure the ATR 360 degree prism reading errors.

Previous research was investigated in depth within chapter 2, determining what had already been documented, noting their testing methods and how they dealt with eliminating the systematic measuring errors within their testing regime. The adjustment procedure for ATR sighting alignment and the measuring corrections for the Earth's curvature and refraction for high precision measurements was also covered.

Chapter 3 details the calculations, preliminary testing and designed procedures that were used to measure the ATR 360 degree prism errors. The preliminary design consideration calculations were highlighted from the literature review and were used in determining the constraints for the testing regime. The preliminary testing confirmed the stability of the measuring platform and the designed testing procedures to accurately measure the ATR 360 degree prism errors.

The designed testing procedures have been provided in detail discussing the reasoning behind the selected method and the necessary calculations required to obtain the desired ATR 360 degree prism errors.

Chapter 4 displays the results for each instrument, providing a comparison between the three instruments tested, identifying any underlining errors that appear within the measured error data sets while explaining its possible cause.

Chapter 5 concludes the project with the findings and provides recommendations that reduce the 360 degree prism effects on the ATR measurements.

1.7 Summary

This project aims to determine the accuracy of the measurements gathered using ATR when sighting to a 360 degree prism. The research is expected to result in a more thorough understanding of the limitations of ATR and the likely accuracies that can be achieved with this method of survey. A review of literature for this research will identify the main components that contribute to the accuracy of measurements achieved using Automatic Target Recognition. The outcome of this study will be used for the design and development of a procedure to measure the variations of measurements caused by the design of the 360 degree prism.

Chapter 2 – Literature Review

2.1 Introduction

This chapter reviewed literature to gain an understanding of the workings for the ATR system and identified the key elements that effect the measurements gathered. This understanding was used to design a procedure to test the accuracy of measuring to a 360 degree prism with the ATR system.

2.2 Electronic Distance Measurement

Electronic Distance Measurement (EDM) is a system used to measure the distance between the instrument and a reflective target. EDM is a technology within the total station that calculates the distance once the ATR system has located the target. EDM derives distances by converting the time taken for an electromagnetic wave to travel from the instrument to the reflective target and return. By knowing the velocity of the electromagnetic wave in the prevailing atmosphere and calculating the number of full and partial waves this is possible (Ghilani & Wolf 2002).

Kirschner and Stempfhuber (2008) concluded during their research on ‘The kinematic potential of modern tracking total stations’ that the distance derived by the EDM was affected by the physical attributes of the 360 degree prism design. The physical attributes of the 360 degree prism which causes the effect to the distance measurement, is the prisms’ inability to be vertically aligned to the instrument. This was confirmed by Mao and Nindl (2009) concluding that the distance measured is affected by the alignment of the prism to the instrument.

2.3 Automatic Target Recognition

Automatic Target Recognition is a system that recognises a reflective target from a field of view and determines the centre of that target. The system aligns the instrument to the target which enables accurate angle and distance measurements without the need for manual fine sighting, making surveying robotically possible.

Automatic Target Recognition is the commonly known name for this system; however manufacturers have different names for their system like Topcon's Auto Tracking, Sokkia's Auto Pointing and Trimble's Autolock. The basic process of the ATR system is relatively similar between manufacturers (see figure 2.1), only their components and reductions differ (Artman et al. 2002; Lemmon & Mollerstrom 2007; Position Partners n.d.; Stempfhuber 2009).

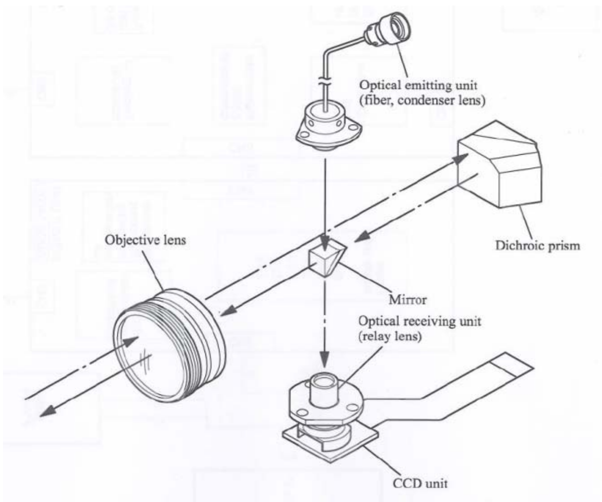

Figure 2.1: Basic optical arrangement (Position Partners n.d., p. 1).

The ATR system works by transmitting an infrared laser beam coaxial with the instruments optics through the objective lens. This beam is reflected back by a prism along the same axis as it was received (Lemmon & Mollerstrom 2007). The reflected beam along with stray light enters the objective lens of the instrument (Artman et al. 2002). The beam and stray light passes through a dichroic prism that splits the reflected beam from the stray light to limit any interference with the signal (*Dichroic prism* 2011; Position Partners n.d.). The separated reflected beam is guided through several mirrors and condensed by a relay lens on to a detector/sensor where it is imaged, see figure 2.1 (Artman et al. 2002; Position Partners n.d.).

The beam appears as a Gaussian spot (see figure 2.2) on the sensor's surface, its size being dependent on the distance to the target (Kirschner & Stempfhuber 2008; Stempfhuber 2009). The spot appears more intense where light has reflected from the central point of the reflective prism.

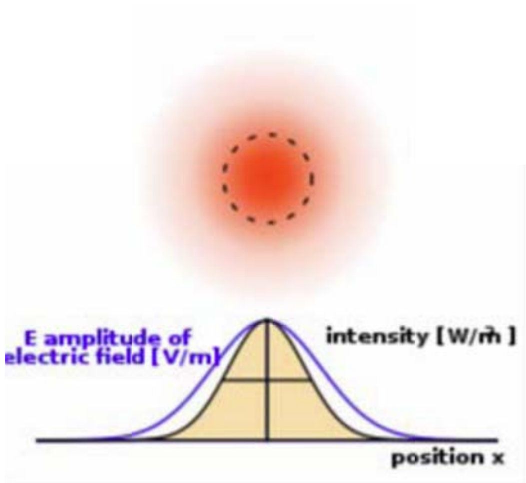

Figure 2.2: The Gaussian spot (*Gaussian beam* 2011).

The pixels within the sensor's surface gather an electric charge proportional to the light intensity shone upon it. This electronic charge is then converted to a voltage (*Charged-coupled device* 2011). This voltage is used to produce a digital image of the signal where an accurate position of the centre of the target is determined. The offset position of the centre of the target to the telescope reticle of the instrument is then calculated, see figure 2.3. (Artman et al. 2002).

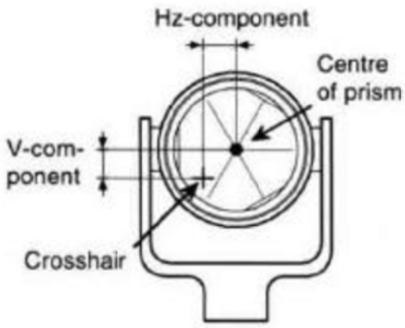

Figure 2.3: Optical offset correction (Artman et al. 2002, p. 8).

There are two ways for the instrument to apply the calculated offset corrections with the method dependent upon the instrument manufacture or settings within the instrument. The first method adjusts the instruments alignment so that the telescope reticle (cross hairs) and centre of target are in line. The other method adjusts the angular readings to the prism by the calculated offset corrections and displays the adjusted angular measurements, as though the instrument was aligned to the centre of the target (Lemmon & Mollerstrom 2007; Sokkia Corporation 2006; Topcon Corporation 2003).

Automatic Target Recognition Range

ATR has a reading range which is dependent on the field of view of the infrared laser beam transmitted, the reflected signal source upon the sensor's surface and the sensor's resolution.

The field of view or spot size of the infrared laser beam transmitted is 0.5 degrees (Artman et al. 2002). This limits the reading range of ATR when reading to a 360 degree prism. If the prism is not fully encompassed by the laser beam, only a portion (or a single prism) of the 360 degree prism may reflect the signal, causing the sensor to calculate an incorrect prism centre. The size of the Gaussian spot on the sensor's surface is dependent on the distance of the prism from the instrument. If the prism is too close, the signal source would fully encompass the sensor's surface with a strong signal. The sensor, unable to distinguish the intensity of the beam, would result in the calculation of an inaccurate prism centre. The same applies if the target is too far away. The signal source on the sensor's surface is too small to register, providing a null reading with no prism identified (Kirschner & Stempfhuber 2008). The maximum distance achievable being restricted by the resolution of the sensor. Kirschner and Stempfhuber (2008) investigated the accuracy of ATR angles over distance. Their findings are displayed in figure 2.4 below.

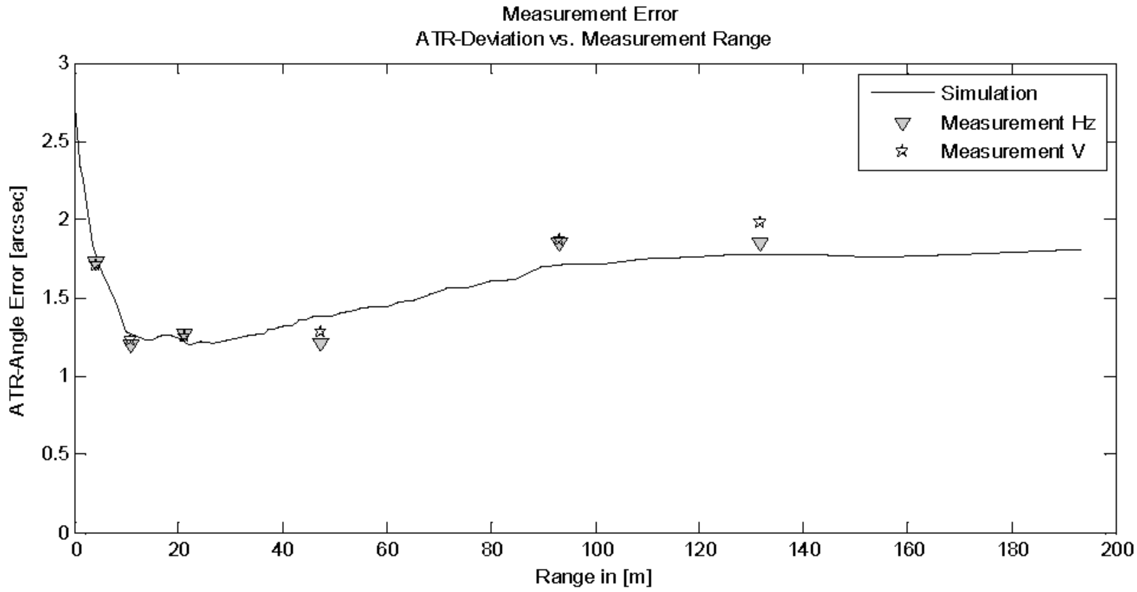

Figure 2.4: ATR errors versus prism range (Kirschner & Stempfhuber 2008, p. 6).

The ATR angle errors will need to be considered in the procedure to investigate the centring errors to a 360 degree prism. From figure 2.4, it can be seen that by reading to a target placed within the range of 10m to 30m, will reduce the ATR angle error to around 1.25".

To understand the limitations of ATR, the main contributing components of the system will be further investigated, these are:

- Prisms.
- Sensors.
- Calibration of ATR.

2.3.1 Prisms

The commonly used reflective targets for most surveys are prisms. Prisms are specifically designed and constructed to reflect light back upon the same path it was received. There are many types and sizes of prisms, all specifically designed for different applications. The prism selected for each task is based off their dominating ability such as: their multi directional ability, high accuracy or measuring range (Mao & Nindl 2009).

To better understand prisms and their effects upon ATR centring; their assembly, constants and sighting alignments will be further discussed.

Prism Assembly

The two main types of prisms are the standard round prism and 360 degree prism.

Standard Round Prism

The standard round prism consists of a triple-prism glass assembly, the three corners being grinded down to fit correctly within the circular housing, see figure 2.5 below (Mao & Nindl 2009).

Figure 2.5: Round prism components (Mao & Nindl 2009, p. 4).

360 Degree Prism

360 degree prisms are constructed in two ways, they are:

- Full array – The full array type consists of six triple-prism glass bodies tightly assembled with slightly grounded corners, producing a full prism array (Mao & Nindl 2009). See figure 2.6.

Figure 2.6: Full array prism (Mao & Nindl 2009, p. 5).

- Multi prism – The multi prism type consists of multiple small-triple prism glass bodies all surrounding one axis, see figure 2.7.

Figure 2.7: Multi prism.

Prism Constants

Measurements that have been derived from reflective targets are referenced to two points. One is the central axis of the instrument and the other is the prism's mounting axis. Corrections are applied to the raw distances measured to make this so. One of these corrections is the prism constant. The prism constant correction moves the measurement axis of the prism (point D) to a desired point (point B), which is the mounting axis of the prism, which coincides with the alignment of the pole's axis when adapted (Mao & Nindl 2009). The prisms true measurement axis is outside the prism (point D) see figure 2.8 below.

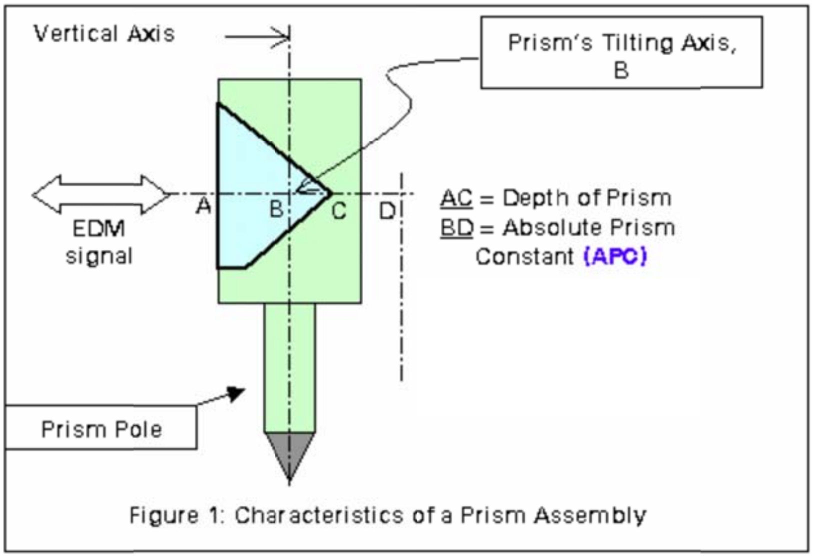

Figure 2.8: Prism axis and measuring points (*Leica FAQ – prism offsets* 2002).

This is caused by an effect the prism's glass has on the measurement signal. The glass affects the signal by decelerating the electromagnetic wave as it enters the glass body. This effect extends the actual measured distance (Mao & Nindl 2009).

Some instrument manufacturers apply an additional correction to counter this effect. They apply a constant value to move the true measurement axis of the prism to coincide with a symmetric point within the prism. A further 'manufacturer prism constant' adjustment is still required to adjust the measurement axis from the symmetrical point to align with the mounting axis of the prism, see figure 2.9 below (Mao & Nindl 2009).

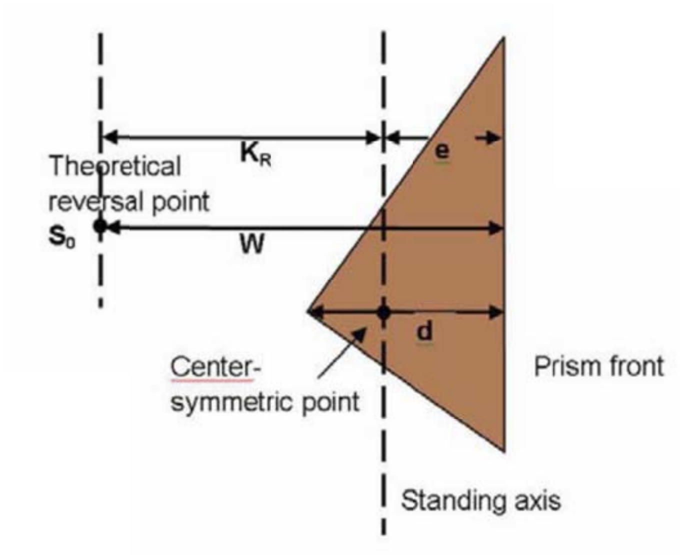

Figure 2.9: Symmetric point within prism (Mao & Nindl 2009, p. 6).

Leica uses this method by applying a constant value of -34.4mm to all its prisms to align the true measurement axis with that of the prism symmetric point (*Leica FAQ – prism offsets* 2002).

The two types of prism constants can cause confusion. The operator needs to perform a three peg test to know for certain which prism constant is stamped on the prism, whether it is the actual prism constant or the manufacturer's prism constant.

Sighting Alignments

In order to achieve high accuracy measurements the prism must be aligned to face the instrument, any misalignment affects the horizontal angle (see figure 2.10) (Kirschner & Stempfhuber 2008). Standard round targets have been modified to counter this issue by fixing gun sights to the target for ease when sighting to the instrument for alignment. Sighter targets have also been attached around the prism to rotate around the mounting axis of the prism. This allows the operator to eliminate any misalignment effects on the horizontal angle, by not sighting to the visual prism centre, but rather sighting to the target. As the prisms are symmetrically designed the effects are also apparent for the vertical angle. The vertical angle effects were eliminated by modifying the round prisms to allow for prism tilt, enabling correct vertical alignment to the instrument (Mao & Nindl 2009).

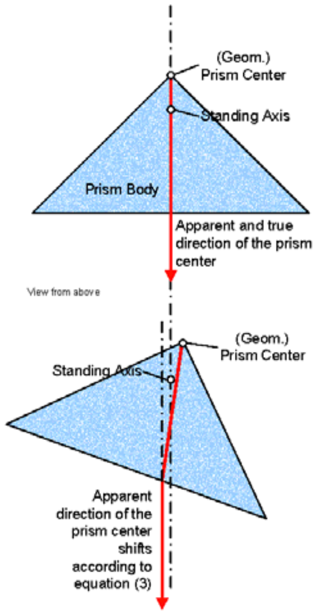

Figure 2.10: Horizontal shift caused by prism misalignment (Mao & Nindl 2009, p. 11).

Mao and Nindl (2009) graphed the horizontal distance error, caused by prism misalignment in relation to the prism's angle of incidence, see figure 2.11 below.

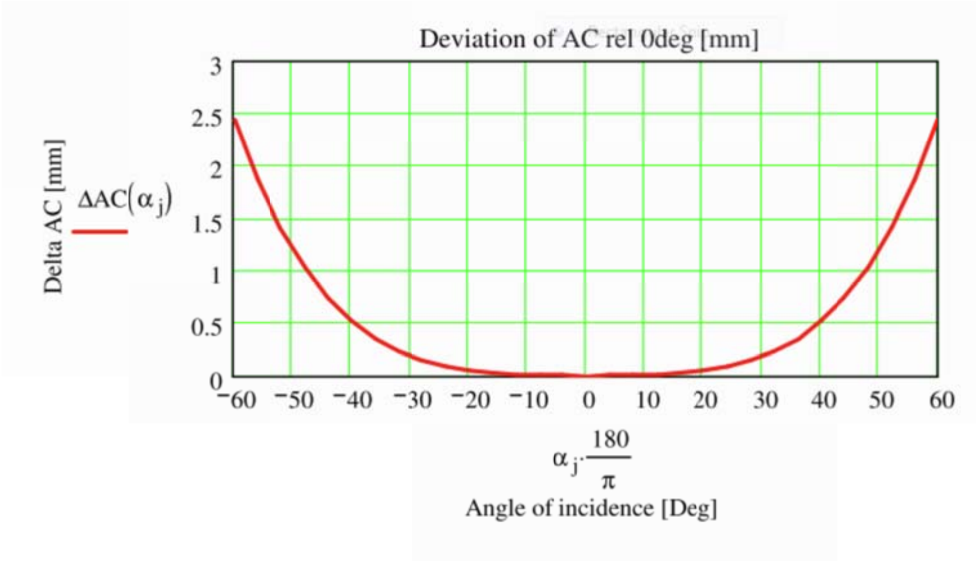

Figure 2.11: Horizontal distance error to prism's angle of incidence (Mao & Nindl 2009, p. 11).

Figure 2.11 illustrates the magnitude of the horizontal distance error with respect to the prisms' angle of incidence to the instrument.

Mao and Nindl (2009) derived equation 2.1 to calculate the distance error caused by the incorrect prism alignment for a round prism. That equation is:

$$\text{Distance measurement error} = \Delta d = e \cdot (1 - \cos\alpha) - d \cdot (n - \sqrt{n^2 - \sin^2\alpha}) \qquad (2.1)$$

Where:

$\alpha =$ Incident angle of the line of sight referring to front surface of the prism

$d =$ Distance from the front surface of the prism to the corner point of the triple prism

$n =$ Index of refraction of the glass body

$e =$ Distance from standing axis to front face

Topcon instructions manual also brings this error to the operator's attention and outlines that the error changes significantly with respect to the prism constant, see figure 2.12 below.

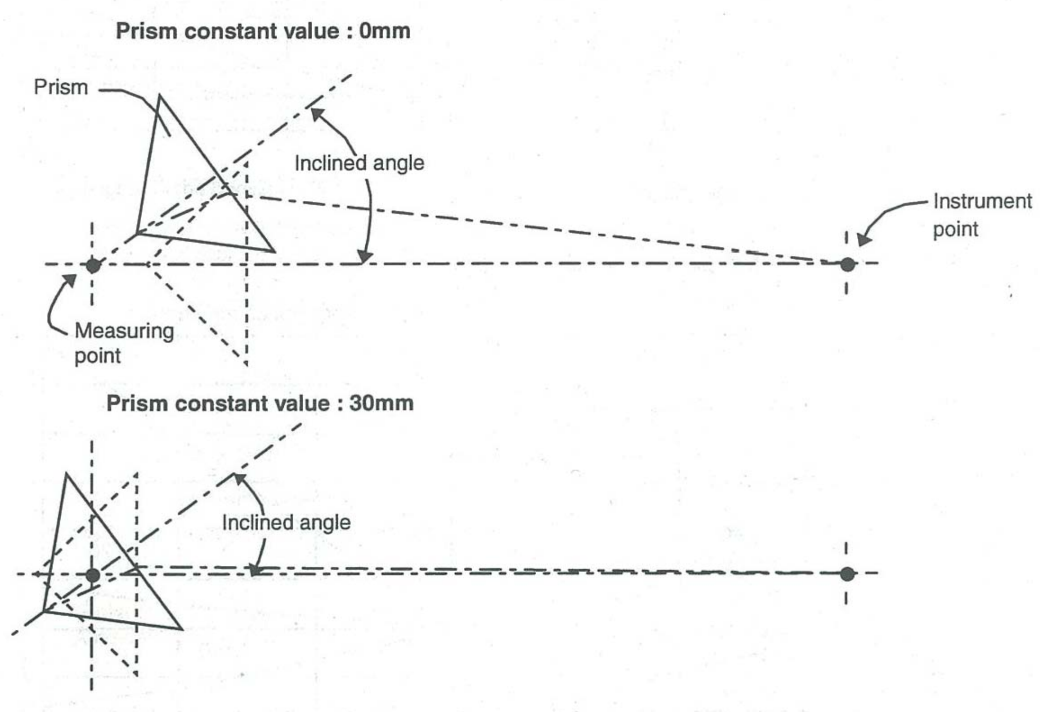

Figure 2.12: Prism constant effect on the prism alignment error (Topcon Corporation 2003, p. 2-10).

Previously this error was cancelled out by correctly aligning the target with the instrument, and always sighting to the target around the prism. However, with robotic instruments it has now been reintroduced. The prism is no longer sighted to manually using the targets but rather centred according to the signal strength received by the ATR sensor.

The 360 degree prisms used in conjunction with robotic instruments have also reintroduced this problem. Previously the assistant holding the pole would face the prism to the instrument reducing the effects. However, with the use of 360 degree prisms, a true pointing alignment is no longer apparent as the prism is not designed to accommodate for any tilt alignment. This leads to vertical and horizontal errors being unknown and difficult to detect (Mao & Nindl 2009).

Kirschner and Stempfhuber (2008) confirmed the alignment errors with reading to a 360 degree prisms, see figure 2.13 below.

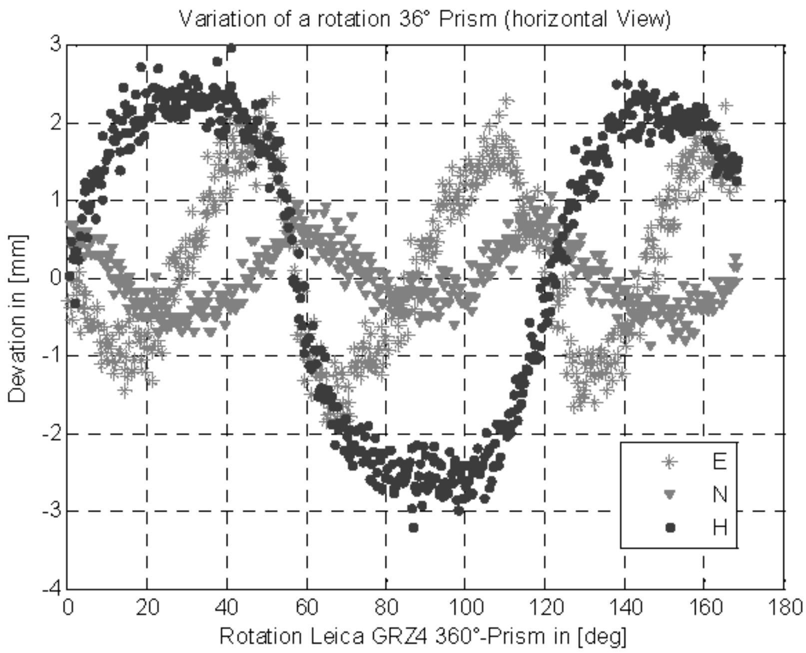

Figure 2.13: 360 degree prism variations to prism rotation (Kirschner & Stempfhuber 2008, p. 7).

Figure 2.13 illustrates the following error patterns for the Leica GRZ4 360 degree prism with respect to prism rotation:

- Easting (E) which is the horizontal angle offset error.
- Northing (N) which is the distance error.
- Height (H) which is the height error.

2.3.2 Sensors

The sensors located within the instrument used in ATR are electronic devices that convert the reflected light upon its surface, into an electrical signal to produce a digital image (*CCD vs. CMOS* 2011; Peterson 2001). The two types of sensors used in ATR are Charged Coupled Device (CCD) and Complementary Metal Oxide Semiconductor (CMOS) (Lemmon & Mollerstrom 2007; Palmetto 2007; Position Partners n.d.; Stempfhuber 2009). See sensor chips below in figure 2.14 and 2.15.

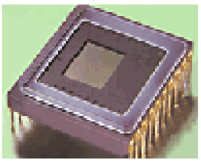

Figure 2.14: CCD sensor (Peterson 2001).

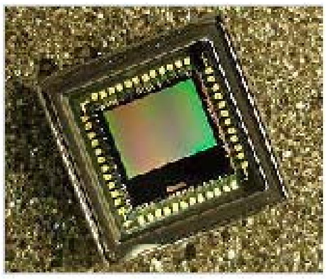

Figure 2.15: CMOS sensor (*Active pixel sensor* 2011).

Both sensor types are pixelated metal oxide semiconductors but each has their advantages over the other and both are continuously evolving as new technologies become available. These enhancements consist of greater resolution, size and power consumption to name a few (*CCD vs. CMOS* 2011). Each sensors basic operations and characteristics are discussed further.

2.3.2.1 Charged Coupled Device (CCD)

When a CCD sensor is exposed, each pixel in the capacitor array (the photoactive region) receives an electric charge proportional to the intensity of the light it received (*Charged-coupled device* 2011). Each compositor vertically shifts its charge on to the next, to a horizontal shift register until eventually reaching an on chip amplifier where the charge is converted to a voltage (*Characteristics and use of FFT-CCD area image sensor* 2003). These voltages are then sent off the sensor to a digital device for further processing, see figure 2.16 below (Peterson 2001).

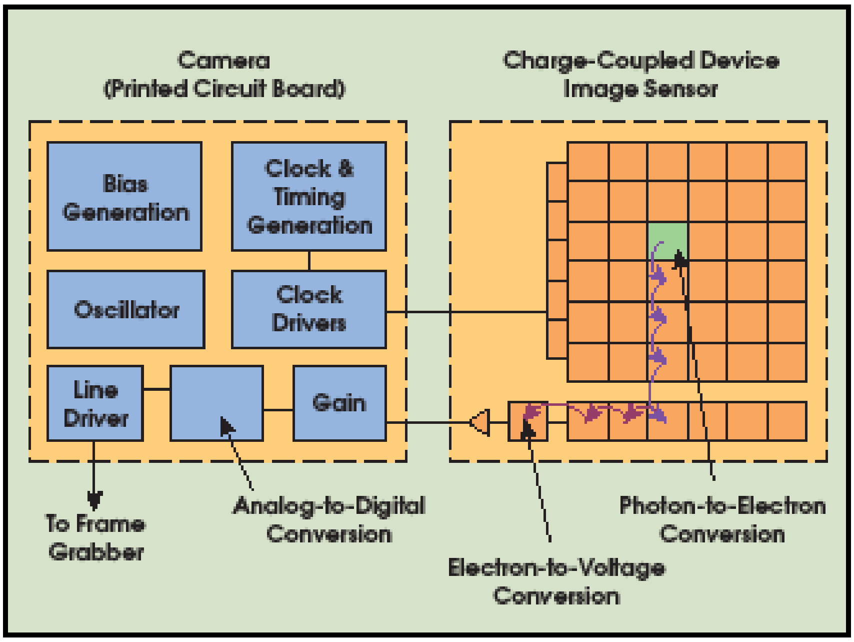

Figure 2.16: CCD sensor process (Litwiller 2001, p. 1).

CCD sensors are used for a wide range of applications; they are used in facsimile machines, photocopiers, bar-code readers, video cameras, televisions and all sorts of sensitive light detectors (Peterson 2001). As there are a number of applications there are also a variety of types of CCD sensors. They are categorised into two main types: linear (one dimensional) and area (two dimensional) (*Characteristics and use of FFT-CCD area image sensor* 2003).

The advantages of the CCD sensor include: smaller in size, easy analogue signal output, less image noise, the charge to voltage conversion is slightly more uniform and has superior shuttering (*CCD vs. CMOS* 2011; Litwiller 2001).

2.3.2.2 Complementary Metal Oxide Semiconductor (CMOS)

Like the CCD sensor once the CMOS sensor is exposed, each pixel in the photoactive region receives an electronic charge proportional to the intensity of the light on that pixel. However, unlike the CCD sensor, each pixel has its own charge to voltage converter, see figure 2.17 (Litwiller 2001). The image processing and a variety of operations are all on chip with a digital output (Graeve & Weckler 2001).

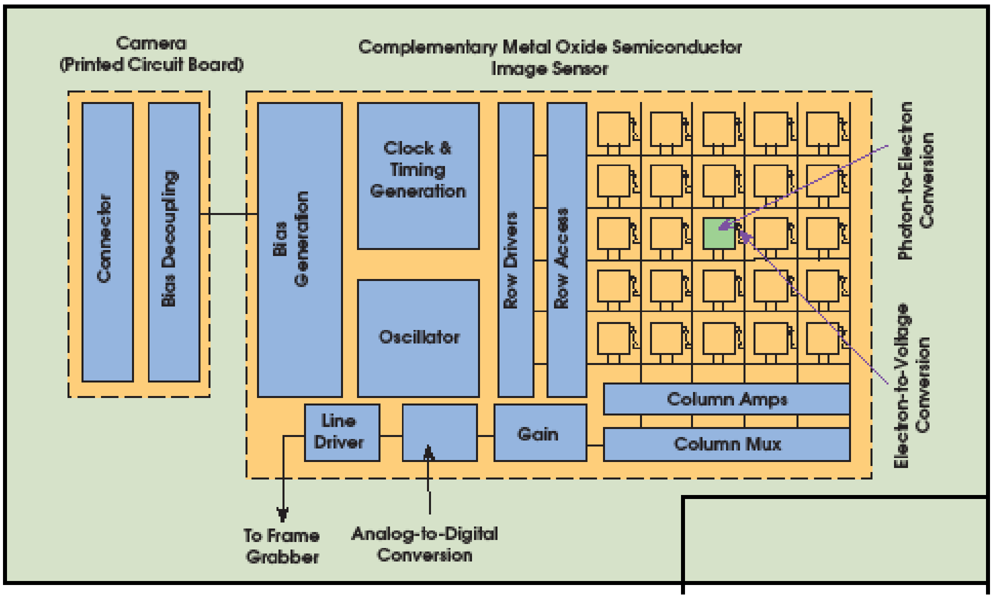

Figure 2.17: CMOS sensor process (Litwiller 2001, p. 2).

CMOS sensors are matrix in type and also cover a diverse field of applications just like the CCD sensors but tend not to cover the small high resolution electronics as CCD sensors like space imagery telescopes (Litwiller 2001). CMOS sensors have the ability of windowing out signal source, which enables multi quadrant detection and processing (Dubois et al. 2008; Litwiller 2001).

The advantages of the CMOS sensor include: more responsive, faster processing, greater processing ability, windowing abilities, natural blooming immunity and more reliability as all circuit functions can be placed on one chip (Litwiller 2001).

2.3.3 Calibration Process

Like any high precision system, the ATR system needs to be constantly checked and calibrated to ensure high precision measurements are obtained. The calibration process of ATR consists of setting up a target with the same level 100 meters away from the instrument. An on-board program is executed and both faces are read to the instrument either manually or automatically, depending on the instrument. These angles are then reduced and the offset correction from the centre of the target to the telescope reticle in the instrument is determined (see figure 2.18). The operator is usually prompted with the original and new correction values, to determine if any adjustment is necessary. Some ATR systems align the telescope reticle with the centre of the prism. This enables the operator to visually confirm the ATR adjustment (Sokkia Corporation 2006; Topcon Corporation 2003; *Trimble S series total station user guide* 2008).

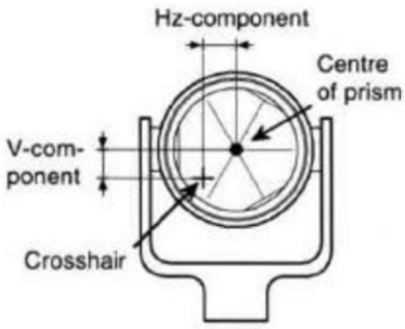

Figure 2.18: Prism offset correction (Artman et al. 2002, p. 8).

ATR centring on targets differs between instrument manufacturers. There are two methods of applying the offset corrections in ATR. The first method applies the offset corrections so that reticle aligns with the centre of the target. This method allows the operator to check the pointing precision of the instrument with ease. The second method applies the offset corrections to the raw angles observed and displays the corrected observations to the centre of the prism, without fully aligning the reticle with the centre of the target. This method is faster and is usually used for rapid/fast capture mode. However, the operator cannot visually check the instrument's alignment to the prism, confirming correct angle observations.

2.4 Curvature and Refraction

The curvature of the Earths' surface and atmospheric refraction affect the vertical line of sight which impacts on vertical angle observations, these affects and their significance will need to be considered when designing the field testing procedures. The instrument determines a level flat plane by gravity at that point. However this is not the case, as a level surface is determined by gravity which varies at each point. The line of sight is not a straight line either; refraction (caused by the prevailing atmosphere) bends the line of sight causing an incorrect position of an object, which affects the vertical angle observed. Both these effects increase as the distance increases, see figure 2.19 below (Anderson & Mikhail 1998).

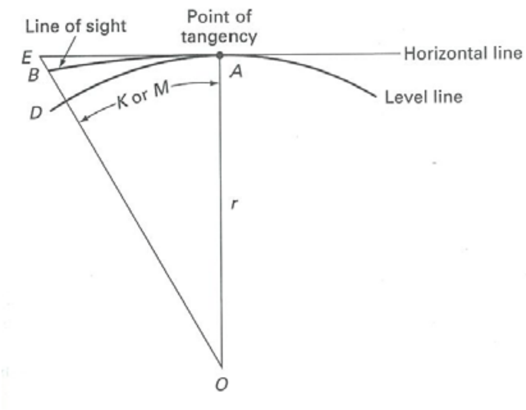

Figure 2.19: Curvature and refraction effects (Anderson & Mikhail 1998, p. 167).

Surveyors use a combined formula to correct for curvature and refraction. However instrument manufacturers modify this formula to suit the EDM's electromagnetic wave used for the instrument.

SVY2106 Geodetic surveying A: study book (2006) states the combined correction formula for curvature and refraction is:

Combine curvature and refraction correction $= c - r = \dfrac{\ell^2}{R}(0.5 - k)$ (2.2)

Where:

$c =$ Curvature correction

$r =$ Refraction correction

$\ell =$ Length of sight in meters

$R =$ Radius of earth in meters (About 6367510m)

$k = \dfrac{R}{2\rho =}$ Coefficient of terrestrial refraction

$\rho = 7R =$ Radius of the path of the light or $\rho = 4R =$ Radius of the path of the microwaves

2.5 Summary

The literature review in this chapter has provided an understanding of the process and elements that contribute to the effects causing a variation in the measurements achieved by ATR. The understanding of how ATR determines the centre of the prism; the characteristics of the 360 degree prism and the known effects of prism misalignment, will be used to design a procedure to measure the variations that occur. This will enable a determination of the likely accuracies achieved with this method of survey.

Chapter 3 - Method

3.1 Introduction

This chapter covers the testing procedures used to accurately measure the ATR 360 degree prism errors. The testing procedure has been developed from design considerations that were deemed necessary from the review of literature in chapter 2.

Calculations were conducted to determine the testing constraints and implications that would affect the error reading measurements gathered. This involved preliminary testing the designed procedure, to ensure there were no systematic errors inclusive of the measured ATR 360 degree prism errors.

3.2 Design Considerations

The review of literature in chapter 2 highlighted a number of factors that needed to be considered before designing the procedures to measure the ATR 360 degree prism errors.

The factors highlighted from the literature review requiring further investigation before developing a testing procedure were:

- The measuring specifications and correct ATR calibration procedure for each instrument selected for testing.
- The calculation of the distances that each 360 degree prism was to be tested over.
- Confirmation of the prism constants for each prism selected for testing.
- The required error measurement information that would allow for a thorough analysis of the measured results to determine the maximum and minimum errors for the two causes of the 360 degree prism reading errors:
    - The multi prism design (horizontal testing).
    - Inability to tilt prism (vertical testing).
- The curvature and refraction interference over the testing distances.

- The other standard measuring interferences that would conflict with the ATR prism error measurements.

These factors have been investigated in detail below to derive their influence on the testing procedure and to better determine the proper measures necessary to reduce any measurement interference.

3.2.1 Instruments Specifications and ATR Calibration Procedures

To understand the measuring capability of each instrument selected for testing, a review of their specifications and calibration procedure was completed. The instruments selected for testing in this project were: Topcon's GPT-8205A, Sokkia's SRX5 and Trimble's S6. These instruments were selected due to their mixed 360 degree prism types, years of separation between releases and accessibility.

Topcon GPT-8205A

Topcon Corporation (2003) states the following specific about the instrument.

Release:	2003
Angle measurement accuracy:	5" standard deviation
Distance measurement accuracy:	±(2mm + 2ppm x Distance)
ATR measurement accuracy:	3" standard deviation
ATR range:	10 to 500m
ATR sensor:	CCD sensor
ATR field of view	±30'
ATR adjustment:	Aligns reticle to centre of target
360 degree prism type:	A3 (6 small prisms scattered around a single point)
360 degree prism constant:	0mm (Actual Prism Constant)

Topcon ATR Calibration Procedure

This was performed by placing a prism, level with the instrument and more than 100m away, running the adjustment program and sighting to the prism in both faces manually. The program calculates the sensor shifted quantities and collimation correction for the horizontal and vertical angle from the observed faces. The instrument then auto points to the centre of the target for visual inspection and prompts the operator for adjustment confirmation. Once accepted the shift and collimation corrections are applied to future ATR angles to ensure the reticle alignment with the centre of the target (Topcon Corporation 2003). The calculated shift corrections do not change over various distance, however greater accuracy is achieved by measuring to a distant target (within ATR range), providing a more precise definition of the observed angle used in the calculation of the collimation correction.

Sokkia SRX5

Sokkia Corporation (2006) states the following specific about the instrument.

Release:	2007
Angle measurement accuracy:	5” standard deviation
Distance measurement accuracy:	±(2mm + 2ppm x Distance)
ATR measurement accuracy:	2mm <100m< 3”
ATR Range:	2 to 600m
ATR sensor:	CCD area sensor
ATR field of view	±45’
ATR adjustment:	Aligns reticle to centre of target
360 degree prism type:	ATP1 (full 360 array)
360 degree prism constant:	-7mm (Actual Prism Constant)

Sokkia ATR Calibration Procedure

This adjustment corrects the offset values to position the CCD sensor in relation to the telescope reticle. This procedure requires the operator to place a prism level with the instrument at approximately 50m. An on-board program is executed which instructs the operator to sight to the centre of the prism manually in both faces. This program then calculates the CCD sensor offset to the telescopic reticle and displays the results along with the previous adopted offsets. This allows the user to compare the readings and make the decision to adopt the adjustments or if the new offsets are within tolerance of the original offset, then no adjustment is necessary and the adjustment can be disregarded (Sokkia Corporation 2006).

Trimble S6 DR 300+

Trimble S6 total station: datasheet (2009) states the following specific about the instrument.

Release:	2007
Angle measurement accuracy:	3" standard deviation
Distance measurement accuracy:	±(2mm + 2ppm)
ATR measurement accuracy:	2mm at 200m
ATR Range:	0.2 to 800m
ATR sensor:	CMOS 4 quadrant detector
ATR adjustment:	Applies corrections to the measured readings
360 degree prism type:	Robotic target kit (7 small prisms scattered around a single point)
360 degree prism constant:	+2mm (Actual Prism Constant)

Trimble ATR Calibration Procedure

A prism is set up level with the instrument, no shorter than 100m from the instrument. This instrument, like the others, has a special program that reduces the observations and makes the necessary adjustments. It first displays the current collimation values, it then instructs the user to accurately aim towards the prism. The instrument will automatically sight using ATR to the prism in both faces, reducing the observations and providing the operator with the adjusted values. The operator is prompted with the option of storing the correction or cancelling the adjustment to use the original collimation correction (*Trimble S series total station user guide* 2008). Unlike the Topcon and Sokkia ATR adjustments, Trimble only adjusts for collimation errors. The centre of the prism determined by the sensor is used for all observations disregarding the reticle alignment. The reticle alignment can be adjusted by instructing the specially trained service technicians when the instrument undergoes its normal six monthly service.

3.2.2 ATR Selected Testing Distances

The field distances for testing the ATR prism errors were calculated for determining the reading platforms and environments for testing. Three testing distances were selected for the horizontal testing regime, with the minimum distance to be adopted for the minimum reading distance in the vertical testing regime.

Before selecting the three testing distances a few conditions were considered. These were:

- The testing distances for the three instruments all had to be the same; this allowed the instruments to be compared against each other, eliminating any additional ATR errors that would have resulted from different measuring distances.
- The testing distances were common distances normally observed in ATR survey practise and within the ATR reading range specifications of all three instruments.
- The minimum distance selected was to allow the prism to be fully encased within the ATRs' beam width (field of view). This ensured that the prism was detected as a whole and not a single prism causing an inaccurate centre determination.

The minimum distance (5m) selected was one that calculated the prism to be fully encased within the ATRs' beam width (field of view) to ensure that the prism is detected as a whole and not a single prism, causing gross errors. Although it was under the minimum reading specification for the instrument, it was adopted due to it being within the common distances normally observed within ATR survey practise. The minimum distance selected for horizontal and vertical testing was 5m.

The maximum distance (50m) selected was a distance that the prism could be observed without including an instrument angle accuracy reading error greater than 1mm. Adding to the errors being measured. The maximum distance selected for horizontal testing was 50m.

The middle distance (20m) selected was determined by being about halfway between the maximum and minimum distance and from the previous research conducted by Kirschner and Stempfhuber (2008) that found the ATR measurement accuracy was most precise at 20m. The middle distance selected for horizontal testing was therefore 20m.

3.2.3 Confirmation of Prism Constants

The prism constants for all the prism that were selected for testing was confirmed by performing three peg tests. The three peg test determined the correct prism constant to be entered into the instrument in order to measure correct distances.

This test was carried out for each instrument using their accompanying 360 degree prisms and the standard round prism selected for testing. This ensured that no prism constant errors were incorporated into the testing regime through the interchanging of different manufacturer prisms. The four steps for the three peg test procedure are outlined below.

1. Three pegs were placed on flat ground in a straight line with an overall distance of about 100 metres.

2. With the assumed prism constant (as stated by the manufacturer or preset within the instrument) for each prism entered into the instrument. The overall horizontal distance between the two outer pegs was measured.

3. The two inner distances between the middle peg and the two outer pegs was than measured.

4. By adding the two inner segment measurements together and subtracting the measured overall distance, the correction to the prism constant was calculated. The measuring accuracy of the instrument was also considered before applying the calculated prism constant correction.

The three peg tests revealed that all three instruments used the same prism constant type and that the prisms were all interchangeable between instruments with no additional correction required to the manufacturers' prism constant.

3.2.4 Sufficient Information to Conclude Results

The measurements gathered had to be sufficient to determine the error pattern with respect to the prism's alignment and the maximum and minimum values that could be observed. The literature review in chapter 2 covered previous work that graphed the measured errors with respect to prism alignment; using this knowledge the degree of rotation between measurements was calculated.

The maximum and minimum vertical angle observation range for each 360 degree prism was calculated. This determined the observation range for the vertical testing that had to be measured to calculate the magnitude of the errors that could be observed. These calculations have been further explained below.

3.2.4.1 Prism Rotations

The degree of rotation between measurements for the horizontal testing depended on the error pattern likely to be achieved; the amount of data required predicting the maximum deviations and the common reading points around the 360 degree prism that would provide an accurate measurement. These considerations have been investigated below.

Error Pattern

Previous research conducted by Kirschner and Stempfhuber (2008) identified that the centring errors associated with reading to a 360 degree prism using ATR follows a sine wave pattern when the prism is rotated, see figure 3.1.

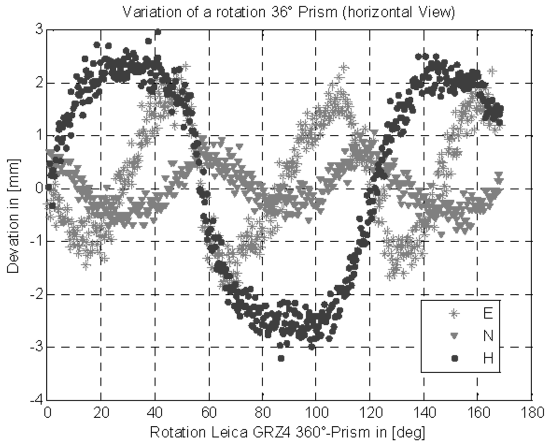

Figure 3.1: 360 degree prism variations to prism rotation (Kirschner & Stempfhuber 2008, p. 7).

Figure 3.1 illustrates the sine wave pattern measured for the Leica GRZ4 full array prism.

Number of Measured Error Points Required

From figure 3.1 it was determined that reading nine points along a single sine wave would provide sufficient information to determine the maximum reading deviations, and provide enough information to determine the best fit sine curve of the error with respect to prism rotations, see figure 3.2.

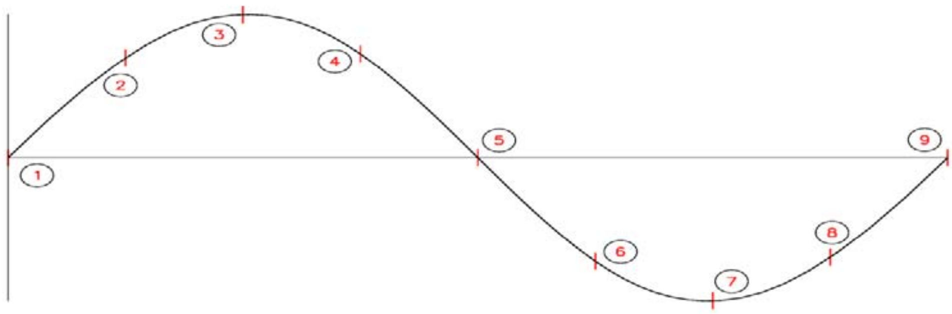

Figure 3.2: Nine points selected along the sine wave for measuring.

Common Reading Points

The operators' manual for each instrument informs the operator that in order to achieve accurate measurements a single prism of the multi 360 degree prism should be correctly aligned to the instrument. This was also the case for the full array 360 degree prism but instead of a single prism, the most accurate reading alignment was when one of the rubber pointers surrounding the prism was aligned to the instrument. This ensured that the full array prism was halfway between two prisms, allowing equal sighting to both prisms producing an average accurate position.

Every accurate reading point was a common reading point, the sum of each accurate reading point would provide the total number of times the error pattern would repeat itself. Studying the 360 degree prisms and understanding how the ATR sensors calculates the centre of the prism, it was determined that when the 360 degree prism was halfway between the accurate reading points (single prism or rubber pointer) there must be a point where the horizontal offset error is zero, the point half way along the sine curve.

Calculating the Degrees of Rotation

To calculate the degrees of rotation for the nine desired readings required to determine the maximum horizontal offset error and to determine the best fit sine curve, each 360 degree prism was divided up into the number of accurate reading points around that prism. The Topcon and Sokkia prisms divided by six with the Trimble prism divided by seven. The rotation between the common reading points was then divided up into the nine desired rotations along the sine curve. This calculated to 7.5° per a rotation for the Topcon and Sokkia prisms and 6.4286° per a rotation for the Trimble prism.

3.2.4.2 Maximum and Minimum Vertical Observation Range

Before the maximum and minimum vertical angles for the 360 degree prisms could be calculated, the position of the visual centre point within each prism was determined. This was calculated by modelling the 360 degree prism in a CAD drafting package.

Modelling of the 360 Degree Prisms

The three 360 degree prisms that were to be used for testing were modelled up in a CAD drafting package (see figure 3.3) using physical measurements attained from vernier calipers. The vernier calipers were able to measure to an accuracy of 0.02mm, this allowed a more accurate model of their physical attributes.

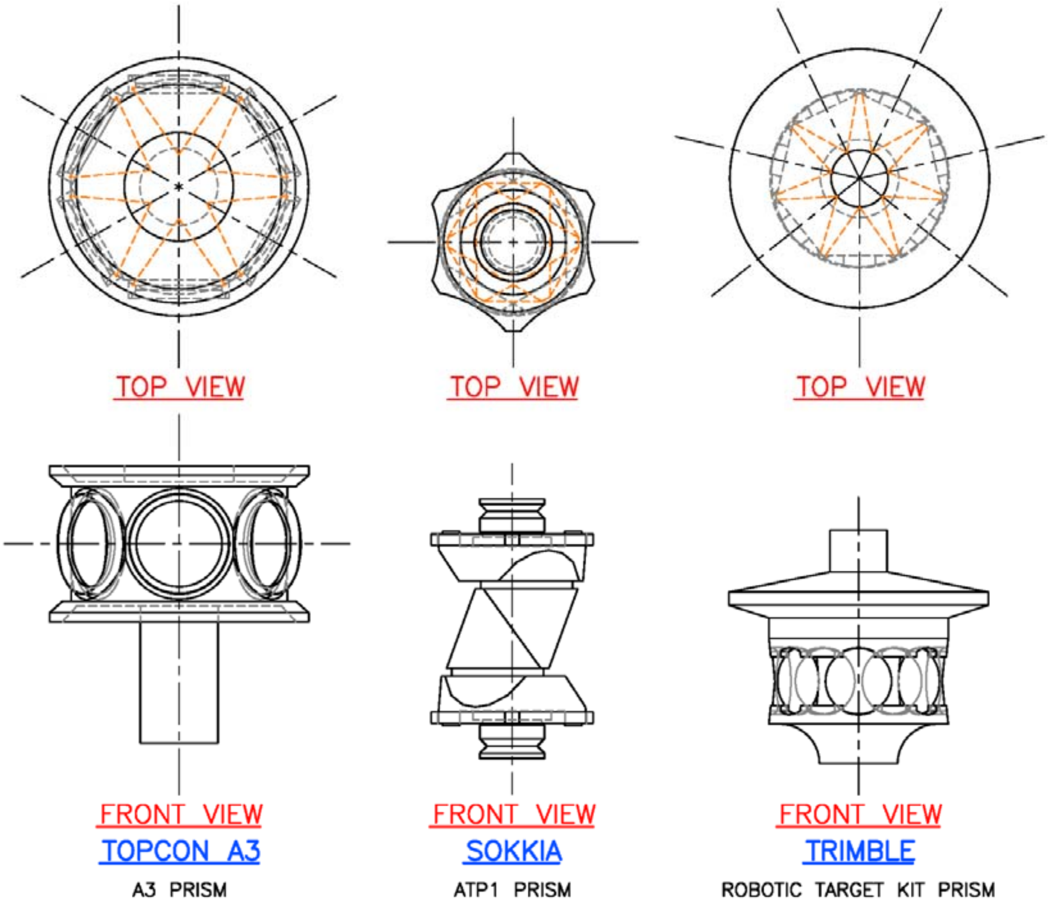

Figure 3.3: 360 degree prism models.

The prism models provided an accurate model that allowed precise distances to be extracted such as the distance from the prism face to the mounting axis of the prism, which was indicated by Mao and Nindl (2009) as a critical distance that was used in computing the effects of a poorly aligned prism.

Visual Centre Point Determination

A standard round prism that was able to be dissembled and reassembled was also measured and modelled up to predict the probable position of the visual centre within the prism caused by the refraction of the prism's glass. See figure 3.4 below.

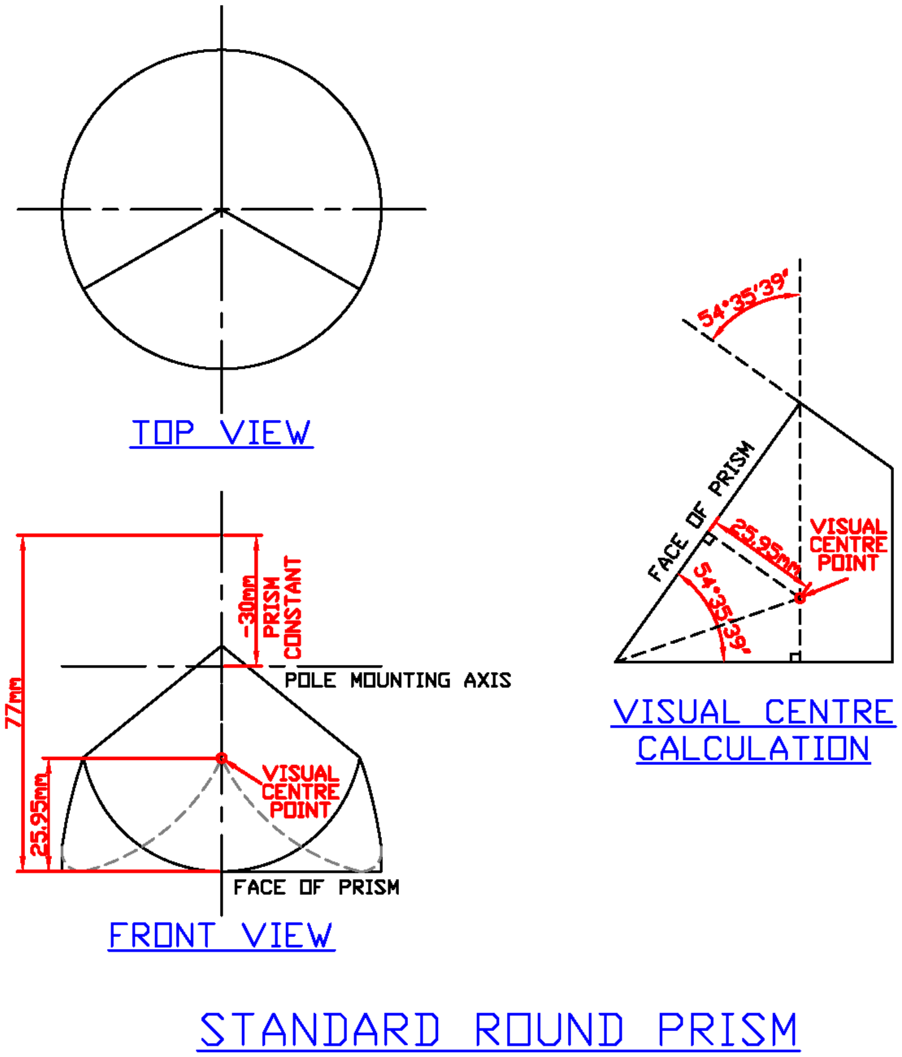

Figure 3.4: Visual centre point prediction.

The predicted visual centre point for the 360 degree multi prism types were calculated by scaling the standard round prism's predicted visual centre point onto the 360 degree prisms. This was scaled using the measurement from the front of the prism's face to the mounting axis of the pole while considering the prism constant. See figure 3.5.

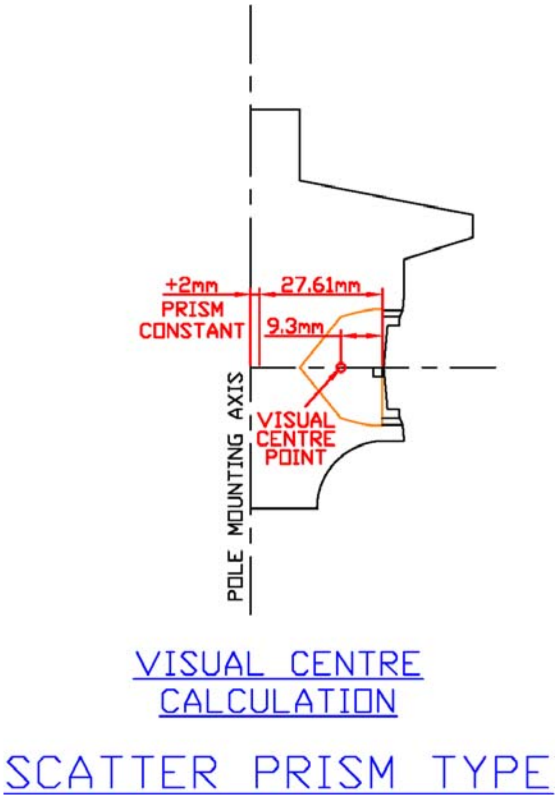

Figure 3.5: Multi prism type visual centre calculation.

The visual centre position for the full array prism type was calculated differently. Palmetto (2007) produced a presentation about the new advancements of the Sokkia SRX. The presentation covered some design considerations used in the construction of their full array type 360 degree prism, detailing how the visual centring of each individual prism was aligned horizontally to reduce the vertical error caused by refraction of the tilting prisms within the constructed 360 degree prism.

From the previous calculations of the visual centre point for the standard round prism it was predicted that the visual centre point was along the prisms axis from the centre of the face of the prism. Applying this knowledge along with Palmetto (2007) design considerations, the predicted position of the 360 degree full array prism was calculated, see figure 3.6.

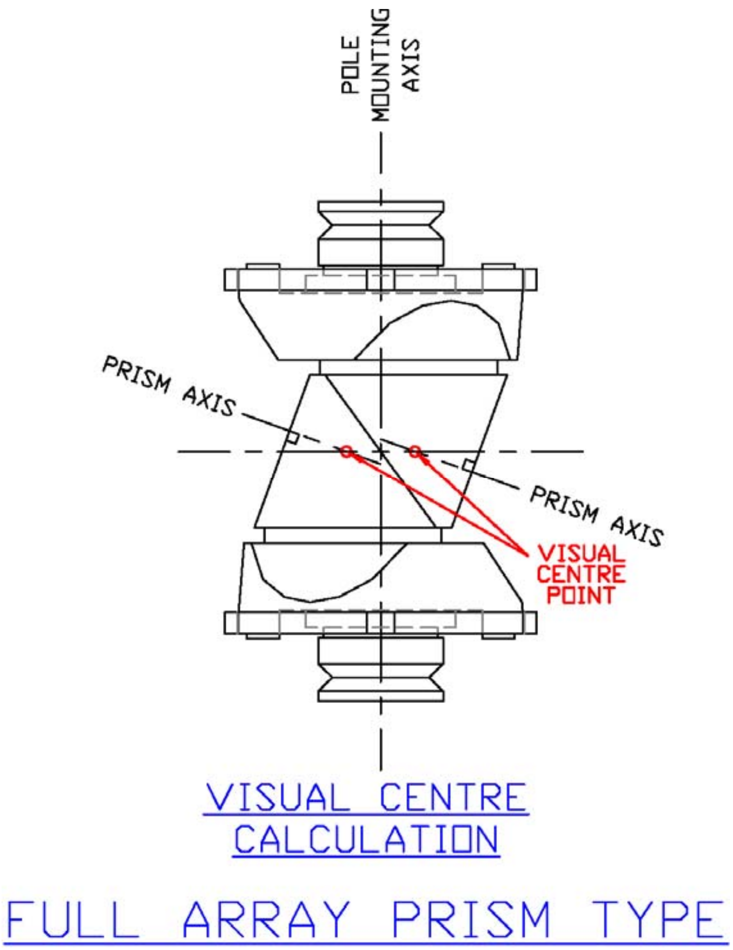

Figure 3.6: Full array prism type visual centre calculation.

Maximum and Minimum Vertical Angles

Knowing the predicted visual centring position for each of the 360 degree prisms, it was possible to predict the maximum and minimum vertical angle observations where each prism could be read. Figures 3.7(a), 3.7(b) and 3.7(c) illustrates the maximum and minimum vertical angles calculated for each of the 360 degree prisms based on their predicted visual centre point within the prism and the physical attributes of that prism.

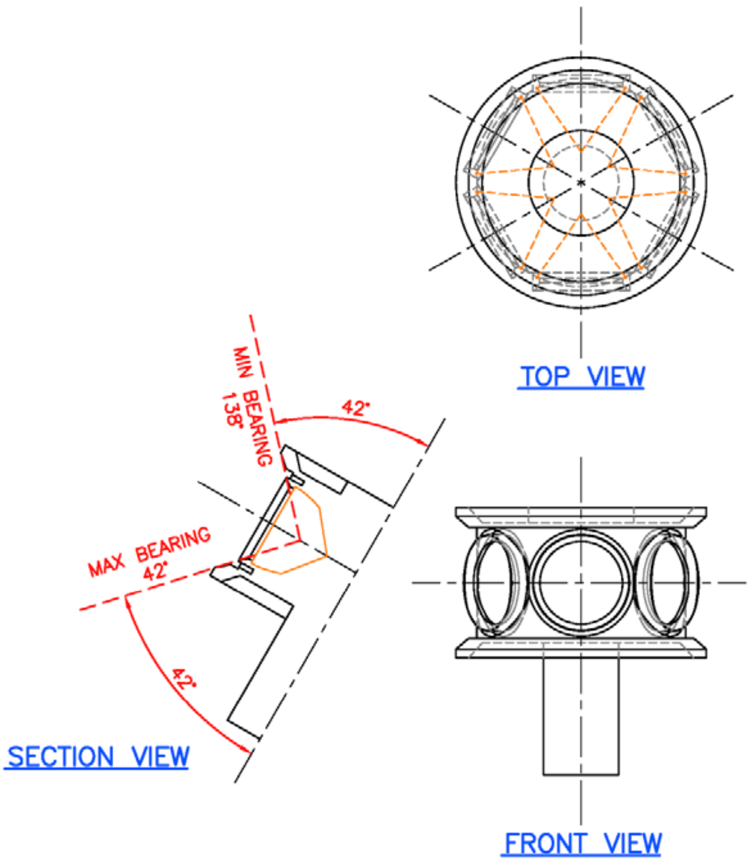

Figure 3.7(a): Topcon A3 prism predicted vertical angle range.

Figure 3.7(a) illustrates the predicted maximum vertical bearing observable to the Topcon A3 prism to be 42° and the minimum vertical bearing to be 138°.

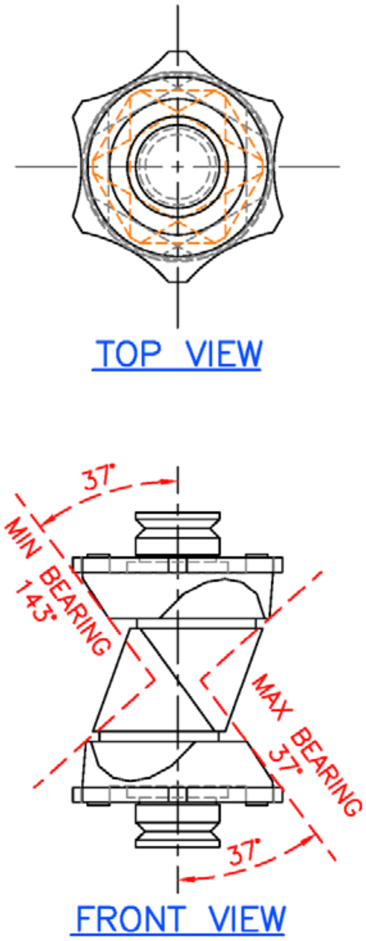

Figure 3.7(b): Sokkia ATP1 prism predicted vertical angle range.

Figure 3.7(b) illustrates the predicted maximum vertical bearing observable to the Sokkia ATP1 prism to be 37° and the minimum vertical bearing to be 143°.

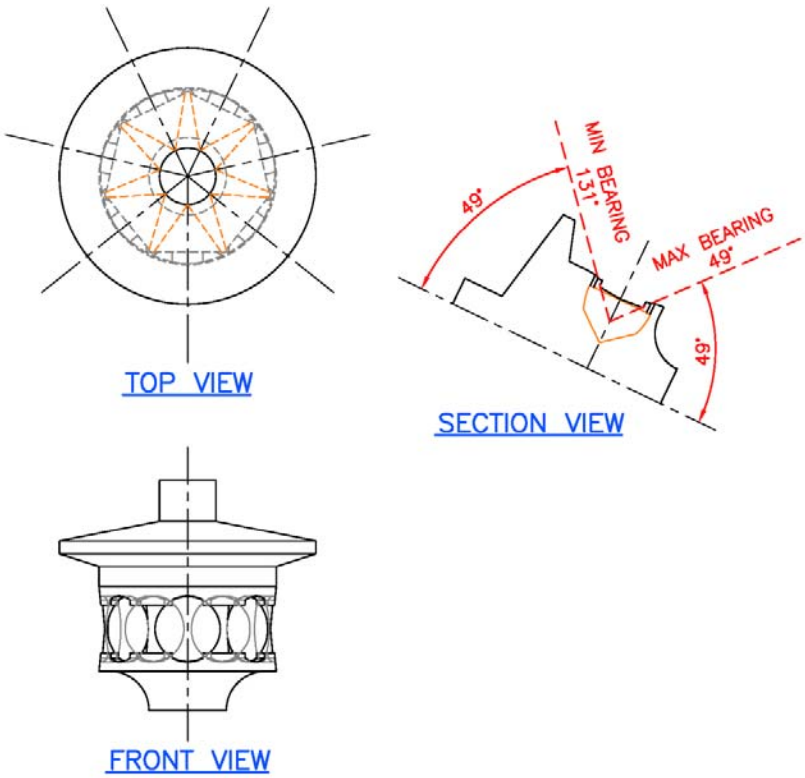

Figure 3.7(c): Trimble robotic target kit prism predicted vertical angle range.

Figure 3.7(c) illustrates the predicted maximum vertical bearing observable to the Trimble robotic target kit prism to be 49° and the minimum vertical bearing to be 131°.

3.2.5 Curvature and Refraction Interference

Curvature of the earths' surface and atmospheric refraction effects was considered when reading measurements for field testing. Curvature and refraction affects the line of sight which impacts on the vertical angle readings. *SVY2106 Geodetic surveying A: study book* (2006) states that the combined curvature and refraction correction for a distance of 100m is 1mm.

The robotic instruments selected for testing have an on-board curvature and refraction correction, that when selected applies the correction to the measured distances. This would mainly impact on the vertical angle readings for the vertical testing. The on-board curvature and refraction correction was turned on to reduce any affects to the measurements gathered.

3.3 Preliminary Testing Considerations

Preliminary testing was carried out for both the horizontal and vertical testing regimes. This ensured that the measurements obtained were accurate ATR 360 degree prism errors and were not inclusive of any significant systematic errors.

3.3.1 Horizontal Pretesting Considerations

Before preliminary horizontal testing was conducted considerations such as the measuring platform selected for use, the vertical circle influences, the prism tribrach rotation markings, the sighter target, the testing environment and the data collection mode was addressed.

3.3.1.1 Measuring Platform

The ideal reading platform was a stable pillar baseline; this would have eliminated any errors caused by movement to the instrument or prism tribrach, as well as any optical plummet alignment errors.

The closest pillar baseline was located two hours drive away, due to travel time, assistant availability, equipment cartage and booking of the baseline this was not utilised. Therefore tripods had to be used as a reading platform, as installing a pillars baseline closer, was too costly and getting approval would take a considerable amount of time.

To be able to use tripods for a reading platform the movement, tilt displacement and optical plummet errors had to be addressed. These were reduced as follows.

3.3.1.1.1 Movement

Any significant movement to the tripod resulted in the instrument or tribrach being shifted off the desired mark and knocked off level. To ensure minimal movement to the tripod, the tripods' feet were placed on a stable surface such as concrete or firm bare dirt. Surfaces such as bitumen and grass were not suitable as they tend to move with heat or spring back slowly once compressed. Having a good spread between the tripods' feet also helped brace the tripod, limiting easy movement as a result of strong wind or a bump from the operator.

To confirm that no significant movement occurred that would affect the measurements gathered was easily determined by setting the instrument and prism tribrach over precise marks so that they could be rechecked for position after the measurements were gathered. Checking the level of the instrument and prism tribrach also identified any significant movement throughout the readings.

3.3.1.1.2 Tilt Displacement

An incorrectly levelled instrument or prism tribrach resulted in inaccurate measurements. The instrument was of more concern as a tilting instrument affects all measurements, where a tilting prism tribrach only affects the measurement to itself and any other measurements with respect to that prism tribrach. The tilt errors were reduced by performing the following procedures.

Tilt Compensators

To counter this issue instruments have been designed with tilt compensators to reduce tilt measurement errors. The tilt compensators only compensate within a certain tilt range. To ensure the instruments' tilt compensators allowed for any tilt, a known bearing was set to a sighting target before readings and rechecked after gathering the readings. This confirmed the closing bearing was within tolerance, indicating that all tilt errors had been compensated for and the observations could be accepted.

Setup Height

The optical plummet alignment error caused by tilt displacement is magnified by the setup height of the prism or instrument. To reduce this error the prism and instrument was not setup at an excessive height. Calculations to identify the limit of allowable tilt before any significant impact to the readings were also undertaken. They revealed that for a 1.5m high prism or instrument and allowing a 0.5mm offset error, the allowable tilt was calculated to be approximately 1′ tilt displacement.

Precise Plate Bubble

A precise plate bubble was used to achieve a more precise level definition that would provided equal spread of the tolerance, improving the chance of staying within the acceptable limits. It also provided a visual warning of when the tilt was starting to approach the acceptable limits. Whereas using a coarse plate level would not have been accurate enough, as it only indicated that the level was out of tolerance after a significant error had already been included in the measurement.

The prism tribrach had a plate bubble that was accurate to 90″, where as the instruments' digital level could be set lower than 10″. The instrument that is paired with the prism tribrach was used to set and confirm the prism tribrach level. This proved difficult during testing, as the instrument used for levelling the prism tribrach was also selected for testing.

3.3.1.1.3 Optical Plummet Alignment

The optical plummet alignment impacts on the accuracy of measurements between marks. If the tribrach is not centred over the mark correctly, as a result of the optical plummets accuracy, then the reading can only be as accurate as the optical plummets accuracy. This issue was addressed when testing.

The optical plummet centring error was eliminated through measurement reductions, by comparing all measurements to the initial prism reading, instead of the mark positioned over. This provided the variations in the horizontal offset measurements with respect to the initial prism reading however, if the initial readings were not accurate then the offset variations would have no meaning or order. This made analysing the offset error very difficult, as it only gathered a spread of variations in relation to an inaccurate reading. To address this issue the initial prism reading was setup so that the 360 degree prisms' most accurate point was aligned to the instrument, resulting in the spread of variations relating to the correct position.

3.3.1.2 Vertical Circle Interference

The vertical circle observations are used to reduce slope distances into horizontal distances. When measuring the horizontal errors, the vertical circle influence was reduced by observing all measurement within a calculated vertical angle range. This reduced any influences of the vertical circle leaving only horizontal and distance reading errors. The vertical reading range where the slope distance can be considered the same as the horizontal distance was calculated for each testing distance. This was determined by calculating the vertical angle off the horizon, where the slope distance differed from the horizontal distance by less than 0.5mm. Table 3.1 outlines the limits of the vertical angle reading ranges for the horizontal testing.

Table 3.1: Vertical angle range where slope distances ≈ horizontal distances.

Distances	5m	20m	50m	100m
Max. Vertical Angle	89°11'52"	89°35'56"	89°44'47"	89°49'14"
Min. Vertical Angle	90°48'08"	90°24'04"	90°15'13"	90°10'46"

3.3.1.3 Prism Tribrach Rotations

The rotation for the prism tribrach was measured to ensure the desired controlled rotations for each 360 degree prism was achieved. The rotations were controlled by placing marks on the top and bottom parts divided by the rotation of the tribrach and aligning them for each desired rotation. The accuracy of the markings affected the rotation angle; a marking accuracy of 1mm equalled a 1°21′33″ rotation error. To reduce this affect the chord distances between the markings for the desired rotations and the initial prism reading marking were calculated to reduce compiling errors through the markings. The markings were placed using vernier calipers to improve accuracy, see figure 3.8.

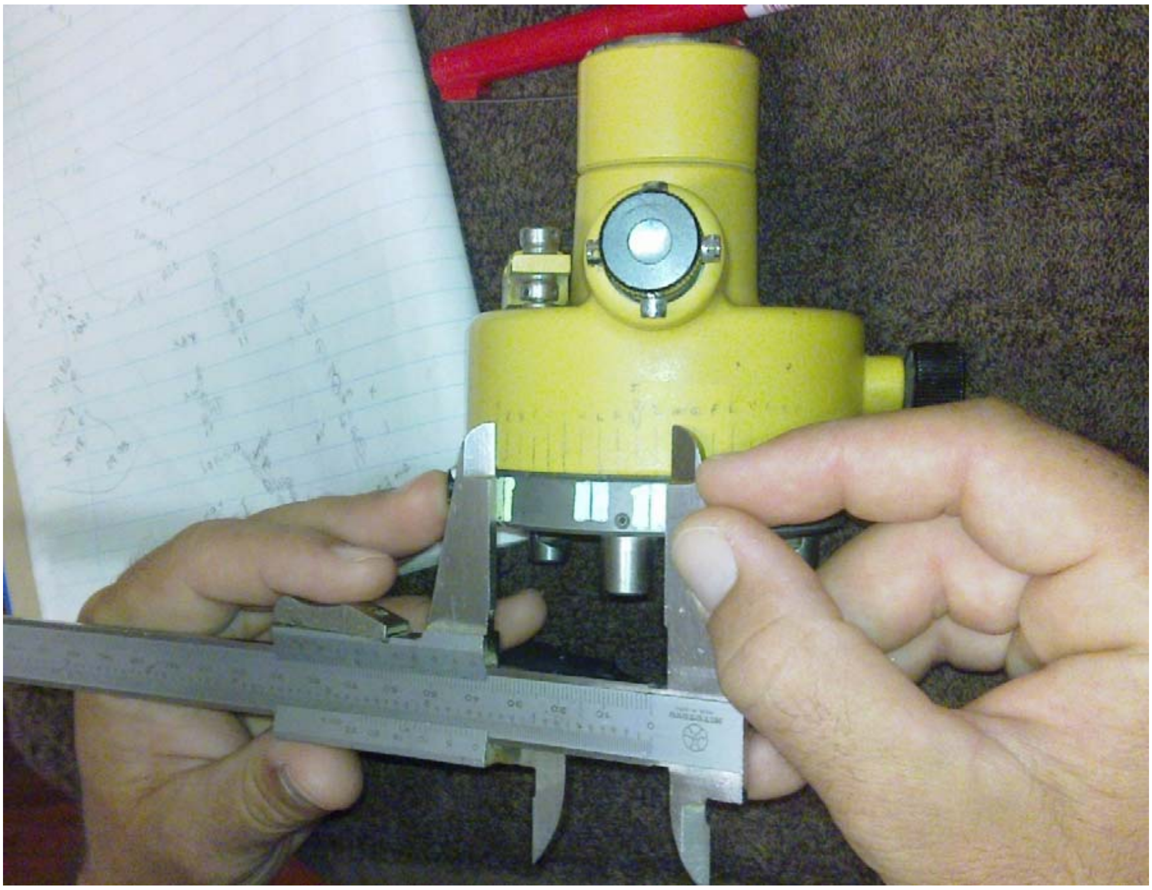

Figure 3.8: Rotation marking on the prism tribrach.

The accuracy of the rotation is reliant not only upon the thickness of the marks but also the manual setting when aligning the rotation marks. This was addressed by placing fine markings using a pacer to achieve a narrower mark on the prism tribrach and taking care when aligning the rotation marks. In the hope of further reducing any inaccurate rotations, an experienced surveyor fully aware of the implications of an incorrect alignment, was responsible for the prism rotations during field testing.

The nine rotation points for each 360 degree prism was marked on the top part of the prism tribrach, the bottom part was divided up by the number of accurate pointing marks on the 360 degree prism, see figure 3.8 above.

3.3.1.4 Sighter Targets

It was beneficial if the sighter targets to be used for positioning the prism and tribrach were also adopted for visual sighting for the instrument. The sighter target provided a measurement to determine the accuracy of the optical plummet, a line of reference to identify any prism misalignment from the initial reading and provided a suitable starting and closing bearing to confirm the existence of any tilt displacement within the readings from the instrument.

A plum-bob was thought ideal but its accuracy was too coarse for accurate bearing sightings, not to mention the drift as a result of the wind. An ideal stable removable target would be a 45° bent steel plate that had a scribe mark which allowed sighting from above for the optical plummet and front on for the instrument, see figure 3.9. The steel plate could also be removed as rawl plugs were used to secure them to the concrete, reducing the chance of them becoming a trip hazard for pedestrians.

Figure 3.9: Sighter target at 20m mark.

3.3.1.5 Testing Environment

The environment where the horizontal field testing was carried out needed to be flat, stable and level. The ideal environment was one that was easily accessible and without much interference by pedestrians and vehicles. Weather also impacted on the selection of the field testing environment, as factors such as wind and rain would affect the testing accuracy.

The kerb out the front of Fredriksen Maclean's Gladstone office was selected. It was protected by surrounding buildings that blocked strong winds. The road was flat and very close to being a level surface. The area was deserted on weekends with the exception of cleaners. This also meant that the carting and transport of survey equipment was not an issue. The road was kerbed either side and in a straight line, making it ideal for installing steel tags and meeting the desired conditions for the field testing environment.

3.3.1.6 Recording of Data

The data gathered through field testing was collected to be reduced for analysis; this process was noted to be easier by storing the measurements in a coordinate format, displaying the northing as the distance and easting as the horizontal offset. The measurements obtained from the horizontal testing were measured and recorded in coordinate mode with the 0m station given the coordinates of 1000E, 5000N. The bearing to the sighter target was set to zero and all observations were stored in a data collector for quick download.

The horizontal pretesting was then carried out to confirm that the procedures and testing elements selected to address the measuring issues, which would impact on the results, would provide viable data.

3.3.2 Vertical Pretesting Considerations

Before a vertical testing regime can be designed, some constraints were calculated as they restricted the design and would have hindered the readings. The constraints considered were; the horizontal testing reductions, the measuring platform, the vertical offset and prism incident angle calculations, the offset affects of the prism adaptor, the prism tribrach rotations and the rotation angle calculations.

3.3.2.1 Horizontal Reductions

From the horizontal testing reductions it was noted that the Topcon instrument had trouble reading to the 360 degree prism over the 5m range. Instead of using the field of view calculation for the minimum reading distance the ATR range minimum was adopted.

3.3.2.2 Measuring Platform

The ideal reading platform was a station on top of a 10m high block wall with the instrument setup on the low side of the wall reading different vertical angles by moving away from the wall and vice versa. There was no suitable platform of this nature located in the Gladstone area.

The next reading platforms considered were a steep road or a high pole that could be adjusted to achieve the desired heights for vertical readings. Both of these options failed as there was no steep roads built to the required incline of over 40 degrees for measurement (as no car could drive up this incline) and holding a 10m high pole still and vertical was a major issue, especially in the wind. A fire escape on the side of a building was considered but upon investigation there was a lot of movement caused by walking up and down the stairs and blocking the emergency escape route was a safety concern. This meant back to the drawing board to rethink another approach.

A testing design was decided upon that would mimic the prism's angle of incident which is experienced when measuring vertical angles. By knowing the angle of incidence of the prism when measuring the vertical offset error, allowed the vertical angle to be calculated linking it to the vertical offset error.

The testing design involved fabricating a 90 degree adaptor that allowed the prism to be mounted on its side while in the prism tribrach, see figure 3.10. By rotating the prism tribrach it, tilted the prism, which replicated a varying angle of incidence that would be observed if viewed with changing vertical angles. By controlling and measuring the degrees of rotation, the incident angle was calculated and the vertical offset errors were able to be referenced in relation to the vertical angle that would experience the same incident angle measured. This allowed the vertical offset errors to be measured horizontally, adopting the same measuring platform and considerations used for the horizontal testing.

Figure 3.10: Standard round prism on 90 degree prism adaptor.

3.3.2.3 Vertical Offset and Prism Incident Angle Calculations

To calculate the vertical offset error the distances from the prism tribrach's axis of rotation (origin) to the centre of the prism (true distance) and to the observed position (observed distance) needs to be known. The vertical offset error is then calculated by subtracting the true distance from the observed distance, as illustrated in figure 3.11.

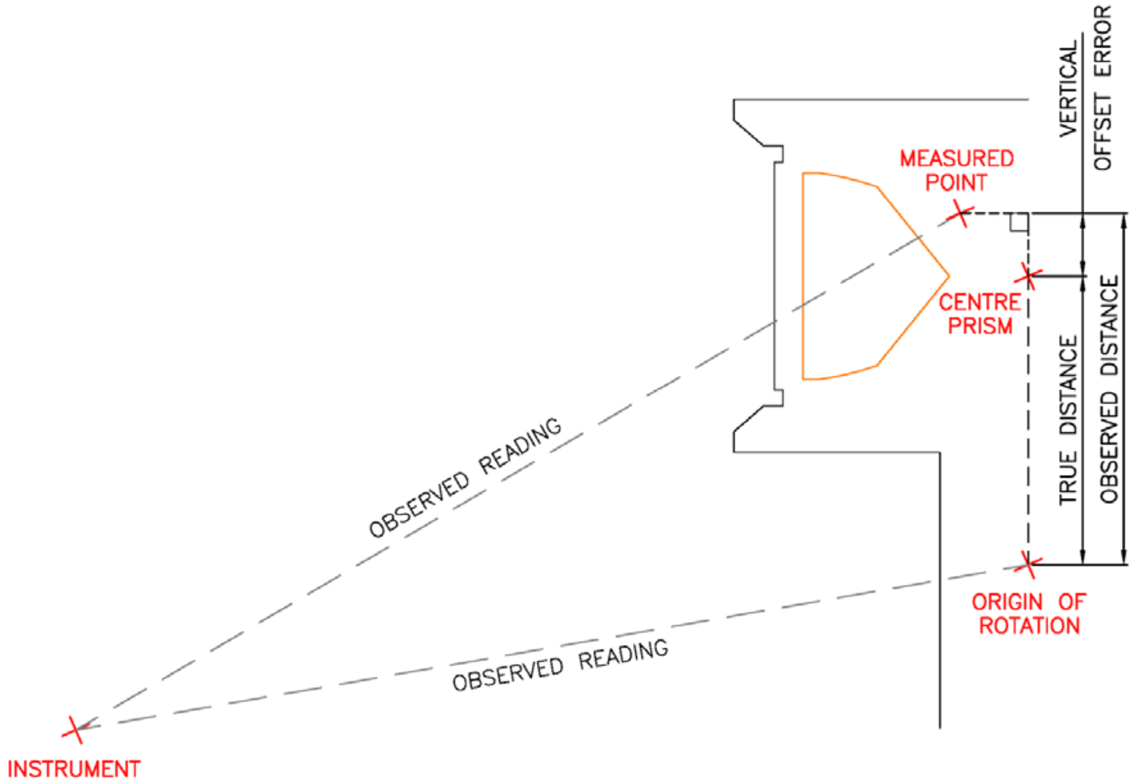

Figure 3.11: Vertical offset error.

The prism incident angle (PIA) was calculated by measuring the prism tribrach rotation angle (PTRA) from a straight on reading and subtracting the instrument reading angle (IRA) between the straight on bearing and the observed prisms rotated bearing, as illustrated in figure 3.12.

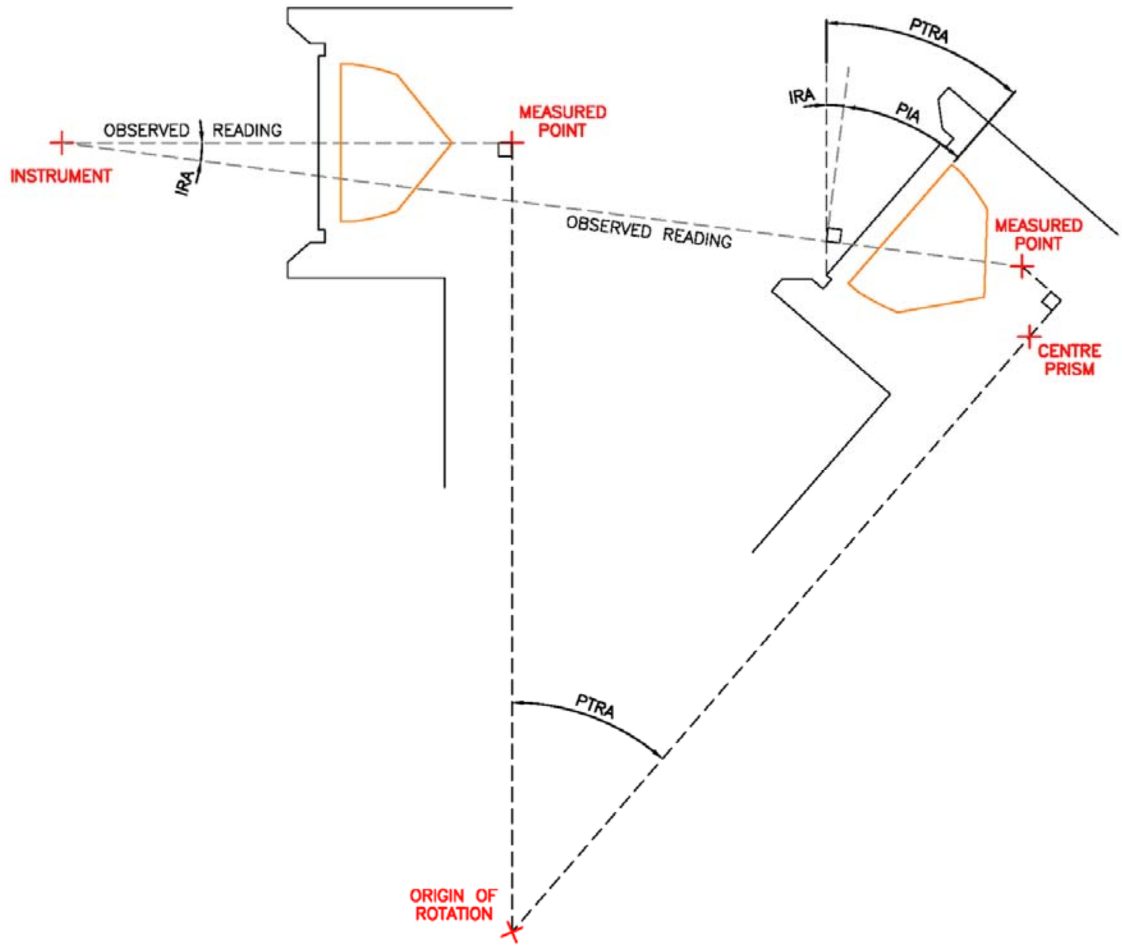

Figure 3.12: Prism angle of incidence calculation.

3.3.2.4 Adaptor Offset Effects

Calculations were preformed to confirm the prism offset from the axis of rotation caused by the 90 degree prism adaptor did not impact on the readings and calculations. This affect was investigated through calculations and preliminary testing. It was determined that the offset from the axis of rotation would amplify the effects of an inaccurate rotation, impacting on the vertical offset and distance errors calculated, see figure 3.13.

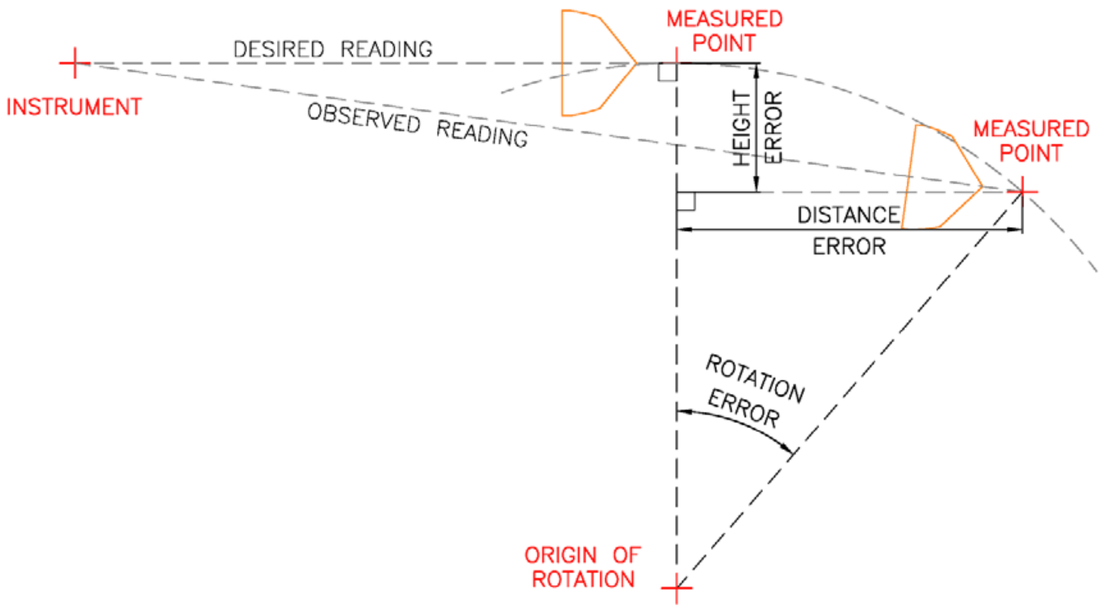

Figure 3.13: Prism offset impacts to height and distance measurements.

The calculated tribrach rotation angle accuracy required before any impact incurred on the vertical offset was calculated, using a prism offset of 95mm and a calculation error tolerance of 0.5mm was 5°52′52″. The calculated tribrach rotation angle accuracy required before impacting on the distance error calculated using a prism offset of 95mm and a calculation error tolerance of 1mm was 0°36′11″.

As calculated in the horizontal design considerations, a marking accuracy of 1 mm on the prism tribrach rotation would equate to a 1°21′33″ rotation error. Therefore, it is crucial that the marking accuracies on the prism tribrach were calculated to confirm the likely impacts on the vertical offset and distance error calculations.

3.3.2.5 Prism Tribrach Rotations

The prism tribrach rotation increment was selected to provide enough sufficient error information, allowing for a clear understanding of the vertical angle effect on the vertical offset and distance errors. The ability to read the error for many rotations while not having to move to achieve the desired vertical angle measurements enabled the selection of a small rotation interval. The selected rotation interval was five degrees, this was set out either side of the straight on reading until the maximum and minimum rotations were achieved.

Using the predicted maximum and minimum vertical angles calculated from the prism visual centre in the design considerations section, the prism tribrach was marked up to allow for rotations of up to ±50°. The procedure to mark up the prism tribrach was the same as stated in the prism tribrach rotation section under the horizontal design considerations to minimise the marking inaccuracies.

The rotations for the marks will still need to be confirmed and adjusted to reduce the inaccuracy impacts on the vertical offset and distance error calculations. This was completed during preliminary testing and reductions.

3.3.2.6 Rotation Angle Calculation

The marking rotation accuracies were determined and adjusted by reading to a standard round prism through each rotation ensuring the prism was always aligned with the instrument. Using the observed angle and distance readings, the angle of rotation between the markings was calculated by a simple close between the readings. The accuracy of the calculation was affected by the reading accuracy of the instrument, being careful that no vertical offset errors were introduced into the calculation of the rotation angles, by ensuring the prism was always aligned to the instrument. These calculated rotation angles between the rotation marks were then used for the vertical offset and distance error calculations.

The accuracy of the rotation angles calculated depended on the instrument reading accuracies and the manual aligning of the rotation marks. To reduce the instrument reading and manual aligning errors six sets of readings were recorded. These six sets of readings enabled an average measurement of a more precise rotation angle between the markings. This provided enough information for an accurate calculation of the standard deviation of accuracy for a single rotation measurement.

In an effort to further reduce the instrument reading errors for the measuring of the rotation angles, the reading platform distance will be amended to 20m, as horizontal testing and previous research revealed this distance to have improved accuracy for the instruments' ATR sighting. The readings were also measured using the Sokkia SRX, which was found to provide a more precise distance measurement than the other instruments in the horizontal testing reductions.

3.3.2.7 Recording of Data

The data gathered through field testing was recorded in a data collector for easy capture and file conversions for downloading. The measurements were stored in a bearing and distance format, allowing easier entering of observations measurements into a close program. The bearing and distance data was extracted from the raw file however the horizontal distance was not displayed. To reduce any vertical circle interference and to allow the slope distance to be adopted as the horizontal distance, care was taken to ensure that the readings did not exceed the vertical angle range calculated in the vertical circle interference under design considerations.

3.4 Preliminary Testing

Preliminary horizontal and vertical testing was essential to ensure that the measurements gathered were useful and accurate. Preliminary vertical testing also confirmed the accuracy of manually rotating the prism tribrach and the actual degrees of rotation between the set rotation marks.

3.4.1 Horizontal Pretesting

This section outlines the procedure for confirming the viability of using the selected reading platform, applying the all previous considerations discussed above in the horizontal pretesting consideration section. This procedure covers the installing of the stations; the adjustment checks to the equipment and the standard round prism readings.

3.4.1.1 Installing Stations

The first step was to install and setup the sighter targets. This involved pacing out the desired testing distances and placing the marks along the kerb to ensure that they did not fall on a driveway or a stormwater pit within the kerb. Once location of the 0m mark was determined and a plug was installed at this position. The instrument was then setup over the plug to provide accurate measurements for setting out the other three desired testing distances (5m, 20m & 50m). The distances were painted up and the rawl plugs for each sighter target at each station was installed, ensuring that the target would be facing the instrument for alignment.

3.4.1.2 Adjustment Checks

Equipment adjustment checks were carried out before any measurements were recorded during each testing session as the field testing took several weekends due to weather and assistant attainability. This ensured that the instruments or prism tribrach had not experienced any significant bumps or knocks throughout the weeks that may have put the equipment out of adjustment.

3.4.1.3 Measuring Systematic Errors

Readings were conducted using the standard round prism for each instrument selected for testing. This pretesting was to identify any systematic errors which may have been caused by a number of things such as the reading platform, the eccentric errors caused by the prism adaptor or the accuracy of ATR centring.

With the instrument centred over the 0m station and the standard round prism setup over the sighter target placed at the 5m station, the bearing to the sighter target was set to zero with a reading in reflector less mode. The standard round prism was then rotated through one set of nine rotations ensuring that the prism was always aligned to face the instrument. A closing measurement was then made to the sighter target confirming no tilt or movement errors to the instrument had occurred. The digital level and optical plummets for the instrument and the prism tribrach were then checked and adjusted if necessary.

This process was continued until the prism tribrach had completed a full rotation, the number of individual rotations depending on the 360 degree prism being tested. If at any time during the readings the closing bearing to the sighter target exceeded the allowable tolerance greater than 1mm offset the observations were discarded and the set re-read. The same procedure was applied regarding the level of the prism tribrach. If at any time when the traversing set instrument was placed on prism tribrach a tilt displacement exceeding 30″ then the observations would be discarded and the set reread.

This procedure was carried out for each instrument over the three testing distances.

3.4.2 Vertical Pretesting

The vertical field testing was conducted on the same reading platform, using the same considerations as mentioned for the horizontal pretesting. The additional considerations mentioned above in the vertical pretesting considerations section were also taken into account.

3.4.2.1 Adjustment Checks

Same as the horizontal readings, the equipment was checked for adjustment before any measurements were recorded, as the field testing was carried out over several weeks due to weather and assistant attainability. This ensured that the instruments or prism tribrach had not experienced any significant bumps or knocks throughout the week that may have put equipment out of adjustment.

3.4.2.2 Measuring the Prism Tribrach Rotations

The first sets of readings were to confirm the prism tribrach rotations using the standard round prism. This would also provide a sample of systematic errors to confirm that the propagation of system errors would not affect the vertical error calculations.

Using the horizontal testing marks the instrument was setup upon the 0m station with the standard round prism secured onto the prism tribrach. It was then centred over the sighter target at the 20m mark and a four step process was followed for testing as described below.

Step 1 - Average Origin Position

Setting a bearing of zero degrees to the sighter target and reading the bearing and distance to the prism tribrach axis of rotation (origin) six times, the average bearing and distance was calculated. The standard round prism was then fixed to the 90° prism adaptor and secured onto the prism tribrach. With the prism aligned to the instrument, the tribrach rotation was set to 0° for an approximate reading. Using the reading to the origin and the approximate 0° reading, the 'prism height' between the prism and the origin was calculated by a close program. The prism reading distance to the correct position of the prism at 0° rotation was calculated. The 90° prism adaptor was then rotated until the calculated prism distance was observed see figure 3.14.

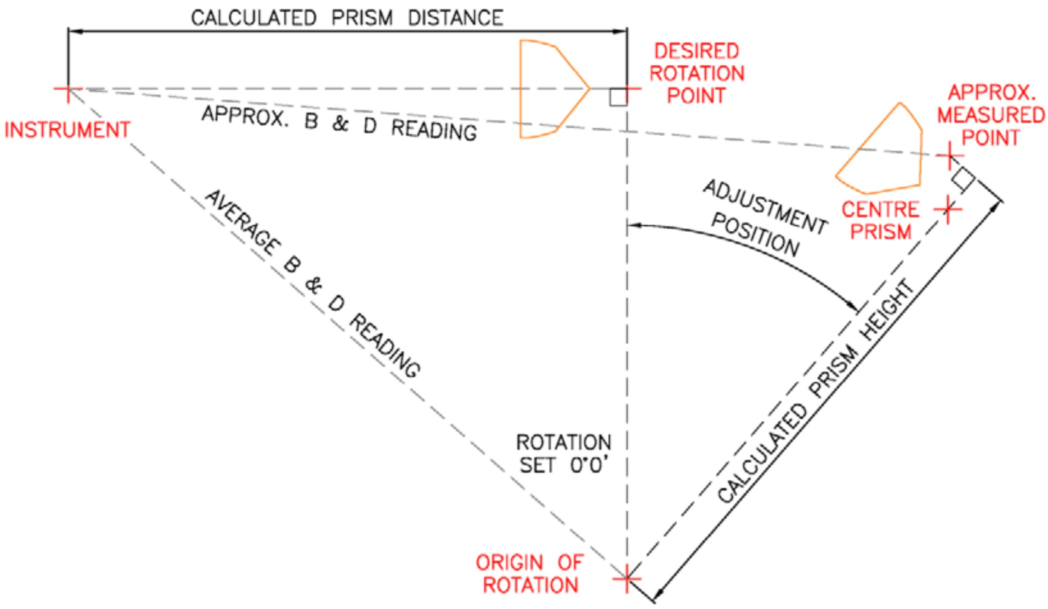

Figure 3.14: Setting prism to read straight onto the instrument at 0° rotation.

This meant that the prism was set straight onto the instrument with the prism tribrach rotation set to 0° and all future readings were measured in relation to this rotation. The 0° rotation was later closed back onto confirming that no movement had occurred, ensuring accurate readings.

Step 2 - Rotations

The prism tribrach was rotated through all the rotation marks from +50° to -50° and then back to 0°. All measurements were observed with the standard round prism aligned to the instrument.

Step 3 – Recheck Origin

The 90° prism adaptor was then carefully removed and the standard round prism placed back onto the prism tribrach. The averaged origin positioned was then staked out to ensure that there was no movement to the prism tribrach.

Step 4 – Final Checks

A closing bearing shot was made to the sighter target confirming that any tilt displacement of the instrument was accounted for. The instrument level was then checked along with the level of the prism tribrach.

At any point during the readings when the 0° prism tribrach rotation was checked and the distance was found to be 1mm or more different to the correct calculated distance, then the readings would be discarded and reread. If the check on the origins' position or sighter target was out by 1mm or more the readings would be discarded and reread also. If the level of the instrument or prism tribrach was found to have a tilt greater than 30″ the readings would once again be discarded and reread.

This process was repeated until six sets of usable observation data had been collected.

3.5 Preliminary Reductions

The reduction process for the horizontal and vertical pretesting confirmed the measuring platforms suitability and the procedures adopted provided accurate measurements without the presence of significant systematic errors.

3.5.1 Horizontal Pretesting Reductions

The reductions for the horizontal pretesting involved, reducing the standard round prism readings to confirm the stability of the testing platform and systematic errors.

3.5.1.1 System Error Reductions

Five steps were used to reduce the standard round prism readings to a meaningful format. These steps have been outlined below, and a sample of calculations has been provided in appendix B.

Step 1 - Data Conversion and Analysis

The testing data was downloaded from the data collector into a Microsoft Excel spreadsheet where the data was displayed in the following columns:

- Observation point identification number.
- Easting.
- Northing.
- Reduce level.
- Description.

The measurements that were noted as affected by movement and were deleted, while the remaining verified data broken up into the six sets of readings.

Step 2 - Distance and Offset Format

The coordinates of each reading was then subtracted by the coordinates of the instrument (1000, 5000) to provide the distance (northing) in relation to the instrument and offset (easting) in relation to the sighter target for the prism. The average distance and offset of each set was calculated along with an overall average of the six sets.

Step 3 - Combined Systematic Errors

To identify the combined systematic distance and offset errors, the overall mean of the distance and offset was subtracted from each of the observed distance and offset readings. This provided errors that were a combination of the following:

- Instrument reading accuracy.
- Eccentric errors of the tribrach and prism adaptor if any exist.

- Prism tribrach optical plummet centring accuracy over the sighter target between sets.

Step 4 - Reduce Systematic Errors

To eliminate the prism tribrach optical plummet centring accuracy over the sighter target, the coordinates for the initial reading of each set was subtracted from each reading within that set. The corrected distance and offset errors would only contain the combination of the instruments reading accuracy and any eccentric errors in the tribrach or prism adaptor.

Step 5 – Average Reading

The instrument reading inaccuracies were reduced by calculating the average corrected distance and offset errors for each set and subtracting them from the corrected distance and offset readings within that set. This provided the residuals of each reading and allowed the overall standard deviation for all the prism readings observed to be calculated with minimal errors.

Step 6 - Standard Deviation of a Single Rotation

The standard deviation of a single rotation from the overall corrected distance and offset errors was calculated. This provided the measurement accuracy likely to be achieved when testing the 360 degree prisms and a sample of data to compare the 360 degree prism errors against.

The standard round prism average distance and offset errors along with the standard deviation of a rotation was tabulated in Microsoft Excel, see table 3.2.

Table 3.2: Horizontal pretesting results.

Instrument	Testing Distance	Mean Offset Error	Std. Dev. Offset Error	Mean Distance Error	Std. Dev. Distance Error
Topcon	5m	0	0	0	1mm
	20m	0	0	0	1mm
	50m	0	1mm	0	1mm
Sokkia	5m	0	0	0	0
	20m	0	0	0	0
	50m	0	0	0	0
Trimble	5m	0	0	0	1mm
	20m	0	0	0	0
	50m	0	0	0	0

From table 3.2, the horizontal pretesting has proved that there are no significant systematic errors within the horizontal testing regime. All errors have all been reduced or cancelled out by the strict measuring procedure. The errors gathered during the pretesting fall within the measuring ability of each instrument. Therefore any errors measured during the horizontal testing can be considered solely that of the 360 degree prism being measured using ATR.

3.5.2 Vertical Pretesting Reductions

The process to reduce the measured field data into the desired vertical height and horizontal distance errors, took nine steps as described below. Note that a sample of the vertical tribrach rotation angle calculations has been provided in appendix C.

Step 1 - Data Conversion

The testing data was downloaded from the data collector and the raw data files were printed out. The usable bearing and distance readings were manually entered into a Microsoft Excel spreadsheet with the bearing in degrees, minutes and seconds format.

Step 2 - Average Origin

The average bearing and distance from the instrument to the origin (prism tribrach axis of rotation) was calculated.

Step 3 - Prism Adaptor Bearing

The bearing and distance observed for the setting of the 0° reading was then used to calculate the bearing alignment for the 90° prism adaptor, assuming the angle between them to be 90°. Using the bearing observed for the initial 0° rotation in that set and the desired rotation angles (which were marked up on the prism tribrach), the bearing alignments for the 90° prism adaptor for each rotation mark was calculated, see figure 3.15.

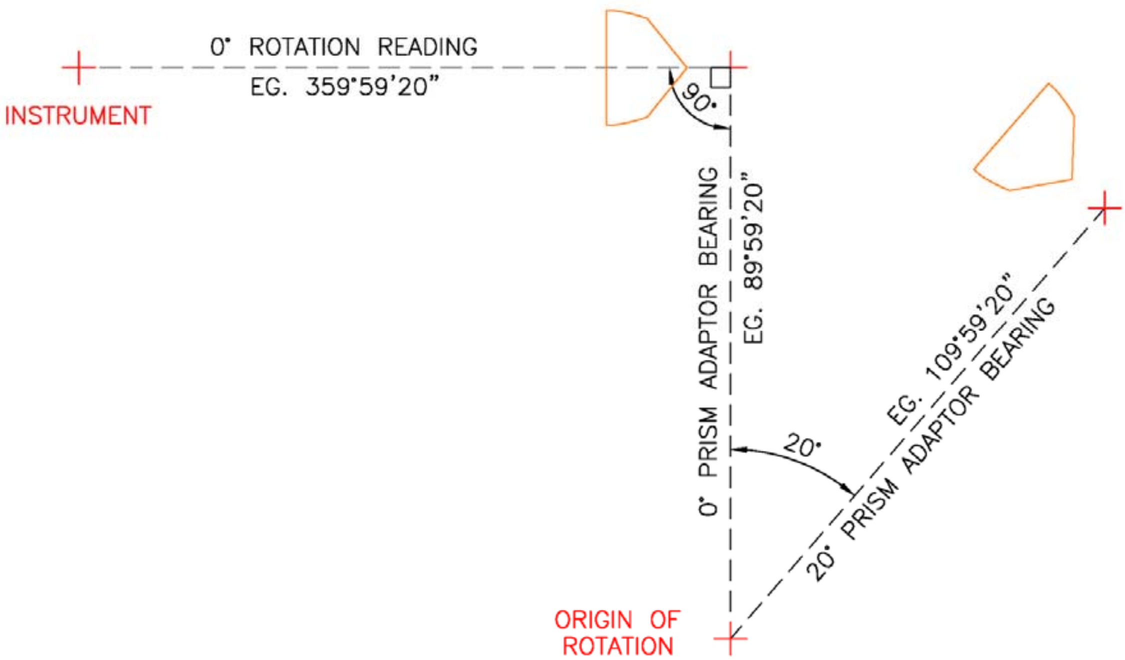

Figure 3.15: Prism adaptor bearing calculations.

Step 4 - Actual Prism Height

The distance and bearing from the prism to the origin was calculated using a close program. By closing the readings from the origin to the instrument and from the instrument to the prism, this information was determined, see figure 3.16.

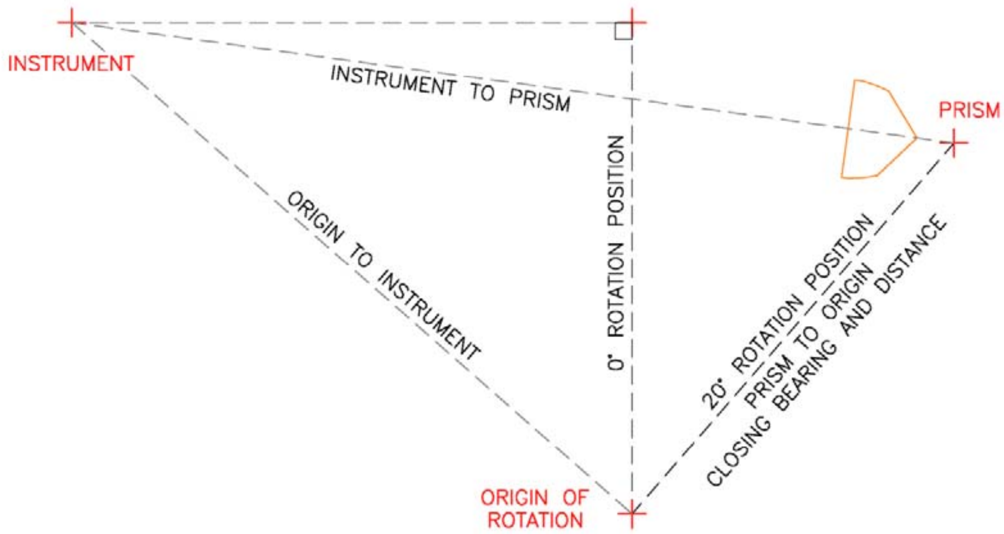

Figure 3.16: Close determining the true rotation for each rotation mark.

Step 5 - Distance and Offset

The distance and offset from the prism to the origin was calculated using the desired prism rotation values for the prism tribrach. This was calculated using a close program, by calculating two missing distances from the following information:

The readings from the origin to the instrument and from the instrument to the prism; along with the calculated bearing for the 90° prism adaptor bearing and the bearing perpendicular to this, see figure 3.17.

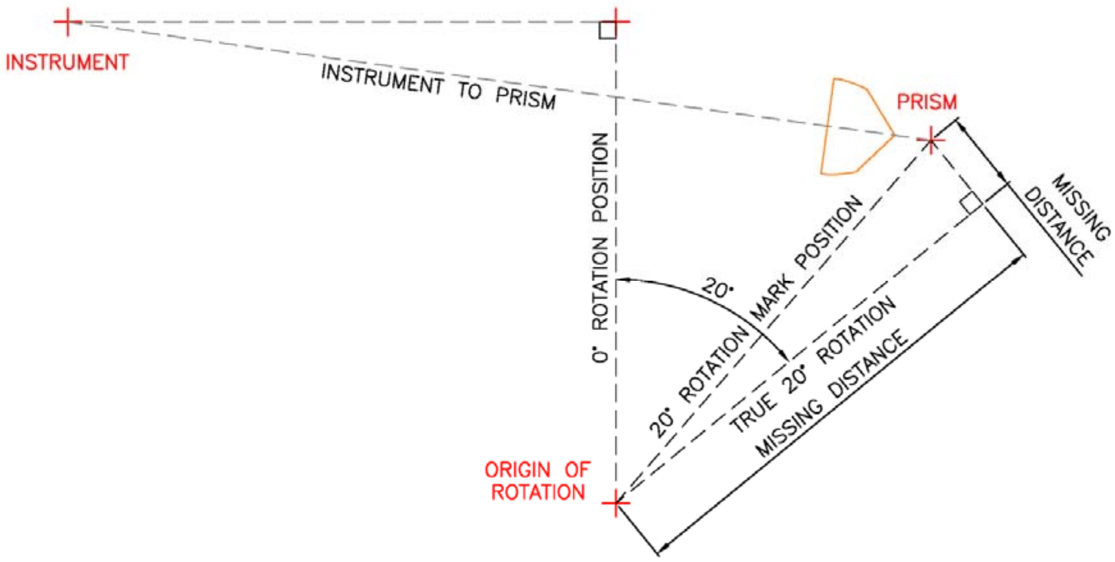

Figure 3.17: Two missing distance calculation.

The two missing distance solution was checked, ensuring that upon entering the two missing distances into the close program, calculated a miss close distance of less than 0.0mm.

This calculation provided the mathematical vertical height distance of the prism in relation to the origin (distance), which was then subtracted by the 0° rotation vertical height distance to calculate the vertical height error. The mathematical horizontal distance error (offset) calculated was a result of the prism tribrach angle rotation accuracy.

Step 6 - Rotation Error

The difference between the two calculated prism adaptor bearings was determined by subtracting the closing bearing from the calculated prism adaptor bearing for each rotation. By comparing the differences across the sets for a single rotation provided a check on the manual entering of the observations. Any calculated difference that grossly differed across the sets was reworked and the measured observations checked against the raw file. If the gross difference was determined to be a reading error as a result of the distance reading accuracy or manual aligning of the marks, then it was taken out of future calculations.

Step 7 - Reading Accuracies

To minimise the instrument reading accuracy and manually alignment of the prism tribrach rotation marks, the average of each desired rotation was calculated along with the standard deviation of a single rotation. The average difference provided a confirmation on the accuracy of the marks placed on the prism tribrach for the desired rotations. The standard deviation of a single rotation, provided the accuracy of the combined manual alignment of the rotation marks on the prism tribrach and the instrument reading accuracy for each measurement.

Step 8 - Adjusted Rotation Angle

Noting that the average standard deviation was around 20′ and that the maximum average difference was about 30′, the rotation angle for the rotation markings were adjusted to the nearest 30′. This reduced the rotation angle accuracy effects on the offset distance error calculation, as this was previously calculated to be affected by about 1mm for an incorrect rotation angle of 30′.

Step 9 - Rotation Angle Confirmation

To confirm the adjusted rotation angles between the rotation markings and their affects on the horizontal distance error, the vertical height and horizontal distance errors were recalculated. This required the 90° prism adaptor bearings to be recalculated using the adjusted rotation angles, which was then used to rerun the two missing distance calculations. The new solutions were then compared to the original two missing distance calculations, to confirm a reduction in the average horizontal distance error.

The vertical pretesting revealed that the method adopted for marking up the prism tribrach for the desired rotations had an accuracy of approximately 20′. Tho the tribrach angle rotations were readjusted for the vertical testing, this information was relevant for the horizontal testing, which can be considered to have the same accurate as that measured during the vertical pretesting.

The standard deviation for a single aligning of the rotation marks was calculated to have an accuracy of approximately 15′. This is under the calculated rotational accuracy allowance from section 3.3.2.4 that if exceed, would impact on the error measurements gathered. Therefore the method designed to perform vertical testing horizontally, would provide accurate error measurements caused by reading to a 360 degree prism using ATR.

3.6 Testing Procedures

The horizontal and vertical testing was able to be completed once the pretesting had proved viability. The procedure for the horizontal and vertical testing has been outlined below.

3.6.1 Horizontal Testing

The horizontal testing procedure was the same as the horizontal pretesting method mentioned in the preliminary testing section above. The only difference was that the 360 degree prism accompanying the instrument undergoing testing was used and the prism was only aligned once to have the most accurate reading point facing the instrument for the initial reading of the set. This process was continued until the prism tribrach had completed a full rotation abiding by the same checks as in the horizontal pretesting.

The horizontal testing procedure was repeated for each instrument with it accompanying 360 degree prism and over each of the selected testing distances.

3.6.2 Vertical Testing

The procedure for testing the 360 degree prism was the same process as measuring the prism tribrach rotations in section 3.5.2, the only difference was that instead of the standard round prism being fixed to the 90° prism adaptor, the 360 degree prism accompanying the testing instrument was used. The 360 degree prism was fixed to ensure the most accurate reading point was aligned to the instrument during the 0° rotation setting and then left alone for the other rotations. Previously the round prism was continuously aligned to face the instrument for each rotation.

Performing the same reading checks used in the vertical pretesting, six sets of usable observation data was recorded for each instrument using their accompanying 360 degree prism.

3.7 Testing Reductions and Analysis

The reductions process to extract the desired error measurements from the numerous observations has been discussed below.

3.7.1 Horizontal Testing Reductions

The same reduction process used in the horizontal pretesting reductions was repeated for the 360 degree prisms, although instead of using the 360 degrees overall mean to convert the data into distance and offset format (step 2), the initial reading for each set for that instrument was used. The average reading calculation (step 5) reducing the instrument reading inaccuracies was also amended, this was calculated by averaging the corrected 360 degree distance and offset errors for each individual rotation across the sets. This provided an average horizontal distance and offset error for the 360 degree prism for each rotation.

Samples of these calculations to obtain the measured errors have been provided in appendix D.

3.7.2 Horizontal Testing Analysis

The 360 degree prism reductions were graphed in Microsoft Excel. This provided an overview analysis of the error pattern with respect to the prism rotation and allowed easy interpretation of the magnitude of the errors measured.

A smooth line was plotted to clearly display the average error for the rotations. This provided a clear picture of the error pattern with respect to the rotation. The offset error pattern closely resembled that of a sine curve as noted in previous research. A formula to predict the error with respect to rotation was created. It was found that Microsoft Excel was not able to calculate a sine regression formula from a sample of data; this therefore had to be calculated manually.

The sine formula was calculated by amending the standard sine or cosine formula with the predetermined information about the error pattern. The predetermined information used was the number of cycles in 360 degree and the error at 0° rotation (Y intersection). From this information, a lease squares adjustment was performed using the 'averaged' offset errors to calculate the magnitude of the sine or cosine formula. This formula was then plotted on the graph and the residuals from the testing data used to calculate the standard deviation for a single observation to confirm the accuracy of the prediction formula.

3.7.3 Vertical Testing Reductions

Note that samples of the vertical 360 degree prism reduction calculations are provided in appendix E.

The 360 degree prism reduction process was similar to that of the vertical pretesting reductions.

Step 1 - Data Conversion

The data was downloaded and the bearing and distance of the usable observations were manually entered into a Microsoft Excel spreadsheet from a printout of the raw data file.

Step 2 - Average Origin

The average bearing and distance from the instrument to the origin was calculated.

Step 3 - Prism Adaptor Bearing

The bearing alignment for the 90° prism adaptor was calculated for each rotation mark, using the bearing observed at the initial 0° rotation for the set and the amended prism tribrach rotation calculated earlier on.

Step 4 - Distance and Offset

Using a close program, the two missing distance calculations for all observations at each rotation was calculated, the solution was rechecked by closing the solution values. The distance, offset and miss close from the solutions were then entered into the spreadsheet.

Step 5 - Vertical Height & Horizontal Distance Errors

This calculation provided the mathematical vertical height distance of the prism in relation to the origin (distance), which when subtracted by the initial 0° rotation vertical height distance, calculated the vertical height error. The mathematical horizontal distance error (offset) as a result of the prism incident angle was also calculated, see figure 3.18.

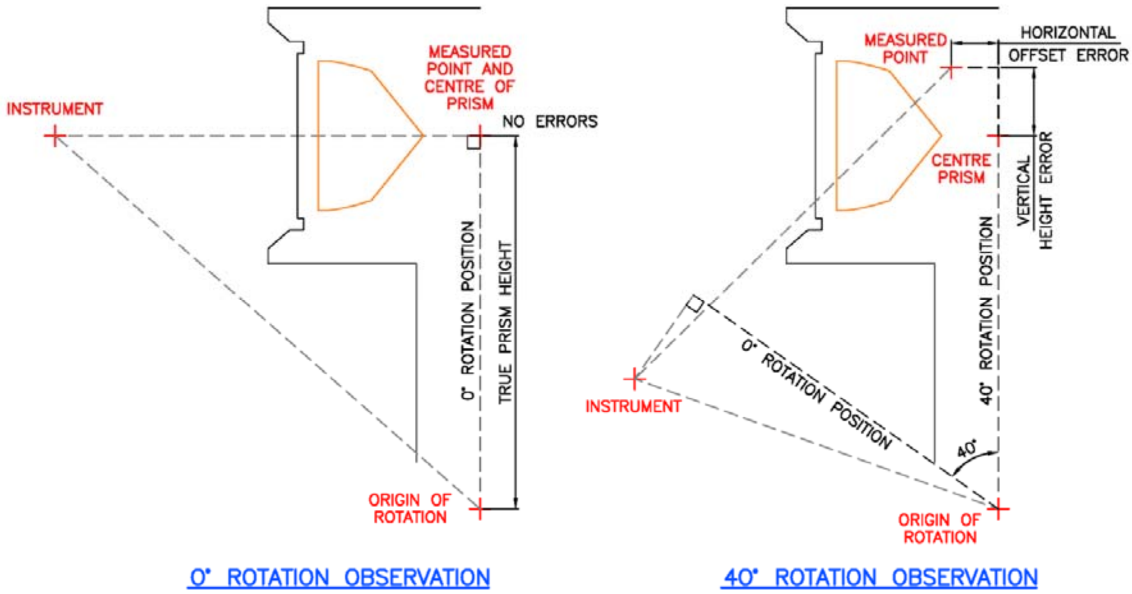

Figure 3.18: Horizontal offset and vertical height errors.

The observed Instrument Reading Angle calculated the 0° rotation observation to each rotation was also calculated to be later applied in determining of the correct prism angle of incidence, refer to figure 3.12 for clarification.

Step 6 - Average Errors

The average deviation, vertical height distance error and horizontal distance error was calculated across the sets for each rotation, along with the residuals from the mean and standard deviation for each observation.

Step 7 - Prism Incident Angle and Vertical Angle

The prism angle of incidence in relation to the 0° rotation observation was calculated. This involved subtracting the average angle of deviation from the amended prism tribrach rotation for each rotation. This was then used to calculate the mathematical vertical angle that would observe the 360 degree prism with that angle of incidence and therefore observe the same vertical height and horizontal distance error. The vertical angle was calculated by subtracting 90° from the prism angle of incidence.

3.7.4 Vertical Testing Analysis

The vertical height and horizontal distance errors were graphed using Microsoft Excel. The errors were graphed in relation to the calculated vertical angle.

From these graphs the error pattern in relation to the calculated vertical angle was able to be identified. Linear regression in Microsoft Excel was used to obtain a formula to predict the errors depending on the vertical angle observed. This linear regression that Microsoft Excel calculates plotted fine on the graph, but the formula it provided was too coarse and when applied against the observed errors, the residuals were too large. A least squares adjustment of the observed error data was performed to calculate a more precise linear regression formula. This formula was used to compare the predicted values against the observed errors with the residuals noted for accuracy.

3.8 Conclusion

This chapter outlined the design considerations, preliminary testing, testing procedures and the reduction process that was used to measure and extract the errors that occur when reading to a 360 degree prism using ATR. The following chapter displays the results obtained, explaining possible causes of outlining measurements and derived formulas that could be used to eliminate these measuring errors, improving accuracy.

Chapter 4 – Results

4.1 Introduction

This chapter has been broken up into two sections, results and discussion. The results section covers the measured results from the horizontal and vertical testing, detailing the error pattern for each measurement component in relation to prism rotation or vertical angle observed to the prism.

The discussion section outlines the overall inaccuracies ranges for the horizontal and vertical testing that would be expected when using this method of survey without reducing any effects. Correction formulae to reduce the vertical testing errors, detailing the formulae accuracy in relation to the measured results have also been provided. These results have been discussed along with any apparent gross error measurements.

4.2 Horizontal Testing Results

The horizontal testing investigated the error measurements caused by the multi prism design. The results have been broken up into the individual measuring components that have been affected by the design, distance and horizontal angle. The horizontal distance and angle errors measured over the three testing distances have been graphed with respect to prism rotation from the most accurate reading point. As the prisms have many accurate reading points, many cycles of error were recorded. These cycles of error data have been averaged to reduce the effects of the instruments reading accuracy, providing the error over a single cycle, allowing a more thorough analysis from the graph.

4.2.1 Horizontal Distance Errors

The horizontal distance error results from the horizontal testing for the three instruments selected for testing are displayed below in figures 4.1(a), 4.1(b) and 4.1(c).

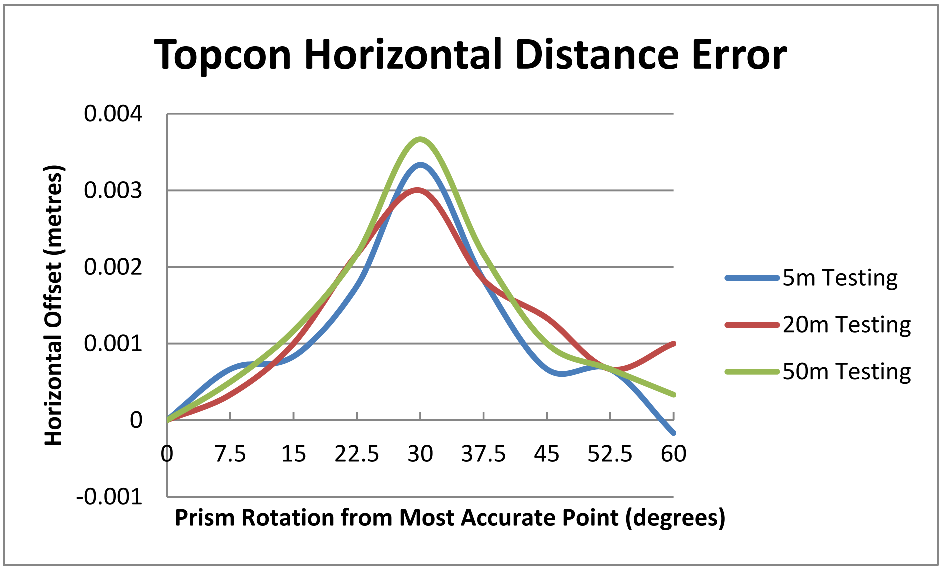

Figure 4.1(a): Topcon A3 prism – horizontal distance results.

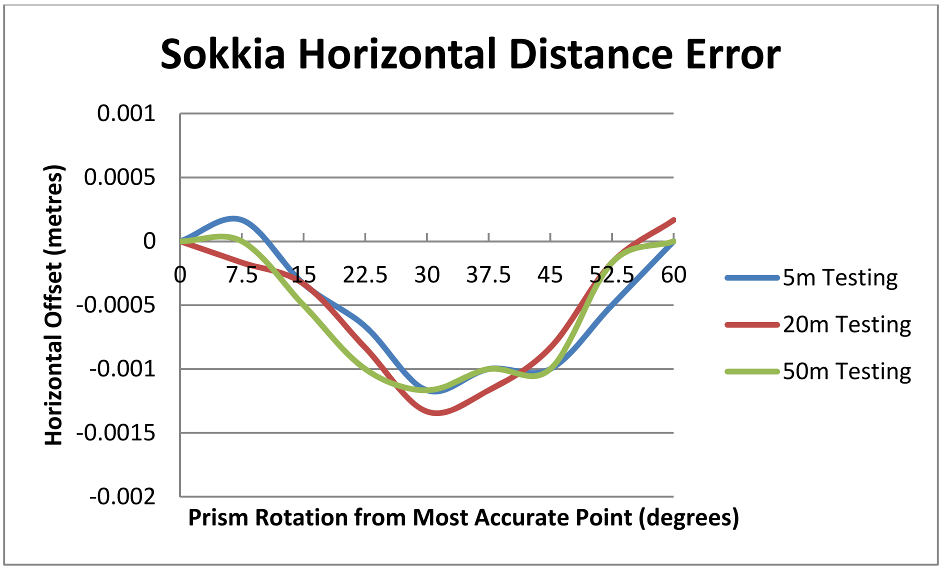

Figure 4.1(b): Sokkia ATP1 prism – horizontal distance results.

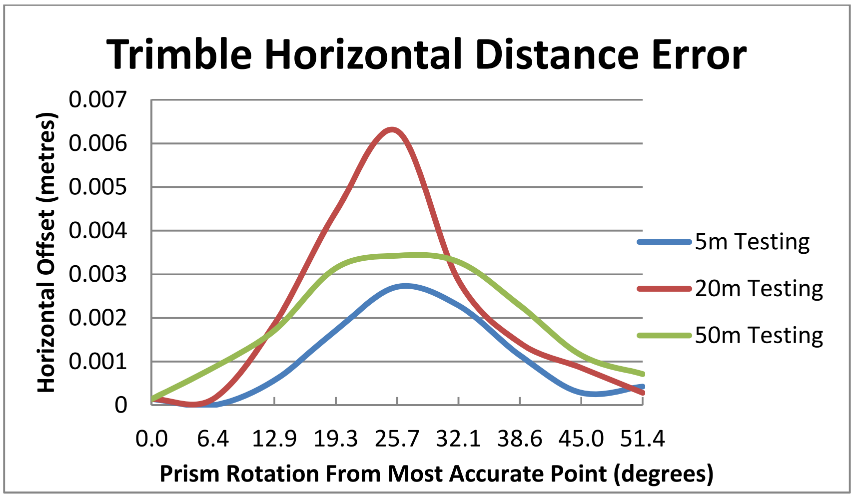

Figure 4.1(c): Trimble robotic target kit prism – horizontal distance results.

4.2.2 Horizontal Angle Errors

Figures 4.2(a), 4.2(b) and 4.2(c) display the horizontal angle offset error results for the instruments and prisms selected for testing over the three testing distances.

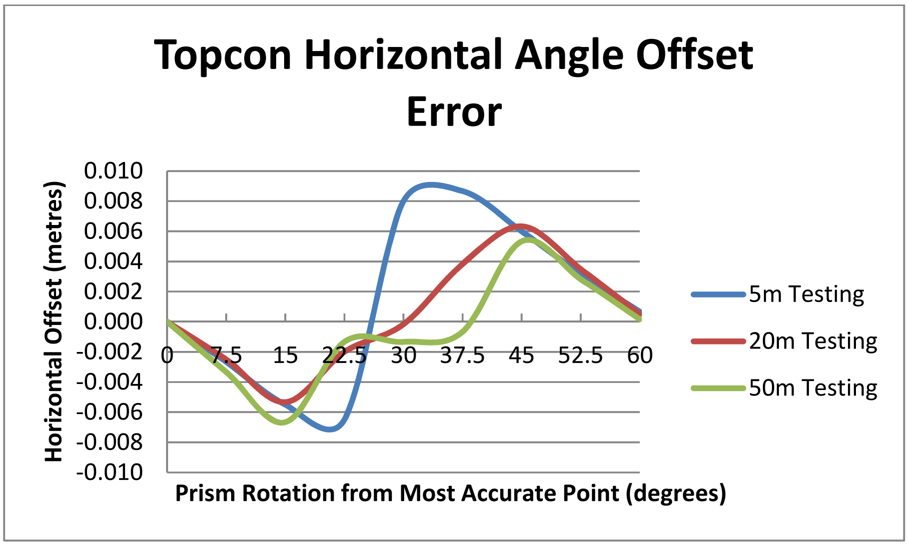

Figure 4.2(a): Topcon A3 prism – horizontal angle results.

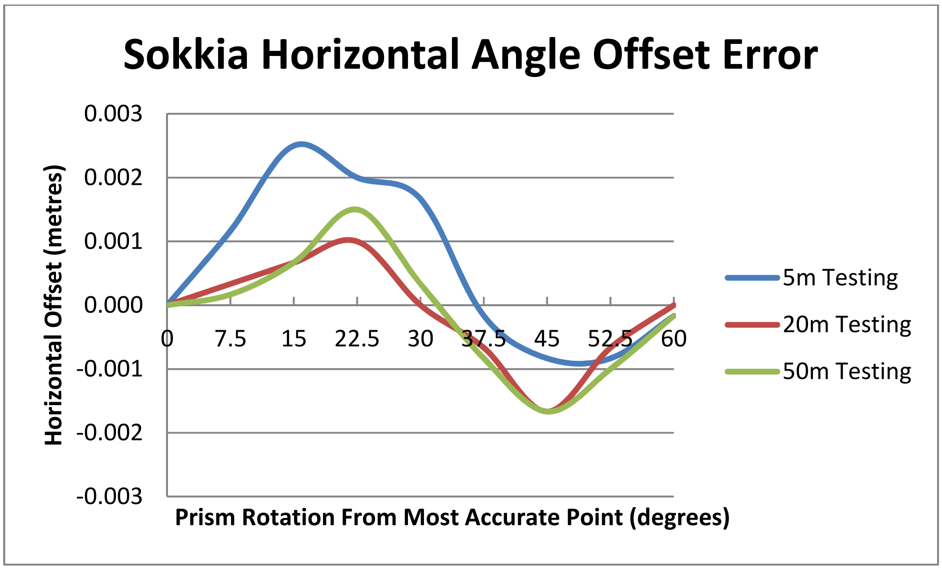

Figure 4.2(b): Sokkia ATP1 prism – horizontal angle results.

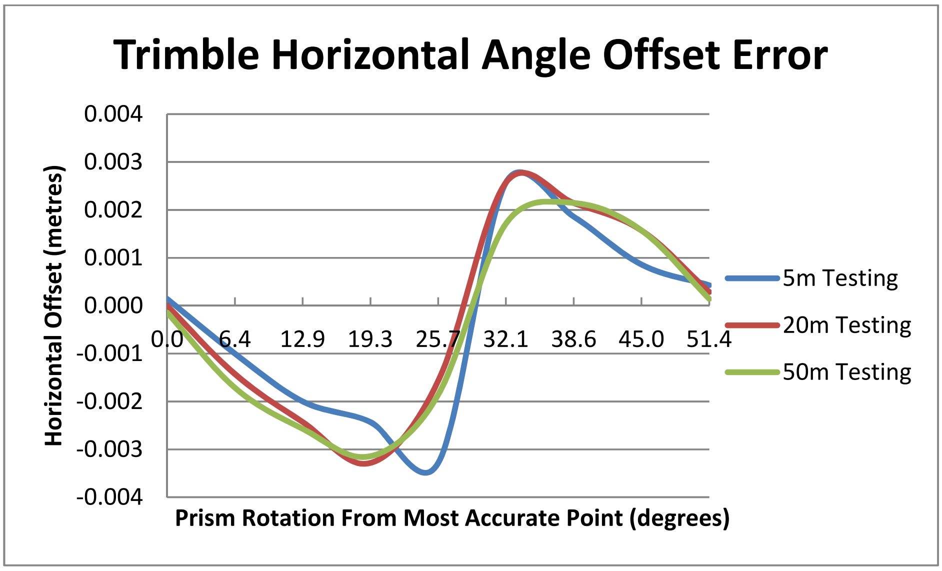

Figure 4.2(c): Trimble robotic target kit prism – horizontal angle results.

4.3 Vertical Testing Results

The vertical testing investigated the measurement inaccuracies caused by the inability to tilt the 360 degree prism vertically to be aligned with the instrument for measurement. The errors measured have been separated up into the individually affected measurement components being horizontal distance and vertical height. These individual component errors have been graphed in relation to the calculated vertical angle observation that experiences the same prism incident angle as that calculated for the measure error.

4.3.1 Horizontal Distance Error

The following figures 4.3(a), 4.3(b) and 4.3(c) display the horizontal distance errors measured for the three tested instruments over the 20m testing distance.

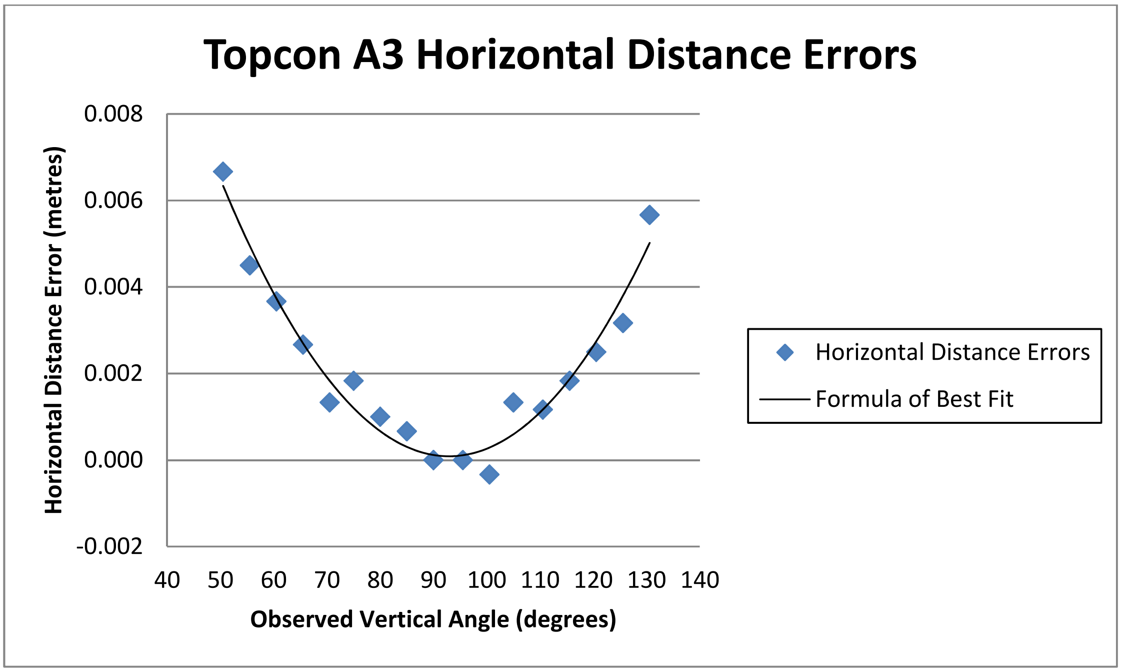

Figure 4.3(a): Topcon A3 prism – vertical distance results.

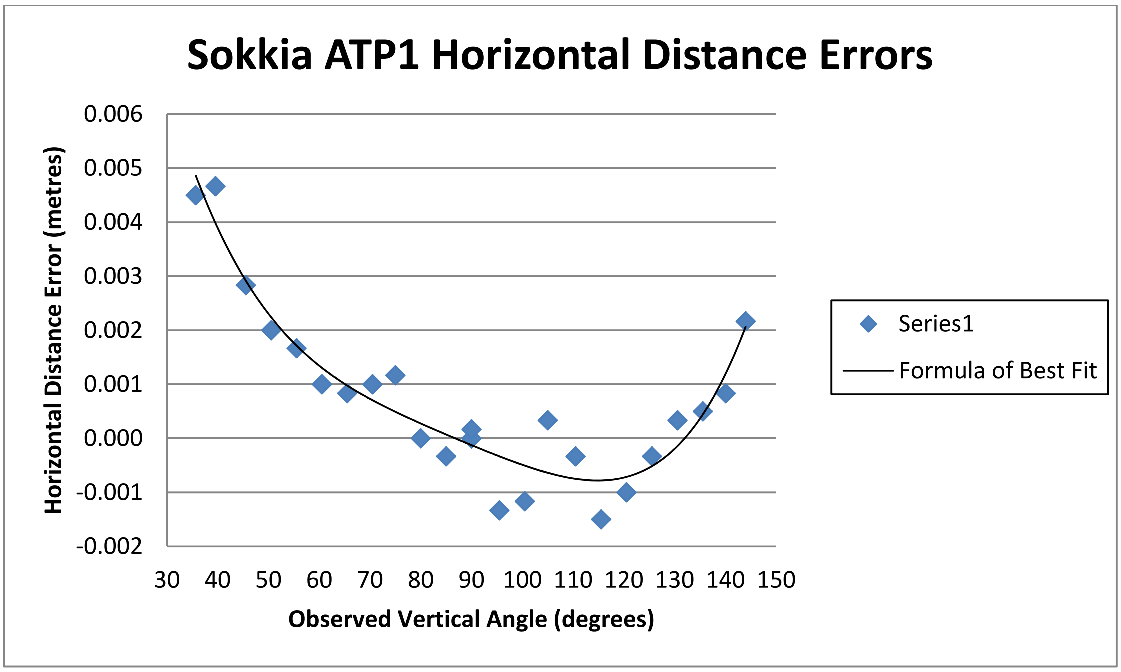

Figure 4.3(b): Sokkia ATP1 prism – vertical distance results.

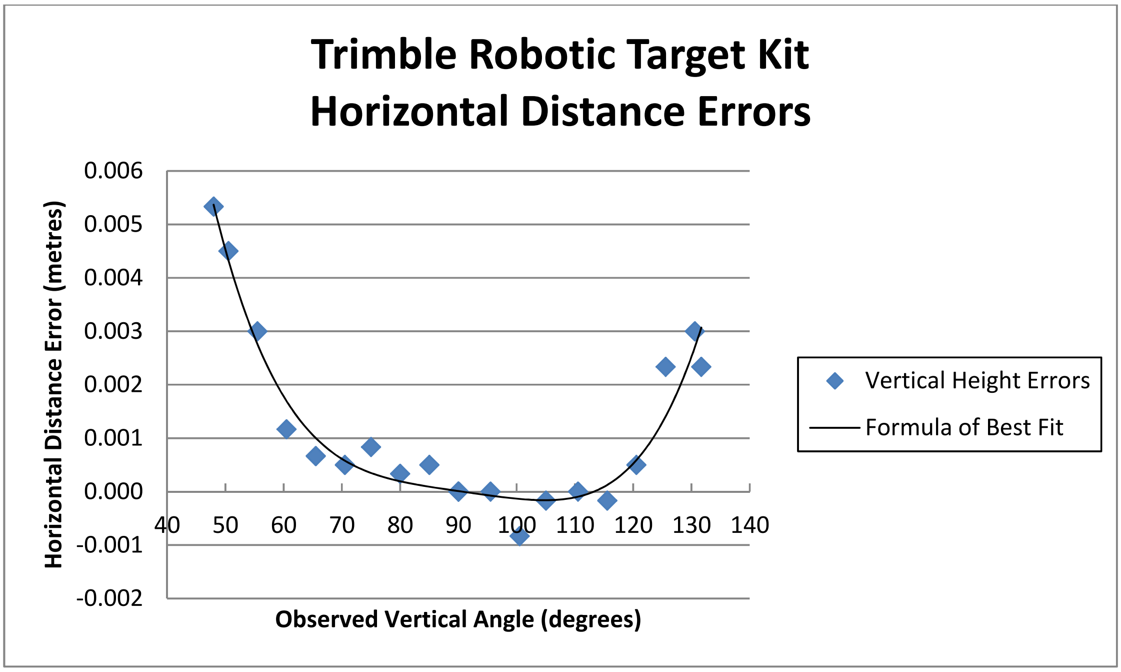

Figure 4.3(c): Trimble robotic target kit prism – vertical distance results.

4.3.2 Vertical Height Errors

The vertical height errors measured over the 20m testing distance for all three instruments with their accompanying 360 degree prism are displayed in figures 4.4(a), 4.4(b) and 4.4(c) below.

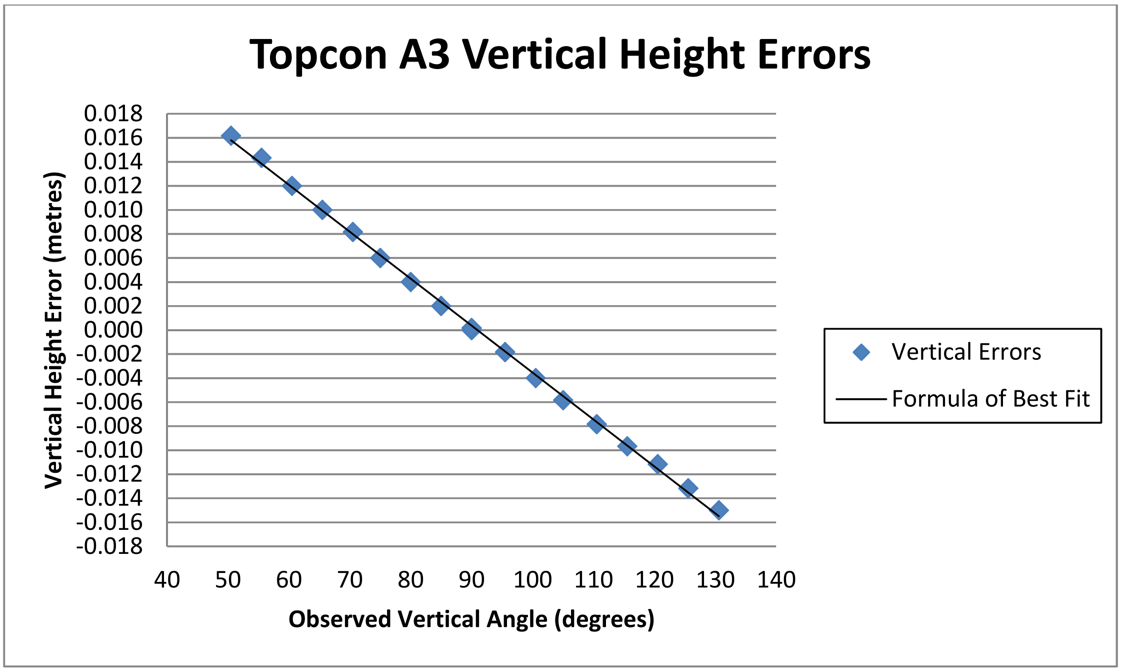

Figure 4.4(a): Topcon A3 prism – vertical height results.

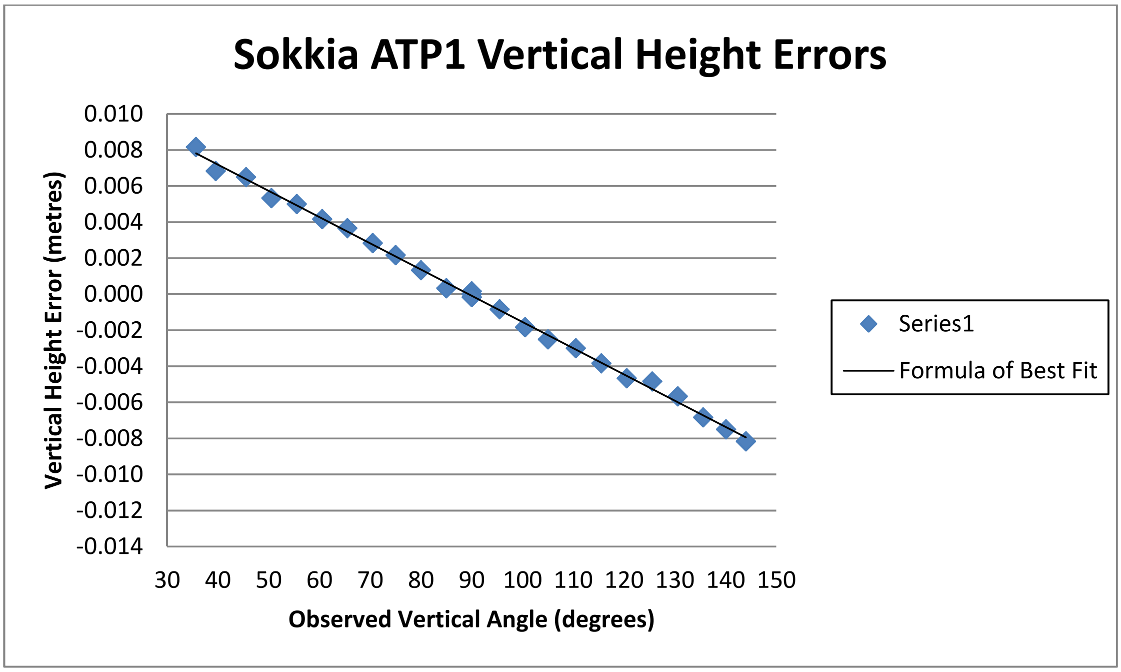

Figure 4.4(b): Sokkia ATP1 prism – vertical height results.

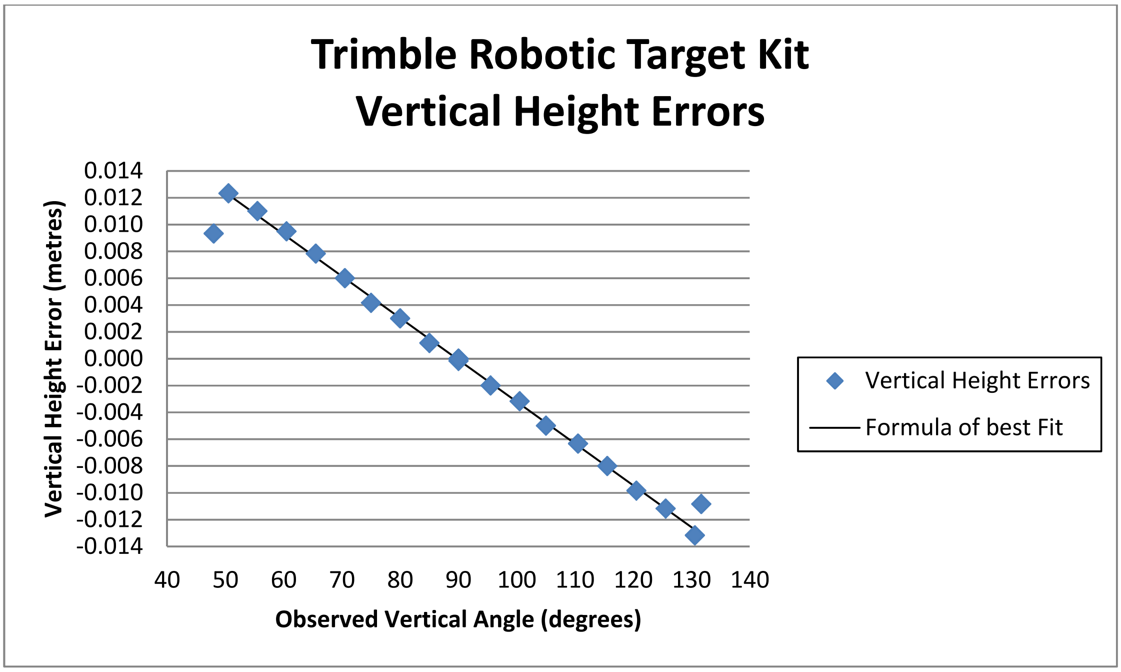

Figure 4.4(c): Trimble robotic target kit prism – vertical height results.

4.4 Discussion

This section discusses the results for the horizontal and vertical testing. It outlines the range of errors measured during the horizontal testing processes. The calculated expected accuracy for this method of survey without taking precautions to reduce any measuring errors is highlighted. Furthermore a discussion identifying any apparent gross errors measured and their possible affects which may have interfered with the measurement is examined. Calculating correction formulae that could be used to eliminate any vertical alignment effects as measured in the vertical testing.

4.4.1 Horizontal Testing Discussion

From the horizontal testing results the error range for each instrument and prism was determined, see table 4.1.

Table 4.1: Horizontal testing error range results.

Instrument	Testing Distance	Maximum		Minimum	
		Offset Error (mm)	Distance Error (mm)	Offset Error (mm)	Distance Error (mm)
Topcon	5m	9	3	-7	0
Topcon	20m	6	3	-5	0
Topcon	50m	5	4	-7	0
Sokkia	5m	2	0	-1	-1
Sokkia	20m	1	0	-2	-1
Sokkia	50m	1	0	-2	-1
Trimble	5m	3	3	-3	0
Trimble	20m	3	6	-3	0
Trimble	50m	2	3	-3	0

Table 4.1 displays that the error ranges were not affected by the distance of measurement, the variations of errors can be explained by the instruments measuring ability. The errors appear to be more of a constant reading error as a result of the 360 degree prism design.

From figures 4.2(a), 4.2(b) and 4.2(c) it can be noted that the horizontal angle offset errors were greatest for the 5m readings, this is when the light intensity on the ATR sensor would have been at its brightest throughout the testing. The Trimble was least affected by this, probably a result of having a significantly smaller minimum ATR range (0.2m) than the other two instruments tested.

The Topcon instrument was tested under its quoted minimum ATR range of 10m. Although the field of view range calculated that the prism would have been wholly contained within the ATR beam, figure 4.2(a) displays that the instrument has locked onto a single prism which provided gross errors.

Figure 4.1(c) provides interesting results for the Trimble 20m horizontal distance testing, the measured errors differs from the other two testing distances by 3mm. This could be the result of the measuring accuracy of the Trimble instrument as all readings indicate the same measurement.

From table 4.1 the following horizontal reading errors for the three tested instruments with their 360 degree prisms can be expected when measuring to the 360 degree prism using ATR:

Topcon GPT-8205A reading to the A3 prism

Horizontal angle error range: ±7mm

Horizontal distance error range: 0mm to +4mm

Sokkia SRX5 reading to the ATP1 prism

Horizontal angle error range: ±2mm

Horizontal distance error range: 0mm to -1mm

Trimble S6 DR300+ reading to the robotic target kit prism

Horizontal angle error range: ±3mm

Horizontal distance error range: 0mm to +6mm

Note that Topcon's 5m reading results should not be considered as they were measured outside the quoted ATR reading range specifications for that instrument.

Overall the Sokkia's advanced full array prism design provided greater measurement accuracy. The horizontal testing errors for the Sokkia ATP1 prism actually measured under the quoted instrument measurement specifications, whereas the multi prism design adopted by Topcon and Trimble appeared to cause significant measuring errors.

The Trimble prism design adopted smaller prisms than Topcons and added an additional prism; this appears to have helped reduce the reading errors. This could be a result of an increase of reflected signal onto the ATR sensor's surface, allowing a more precise centre average of the prism to be determined reducing the chance of a single prism fix.

4.4.2 Vertical Testing Discussion

The vertical testing results have identified that the errors caused by the inability to vertical align the prism with the instrument follow a very distinctive pattern. This means that the error is not irregular and could be eliminated by the addition of formulae in the measurement reduction process.

Figures 4.3(a), 4.3(b) and 4.3(c) all display a constant change of the horizontal distance error, with respect to a change in the vertical angle. This error can also be predicted and corrected by a polynomial equation using the vertical angle as a variable.

Figures 4.4(a), 4.4(b) and 4.4(c) clearly show that the vertical height error gradually increases with respect to an increase in the vertical angle. This error can easily be predicted and corrected by a linear equation using the vertical angle as a variable.

The correction formulae for the three instruments using the tested 360 degree prism were calculated to counter the horizontal distance and vertical height errors. The correction formulae are as follows:

4.4.2.1 Horizontal Distance Correction Formulae

Topcon GPT-8205A using A3 prism

$$y = -3.68 \times 10^{-6}x^2 + 6.8643 \times 10^{-4}x - 3.19713 \times 10^{-2} \qquad (4.1)$$

Where:
$y =$ The correction to the horizontal distance
$x =$ The vertical angle observed for the measurement

This formula was calculated to have an accuracy of $\pm 0.4mm$ when compared to the average measured errors from field testing.

Sokkia SRX5 using ATP1 prism

$$y = -3.695146 \times 10^{-10}x^4 + 31.283718 \times 10^{-7} \times x^3 - 1.684227 \times 10^{-5} \times x^2 + 1.028460 \times 10^{-3} \times x - 2.535998 \times 10^{-2} \qquad (4.2)$$

Where:
$y =$ The correction to the horizontal distance
$x =$ The vertical angle observed for the measurement

This formula was calculated to have an accuracy of ± 0.4mm when compared to the average measured errors from field testing.

Trimble S6 DR300+ using robotic target kit prism

$$y = -1.309291 \times 10^{-9}x^4 + 4.769947 \times 10^{-7}x^3 - 6.535321 \times 10^{-5}x^2 + 3.988665 \times 10^{-3}x - 9.225939 \times 10^{-2} \quad (4.3)$$

Where:
$y =$ The correction to the horizontal distance
$x =$ The vertical angle observed for the measurement

This formula was calculated to have an accuracy of $\pm 0.4mm$ when compared to the average measured errors from field testing.

4.4.2.1 Vertical Height Correction Formulae

Topcon GPT-8205A using A3 prism

$$y = 3.91 \times 10^{-4}x - 3.553 \times 10^{-2} \quad (4.4)$$

Where:
$y =$ The correction to the vertical height
$x =$ The vertical angle observed for the measurement

This formula was calculated to have an accuracy of $\pm 0.3mm$ when compared to the average measured errors from field testing.

Sokkia SRX5 using ATP1 prism

$$y = 1.49 \times 10^{-4}x - 1.3195 \times 10^{-2} \tag{4.5}$$

Where:
$y =$ The correction to the vertical height
$x =$ The vertical angle observed for the measurement

This formula was calculated to have an accuracy of $\pm 0.2mm$ when compared to the average measured errors from field testing.

Trimble S6 DR300+ using robotic target kit prism

$$y = 3.12 \times 10^{-4}x - 2.7993 \times 10^{-2} \tag{4.6}$$

Where:
$y =$ The correction to the vertical height
$x =$ The vertical angle observed for the measurement

This formula was calculated to have an accuracy of $\pm 0.2mm$ when compared to the average measured errors from field testing. Note this formula does not account for the maximum and minimum reading errors, as they disagree with the rest of the results indicating that something may have interfered with the readings.

The maximum and minimum readings for the Trimble, displayed in figure 4.4(c) disagree with the rest of the error measurements. The readings and calculations were recalculated and checked but no calculation or manual errors could be found. It is expected that there was some reflective interference which has impacted on the CMOS sensor reading.

Vertical Comparisons

Figure 4.5 displays the range of errors for each instrument and prism tested during the vertical testing.

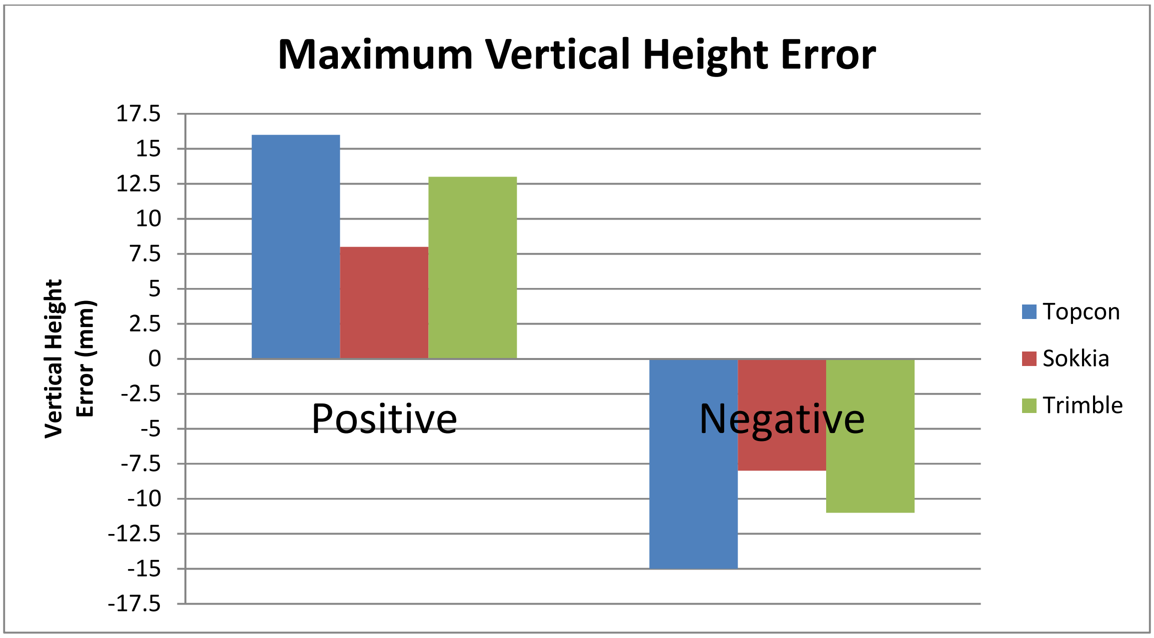

Figure 4.5: Vertical testing instrument comparisons.

Figure 4.5 displays the comparison results between instruments for the vertical testing. The Sokkia ATP1 tilted prism design appears to have reduced the effects caused by vertical alignment to the instrument by reducing the prism incident angle. This was made possible by using tilted prisms that provide an accurate reading when both prisms are averaged, but when viewed vertically, the instrument locks onto only a single prism as the other is obscured from view. The prism reflecting the signal has been designed to tilt towards the instrument, also reducing the horizontal distance errors. The advanced tilting prism design also providing a greater vertical reading range to the prism as measured in the vertical testing.

4.5 Conclusion

In conclusion the reading errors caused by using ATR when sighting to a 360 degree prism should be considered when selecting the method of survey for performing high precision work. These errors will impact more significantly on machine guidance, as this is where large vertical angles are normally observed as a result of the prism being positioned above the graders cabin to limit interference caused by passing motorists and cabin obstruction. With the addition of formulae to the observation reduction process, the horizontal distance and vertical height errors caused by the inability to vertical align the prism can be eliminated.

Chapter 5 – Conclusions

5.1 Findings

The impacts to the measurements derived from measuring to a 360 degree prism using ATR technology for alignment was found to be significantly affected by the vertical angle of the observation. This was concluded to be a result of the prism's construction through the restriction of the vertical alignment of the prism to the instrument. The horizontal alignment deviations, as a result of the multi prism design no longer requiring the prism to be aligned to the instrument, was found to have been accounted for with the designs of the later 360 degree prisms (Sokkia ATP1 and Trimble robotic target kit prism). The significant vertical angle measurement errors that were identified were able to be corrected by applying derived formulae which are a function of the vertical angle being observed.

5.2 Testing Limitations

The maximum horizontal deviations measured through prism rotation may not be the maximum deviations for that prism. The testing was conducted under the premise that the error pattern in relation to the prism rotation would closely match that of a sine curve. However, the error pattern was similar to that of a sine curve in the form of a wave but it was not evenly flowing. This may have been a result of the accuracy of the rotations for the horizontal testing. The marking procedure measured had an accuracy of approximately 20′ with a standard deviation of a single rotation of 15′. The accuracy of this calculation is limited by the reading accuracy of the instrument, with which it was measured.

This rotation inaccuracy also impacts on the accuracy of the horizontal distance error calculation. The calculated horizontal distance error can therefore only be as accurate as ±1mm, even though all the calculated errors agreed to within ±0.5mm.

The maximum and minimum vertical angle testing was very difficult when using the Topcon instrument. The controller software was updated to work for another instrument which affected the communication for the Topcon instrument. This communication change prevented the instrument from being able to be set for tracking mode, which would continually determine the centre of the prism along with continuous distance readings. This resulted in a trial and error method being adopted to determine the maximum vertical angle range for the prism, which meant that only a single reading could be observed. This method also provided results that significantly varied between each set. If software that communicated effectively with the instruments was used, different results may have been obtained.

5.3 Further Research

Further research could be carried out to improve the understanding of these errors by refining the testing procedures to incorporate finer rotations and improving the rotational accuracies. Deriving another method to calculate the vertical reading limits of the prism and more accurately calculating the maximum and minimum errors could be further investigated also. Additionally, the selection of different instruments and prism types for testing would also help identify any reduction of these errors through new technology or prism developments. The first two of these topics are discussed further below.

Smaller rotations of the prism during the horizontal testing would have provided a more thorough analysis of the error to prism rotation. This may provide a different maximum and minimum result for the horizontal alignment deviations, which may suggest a different conclusion to the accuracy of horizontal angles read to the prism. This testing along with the vertical testing would be beneficial by finding a more accurate way of measuring the rotation angles of the prism tribrach, and not being restricted by the reading accuracy of the instrument.

The vertical testing should be performed vertically not horizontally. Another method for vertical testing could be performed by focussing on the maximum and minimum ranges, now that the error pattern has been determined. The accuracy of the vertical angles for the vertical testing was limited as a result of the testing procedure used. This method provided an accurate reading for predicting the vertical height error and horizontal distance errors, only because their effects increased slightly with respect to angle. This method was also used to determine the maximum and minimum vertical angle ranges for the 360 degree prisms which could have been more precise, instead of determining an indication of the likely vertical ranges. The maximum and minimum vertical angle ranges for the prisms may have increased by rotating the prism around the prism's axis.

5.4 Conclusion

In conclusion, knowing the magnitude of the effects of reading to a 360 degree prism using ATR allows a better understanding of the likely accuracies that can be achieved using this method of survey. This knowledge also allows the operator to consider this as a method of survey for set out, whereas before the operator may not have contemplated using it, as the accuracies attained were uncertain. By identifying these effects and their likely impacts on the accuracy of readings, new technology being developed can now consider these results and reduce them through prism designs or the observation reduction process.

References

Active pixel sensor 2011, information document, Wikipedia, viewed 26 April 2011, <http://en.wikipedia.org/wiki/Active_pixel_sensor>.

Anderson, JM & Mikhail, EM 1998, *Surveying: theory and practice,* 7th edn, McGraw-Hill, United States of America.

Artman, D, Brinton, D, Brown, L & Singh, R 2002, *Compensators, stability check, and automatic target recognition,* Oregon Department of Transport, Oregon, viewed 20 April 2011, < http://www.oregon.gov/ODOT/HWY/GEOMETRONICS/docs/Compensators-Stability_Check-ATRhandout.pdf?ga=t>.

CCD vs. CMOS 2011, Teledyne DALSA, California, United States of America, viewed 21 April 2011, <http://www.dalsa.com/corp/markets/ccd_vs_cmos.aspx>.

Characteristics and use of FFT-CCD area image sensor 2003, technical information report, Hamamatsu Photonics, Japan, viewed 21 April 2011, <http://sales.hamamatsu.com/assets/applications/SSD/fft_ccd_kmpd9002e06.pdf>.

Charged-coupled device 2011, information document, Wikipedia, viewed 21 April 2011, <http://en.wikipedia.org/wiki/Charge-coupled_device>.

Dichroic prism 2011, information document, Wikipedia, viewed 21 April 2011, <http://en.wikipedia.org/wiki/Dichroic_prism>.

Dubois, J, Ginhac, D, Heyrman, B & Paindavoine, M 2008, *A 10 000 fps CMOS sensor with massively parallel image processing,* vol 43, no 3, IEEE Journal of Solid-State Circuits, France, viewed 21 April 2011, <http://hal.archives-ouvertes.fr/docs/00/48/27/51/PDF/jssc_march08.pdf>.

Gaussian beam 2011, information document, Wikipedia, viewed 26 April 2011, <http://en.wikipedia.org/wiki/Gaussian_beam>.

Ghilani, CD & Wolf, PR 2002, *Elementary surveying: an introduction to geomatics*, 10th edn, Prentice Hall, New Jersey, United States of America.

Graeve, T & Weckler, GP 2001, 'High-resolution CMOS imaging detector', *Medical Imaging 2001 – Physics of Medical Imaging,* vol 4320, viewed 21 April 2011, <http://www.dalsa.com/public/ls/appnotes/Radicon_AN05.pdf>.

Kirschner, H & Stempfhuber, W 2008, *The kinematic potential of modern tracking total stations – a state of the art report on the Leica TPS1200+,* International Conference on Machine Control and Guidance, Zurich, Switzerland, viewed 19 March 2011, <http://www.mcg.ethz.ch/papres/Kirschner_Stempfhuber_05.pdf>.

Leica FAQ – prism offsets 2002, question and answer document, Heerbrugg, Switzerland, viewed 26 March 2011, <http://www.triginstruments.co.nz/brochures/prism.pdf>.

Lemmon, T & Mollerstrom, L 2007, *Trimble S6 Multitrack: white paper,* Trimble Navigation Limited, United States of America.

Litwiller, D 2001, *CCD vs. CMOS: facts and fiction,* Laurin Publishing Co. Inc., Canada, viewed 21 April 2011, < http://www.dalsa.com/public/corp/photonics_spectra_ccdvscmos_litwiller.pdf>.

Mao, J & Nindl, D 2009, *Surveying reflectors – white paper: characteristics and influences,* Heerbrugg, Switzerland, viewed 19 January 2011, < http://www.leica-geosystems.com/downloads123/zz/accessory/accessories/white-tech-paper/White%20Paper%20Surveying%20Reflectors_en.pdf>.

Palmetto 2007, *SRX product introduction,* online video, authorSTREAM, viewed 20 April 2011, <http://www.authorstream.com/Presentation/palmettoequipment-473629-srx-product-introduction/>.

Peterson, C 2001, ‘How it works: the charged –coupled device, or CCD’, *Journal of Young Investigators*, vol 3, no 1, viewed 20 April 2011, <http://www.jyi.org/volumes/volume3/issue1/features/peterson.html>.

Position Partners n.d., ‘GPT-8200 auto tracking: principles and adjustments’, staff training PowerPoint file, Position Partners, Brisbane.

Sokkia Corporation 2006, *Operators manual: series SRX,* 4th edn, JSIMA, Japan.

Stempfhuber, W 2009, *Verification of the Trimble universal total station (UTS) performance for kinematic applications,* Swiss federal Institute of technology, Zurich, Switzerland, viewed 19 March 2011, < http://www.geometh.ethz.ch/people/former_staff/stwerner/O3D_Wien2009.pdf>.

SVY2106 Geodetic surveying A: study book 2006, University of Southern Queensland, Toowoomba.

Topcon Corporation 2003, *Instruction manual: auto tracking pulse total station GPT-8200A series,* JSIMA, Japan.

Trimble S series total station user guide 2008, 4th edn, Trimble Navigation Limited, United States of America, viewed 13 March 2011, <http://www.geometius.nl/uploads/handleidingen/Trimble%20S%20Series%20Total%20Station%20User%20guide.pdf>.

Trimble S6 total station: datasheet 2009, Trimble Navigation Limited, United States of America, viewed 19 March 2011, <http://www.pacificsurvey.com/pdf/S6.pdf>.

Appendix A

Project Specification

University of Southern Queensland

FACULTY OF ENGINEERING AND SURVEYING

ENG4111/4112 Research Project
PROJECT SPECIFICATION

FOR:	**MATTHEW MCDONALD** (Student Number 0050023688)
TOPIC:	INVESTIGATION INTO THE LIMITATIONS OF MEASURING TO 360 DEGREE PRISMS USING AUTO POINT TECHNOLOGY.
SUPERVISORS:	Assoc. Prof. Kevin McDougall, University of Southern Queensland. Dave William Fredriksen, Fredriksen Maclean & Associates.
ENROLMENT:	ENG4111 – S1, 2011 (External) ENG4112 – S2, 2011 (External)
PROJECT AIM:	This project seeks to determine the accuracy of the measurements gathered using Automatic Target Recognition (ATR) and measuring to 360 degree prisms. Discussing the prism factors that affect the measurements and recommending the appropriate uses for robotic surveys.
SPONSORSHIP:	Self Sponsored
PROGRAMME:	**Issue B, 18th March 2011**

1. Research background information into the basic principles of how ATR systems work for different total stations including the determination of the centre of the prism, the quoted centring accuracies of ATR, calibration processes and the errors associated with reading to a prism not aligned to face the instrument.

2. Design a procedure to measure and assess the possible horizontal, vertical and distance errors that can be found when reading to a 360 degree prism using ATR.

3. Calibrate and adjust three different brand robotic instruments as per their manuals and field test with their accompanying 360 degree prism.

4. Reduce and analyse each instruments prism offset errors depending on the prism rotation/height in relation to the instrument.

5. Evaluate the vertical offset error, the impact of curvature and refraction and derive a possible equation to calculate the vertical distance error at any vertical angle.

6. Construct a CAD model of each 360 degree prism and determine from the prisms' physical attributes, the possible maximum vertical angle that may be read to the prism, and calculate its approximate vertical distance error.

7. Field test the calculated maximum vertical angle and vertical distance error.

8. Present the measurement accuracy findings and recommendations of the possible applications of robotic surveys using a 360 degree prism.

AGREED:

____________________(Student) ____________________,
____________________(Supervisors)

___ / ___ / ___ ___ / ___ / ___ ___ / ___ / ___

Appendix B

Sample Horizontal Pretesting Reductions

Topcon GPT-8205A

Table B.1: Topcon 5m horizontal pretesting sets 1 & 2 reductions.

Topcon 5m Measurement Data Standard Round Prism				Sighter Target Residuals				Initial Reading Residuals			
Rotation	**East**	**North**	**RL**	**Offset**	**Dist**	**Offset**	**Dist**	**Offset**	**Dist**	**Offset**	**Dist**
1A	1000.001	5005.011	10.057	0.001	5.011	0.000	0.001	0.000	0.000	0.000	0.001
1B	1000.001	5005.010	10.057	0.001	5.010	0.000	0.000	0.000	-0.001	0.000	0.000
1C	1000.001	5005.011	10.057	0.001	5.011	0.000	0.001	0.000	0.000	0.000	0.001
1D	1000.001	5005.011	10.057	0.001	5.011	0.000	0.001	0.000	0.000	0.000	0.001
1E	1000.001	5005.011	10.057	0.001	5.011	0.000	0.001	0.000	0.000	0.000	0.001
1F	1000.001	5005.011	10.057	0.001	5.011	0.000	0.001	0.000	0.000	0.000	0.001
1G	1000.001	5005.010	10.057	0.001	5.010	0.000	0.000	0.000	-0.001	0.000	0.000
1H	1000.001	5005.010	10.057	0.001	5.010	0.000	0.000	0.000	-0.001	0.000	0.000
1I	1000.000	5005.009	10.057	0.000	5.009	-0.001	-0.001	-0.001	-0.002	-0.001	-0.001
			Mean	0.001	5.010		**Mean**	0.000	-0.001		
2A	1000.001	5005.009	10.057	0.001	5.009	0.000	-0.001	0.000	0.000	0.000	-0.001
2B	1000.001	5005.010	10.057	0.001	5.010	0.000	0.000	0.000	0.001	0.000	0.000
2C	1000.001	5005.010	10.057	0.001	5.010	0.000	0.000	0.000	0.001	0.000	0.000
2D	1000.001	5005.009	10.057	0.001	5.009	0.000	-0.001	0.000	0.000	0.000	-0.001
2E	1000.001	5005.010	10.057	0.001	5.010	0.000	0.000	0.000	0.001	0.000	0.000
2F	1000.001	5005.009	10.057	0.001	5.009	0.000	-0.001	0.000	0.000	0.000	-0.001
2G	1000.001	5005.010	10.057	0.001	5.010	0.000	0.000	0.000	0.001	0.000	0.000
2H	1000.001	5005.010	10.057	0.001	5.010	0.000	0.000	0.000	0.001	0.000	0.000
2I	1000.001	5005.009	10.057	0.001	5.009	0.000	-0.001	0.000	0.000	0.000	-0.001
			Mean	0.001	5.010		**Mean**	0.000	0.001		

Table B.2: Topcon 5m horizontal pretesting sets 3 & 4 reductions.

Topcon 5m Measurement Data Standard Round Prism				Sighter Target Residuals				Initial Reading Residuals			
Rotation	**East**	**North**	**RL**	**Offset**	**Dist**	**Offset**	**Dist**	**Offset**	**Dist**	**Offset**	**Dist**
3A	1000.001	5005.010	10.057	0.001	5.010	0.000	0.000	0.000	0.000	0.000	0.001
3B	1000.001	5005.010	10.057	0.001	5.010	0.000	0.000	0.000	0.000	0.000	0.001
3C	1000.001	5005.009	10.057	0.001	5.009	0.000	-0.001	0.000	-0.001	0.000	0.000
3D	1000.001	5005.009	10.057	0.001	5.009	0.000	-0.001	0.000	-0.001	0.000	0.000
3E	1000.001	5005.010	10.057	0.001	5.010	0.000	0.000	0.000	0.000	0.000	0.001
3F	1000.000	5005.009	10.057	0.000	5.009	-0.001	-0.001	-0.001	-0.001	-0.001	0.000
3G	1000.000	5005.009	10.057	0.000	5.009	-0.001	-0.001	-0.001	-0.001	-0.001	0.000
3H	1000.000	5005.010	10.057	0.000	5.010	-0.001	0.000	-0.001	0.000	-0.001	0.001
3I	1000.001	5005.009	10.057	0.001	5.009	0.000	-0.001	0.000	-0.001	0.000	0.000
			Mean	0.001	5.009		**Mean**	0.000	-0.001		
4A	1000.000	5005.010	10.057	0.000	5.010	-0.001	0.000	0.000	0.000	-0.001	0.000
4B	1000.000	5005.009	10.057	0.000	5.009	-0.001	-0.001	0.000	-0.001	-0.001	-0.001
4C	1000.000	5005.010	10.057	0.000	5.010	-0.001	0.000	0.000	0.000	-0.001	0.000
4D	1000.001	5005.010	10.057	0.001	5.010	0.000	0.000	0.001	0.000	0.000	0.000
4E	1000.001	5005.010	10.057	0.001	5.010	0.000	0.000	0.001	0.000	0.000	0.000
4F	1000.001	5005.009	10.057	0.001	5.009	0.000	-0.001	0.001	-0.001	0.000	-0.001
4G	1000.001	5005.010	10.057	0.001	5.010	0.000	0.000	0.001	0.000	0.000	0.000
4H	1000.001	5005.009	10.057	0.001	5.009	0.000	-0.001	0.001	-0.001	0.000	-0.001
4I	1000.001	5005.010	10.057	0.001	5.010	0.000	0.000	0.001	0.000	0.000	0.000
			Mean	0.001	5.010		**Mean**	0.001	0.000		

Table B.3: Topcon 5m horizontal pretesting sets 5 & 6 reductions.

Topcon 5m Measurement Data Standard Round Prism				**Sighter Target Residuals**				**Initial Reading Residuals**			
Rotation	**East**	**North**	**RL**	**Offset**	**Dist**	**Offset**	**Dist**	**Offset**	**Dist**	**Offset**	**Dist**
5A	1000.001	5005.010	10.057	0.001	5.010	0.000	0.000	0.000	0.000	0.000	0.000
5B	1000.001	5005.010	10.057	0.001	5.010	0.000	0.000	0.000	0.000	0.000	0.000
5C	1000.001	5005.010	10.057	0.001	5.010	0.000	0.000	0.000	0.000	0.000	0.000
5D	1000.001	5005.009	10.057	0.001	5.009	0.000	-0.001	0.000	-0.001	0.000	-0.001
5E	1000.001	5005.010	10.057	0.001	5.010	0.000	0.000	0.000	0.000	0.000	0.000
5F	1000.001	5005.011	10.057	0.001	5.011	0.000	0.001	0.000	0.001	0.000	0.001
5G	1000.001	5005.010	10.057	0.001	5.010	0.000	0.000	0.000	0.000	0.000	0.000
5H	1000.001	5005.010	10.057	0.001	5.010	0.000	0.000	0.000	0.000	0.000	0.000
5I	1000.001	5005.010	10.057	0.001	5.010	0.000	0.000	0.000	0.000	0.000	0.000
			Mean	0.001	5.010		**Mean**	0.000	0.000		
6A	1000.001	5005.010	10.057	0.001	5.010	0.000	0.000	0.000	0.000	0.000	0.000
6B	1000.001	5005.010	10.057	0.001	5.010	0.000	0.000	0.000	0.000	0.000	0.000
6C	1000.001	5005.010	10.057	0.001	5.010	0.000	0.000	0.000	0.000	0.000	0.000
6D	1000.001	5005.009	10.057	0.001	5.009	0.000	-0.001	0.000	-0.001	0.000	-0.001
6E	1000.001	5005.009	10.057	0.001	5.009	0.000	-0.001	0.000	-0.001	0.000	-0.001
6F	1000.001	5005.010	10.057	0.001	5.010	0.000	0.000	0.000	0.000	0.000	0.000
6G	1000.001	5005.010	10.057	0.001	5.010	0.000	0.000	0.000	0.000	0.000	0.000
6H	1000.001	5005.009	10.057	0.001	5.009	0.000	-0.001	0.000	-0.001	0.000	-0.001
6I	1000.001	5005.010	10.057	0.001	5.010	0.000	0.000	0.000	0.000	0.000	0.000
			Mean	0.001	5.010		**Mean**	0.000	0.000		
		Overall Mean		0.001	5.010	**Overall Mean**		0.000	0.000		
				Std Dev of Obs		0.000	0.001	**Std Dev of Obs**		0.000	0.001

Appendix C

Sample Vertical Pretesting Reductions

Sokkia SRX5

Table C.1: Vertical pretesting set 1 – average origin position

Set 1									
Rotation Origin									
Reading	Bearing						Res	Distance (m)	Res
1	0	°	0	′	17	″	1.2 ″	20.001	0.000
2	0	°	0	′	17	″	1.2 ″	20.001	0.000
3	0	°	0	′	18	″	0.2 ″	20.001	0.000
4	0	°	0	′	20	″	-1.8 ″	20.001	0.000
5	0	°	0	′	17	″	1.2 ″	20.001	0.000
6	0	°	0	′	20	″	-1.8 ″	20.001	0.000
Mean	0	°	0	′	18	″		20.001	

Table C.2: Vertical pretesting set 1 – 0° check readings.

Check Readings							Diff	Distance (m)
0°	359	°	39	′	24	″		20.001
0°	359	°	39	′	20	″	4 ″	20.001
0°	359	°	39	′	22	″	2 ″	20.001

Table C.3(a): Vertical pretesting set 1 – calculate errors.

0° Tribrach Rotation							Distance (m)		
Reading	359	°	39	′	24	″	20.001		
Calc	89	°	39	′	24	″	0.122	Offset	0.000
Close	89	°	49	′	51	″	0.122		
Diff	-0	°	10	′	27	″	0.000	Check	0.000
+35° Tribrach Rotation							Distance (m)		
Reading	359	°	43	′	0	″	20.069		
Calc	124	°	39	′	24	″	0.122	Offset	0.002
Close	123	°	51	′	30	″	0.122		
Diff	0	°	47	′	54	″	0.000	Check	0.002
Adj Calc	124	°	9	′	24	″	0.122	Offset	0.001
+30° Tribrach Rotation							Distance (m)		
Reading	359	°	42	′	6	″	20.061		
Calc	119	°	39	′	24	″	0.122	Offset	0.001
Close	119	°	21	′	14	″	0.122		
Diff	0	°	18	′	10	″	0.000	Check	0.001
Adj Calc	119	°	9	′	24	″	0.122	Offset	0.000

Table C.3(b): Vertical pretesting set 1 – calculate errors.

+25° Tribrach Rotation				Distance (m)		
Reading	359 °	41 ′	13 ″	20.052		
Calc	114 °	39 ′	24 ″	0.122	Offset	0.000
Close	114 °	29 ′	23 ″	0.122		
Diff	0 °	10 ′	1 ″	0.000	Check	0.000
Adj Calc	114 °	9 ′	24 ″	0.122	Offset	0.001
+20° Tribrach Rotation				Distance (m)		
Reading	359 °	40 ′	30 ″	20.041		
Calc	109 °	39 ′	24 ″	0.122	Offset	0.001
Close	108 °	58 ′	15 ″	0.122		
Diff	0 °	41 ′	9 ″	0.000	Check	0.001
Adj Calc	109 °	9 ′	24 ″	0.122	Offset	0.000
+15° Tribrach Rotation				Distance (m)		
Reading	359 °	40 ′	2 ″	20.032		
Calc	104 °	39 ′	24 ″	0.122	Offset	0.000
Close	104 °	33 ′	19 ″	0.122		
Diff	0 °	6 ′	5 ″	0.000	Check	0.000
+10° Tribrach Rotation				Distance (m)		
Reading	359 °	39 ′	36 ″	20.021		
Calc	99 °	39 ′	24 ″	0.122	Offset	0.001
Close	99 °	15 ′	24 ″	0.122		
Diff	0 °	24 ′	0 ″	0.000	Check	0.001
+5° Tribrach Rotation				Distance (m)		
Reading	359 °	39 ′	23 ″	20.011		
Calc	94 °	39 ′	24 ″	0.122	Offset	0.000
Close	94 °	31 ′	38 ″	0.122		
Diff	0 °	7 ′	45 ″	0.000	Check	0.000
0° Tribrach Rotation				Distance (m)		
Reading	359 °	39 ′	20 ″	20.001		
Calc	89 °	39 ′	24 ″	0.122	Offset	0.000
Close	89 °	49 ′	49 ″	0.122		
Diff	-0 °	10 ′	25 ″	0.000	Check	0.000
-5° Tribrach Rotation				Distance (m)		
Reading	359 °	39 ′	28 ″	19.991		
Calc	84 °	39 ′	24 ″	0.122	Offset	0.001
Close	85 °	6 ′	50 ″	0.122		
Diff	-0 °	27 ′	26 ″	0.000	Check	0.001
Adj Calc	85 °	9 ′	24 ″	0.122	Offset	0.000

Table C.3(c): Vertical pretesting set 1 – calculate errors.

-10° Tribrach Rotation		Distance (m)		
Reading	359° 39′ 37″	19.981		
Calc	79° 39′ 24″	0.122	Offset	0.002
Close	80° 23′ 30″	0.122		
Diff	-0° 44′ 6″	0.000	Check	0.002
Adj Calc	80° 9′ 24″	0.122	Offset	0.001
-15° Tribrach Rotation		Distance (m)		
Reading	359° 40′ 7″	19.969		
Calc	74° 39′ 24″	0.122	Offset	0.000
Close	74° 34′ 54″	0.122		
Diff	0° 4′ 30″	0.000	Check	0.000
-20° Tribrach Rotation		Distance (m)		
Reading	359° 40′ 34″	19.960		
Calc	69° 39′ 24″	0.122	Offset	0.001
Close	70° 10′ 11″	0.122		
Diff	-0° 30′ 47″	0.000	Check	0.001
Adj Calc	70° 9′ 24″	0.122	Offset	0.000
-25° Tribrach Rotation		Distance (m)		
Reading	359° 41′ 19″	19.950		
Calc	64° 39′ 24″	0.122	Offset	0.001
Close	65° 2′ 0″	0.122		
Diff	-0° 22′ 36″	0.000	Check	0.001
Adj Calc	65° 9′ 24″	0.122	Offset	0.000
-30° Tribrach Rotation		Distance (m)		
Reading	359° 42′ 8″	19.941		
Calc	59° 39′ 24″	0.121	Offset	0.001
Close	60° 14′ 4″	0.121		
Diff	-0° 34′ 40″	0.000	Check	0.001
Adj Calc	60° 9′ 24″	0.121	Offset	0.000
-35° Tribrach Rotation		Distance (m)		
Reading	359° 43′ 7″	19.932		
Calc	54° 39′ 24″	0.121	Offset	0.001
Close	55° 12′ 10″	0.121		
Diff	-0° 32′ 46″	0.000	Check	0.001
Adj Calc	55° 9′ 24″	0.121	Offset	0.000

Table C.3(d): Vertical pretesting set 1 – calculate errors.

-40° Tribrach Rotation							Distance (m)		
Reading	359	°	44	′	17	″	19.923		
Calc	49	°	39	′	24	″	0.121	Offset	0.000
Close	49	°	53	′	9	″	0.121		
Diff	-0	°	13	′	45	″	0.000	Check	0.000
0° Tribrach Rotation							Distance (m)		
Reading	359	°	39	′	22	″	20.001		
Calc	89	°	39	′	24	″	0.122	Offset	0.000
Close	89	°	49	′	50	″	0.122		
Diff	-0	°	10	′	26	″	0.000	Check	0.000
0° (+45°) Tribrach Rotation							Distance (m)		
Reading	359	°	39	′	19	″	20.001		
Calc	89	°	39	′	24	″	0.122	Offset	0.000
Close	89	°	49	′	49	″	0.122		
Diff	-0	°	10	′	25	″	0.000	Check	0.000
-5° (+40°) Tribrach Rotation							Distance (m)		
Reading	359	°	39	′	26	″	19.990		
Calc	84	°	39	′	24	″	0.122	Offset	0.000
Close	84	°	39	′	9	″	0.122		
Diff	0	°	0	′	15	″	0.000	Check	0.000
-10° (+35°) Tribrach Rotation							Distance (m)		
Reading	359	°	39	′	40	″	19.980		
Calc	79	°	39	′	24	″	0.122	Offset	0.001
Close	79	°	54	′	20	″	0.122		
Diff	-0	°	14	′	56	″	0.000	Check	0.001
0° (+45°) Tribrach Rotation							Distance (m)		
Reading	359	°	39	′	23	″	20.001		
Calc	89	°	39	′	24	″	0.122	Offset	0.000
Close	89	°	49	′	51	″	0.122		
Diff	-0	°	10	′	27	″	0.000	Check	0.000
0° (-45°) Tribrach Rotation							Distance (m)		
Reading	359	°	39	′	20	″	20.001		
Calc	89	°	39	′	24	″	0.122	Offset	0.000
Close	89	°	49	′	49	″	0.122		
Diff	-0	°	10	′	25	″	0.000	Check	0.000

Table C.3(e): Vertical pretesting set 1 – calculate errors.

+5° (-40°) Tribrach Rotation				Distance (m)		
Reading	359 °	39 ′	25 ″	20.011		
Calc	94 °	39 ′	24 ″	0.122	Offset	0.000
Close	94 °	32 ′	6 ″	0.122		
Diff	0 °	7 ′	18 ″	0.000	Check	0.000
0° (-45°) Tribrach Rotation				Distance (m)		
Reading	359 °	39 ′	17 ″	20.001		
Calc	89 °	39 ′	24 ″	0.122	Offset	0.000
Close	89 °	49 ′	48 ″	0.122		
Diff	-0 °	10 ′	24 ″	0.000	Check	0.000

Table C.4(a): Vertical pretesting – average rotation angle.

+0° Rotation Angle Accuracy							
Set	Difference			Residuals			Dist Error
1	-0 °	10 ′	27 ″	0 °	0 ′	0 ″	0.000
2	-0 °	10 ′	27 ″	0 °	0 ′	0 ″	0.001
3	-0 °	10 ′	27 ″	0 °	0 ′	0 ″	0.000
4	-0 °	10 ′	27 ″	0 °	0 ′	0 ″	0.000
5	-0 °	10 ′	26 ″	0 °	0 ′	1 ″	0.000
6	-0 °	10 ′	28 ″	-0 °	0 ′	0 ″	0.000
Mean	-0 °	10 ′	27 ″	0 °	0 ′	0 ″	Std Dev
+35° Rotation Angle Accuracy							
Set	Difference			Residuals			Dist Error
1	0 °	47 ′	54 ″	0 °	27 ′	1 ″	0.000
2	0 °	19 ′	58 ″	-0 °	0 ′	54 ″	0.000
3	0 °	19 ′	57 ″	-0 °	0 ′	55 ″	0.000
4	0 °	21 ′	29 ″	0 °	0 ′	36 ″	0.000
5	0 °	16 ′	52 ″	-0 °	4 ′	0 ″	0.000
6	0 °	26 ′	8 ″	0 °	5 ′	15 ″	0.000
Mean	0 °	20 ′	52 ″	0 °	3 ′	22 ″	Std Dev
+30° Rotation Angle Accuracy							
Set	Difference			Residuals			Dist Error
1	0 °	18 ′	10 ″	0 °	0 ′	39 ″	0.000
2	0 °	14 ′	6 ″	-0 °	3 ′	24 ″	0.000
3	0 °	15 ′	27 ″	-0 °	2 ′	3 ″	0.000
4	0 °	45 ′	28 ″	0 °	27 ′	57 ″	0.000
5	-0 °	11 ′	42 ″	-0 °	29 ′	12 ″	0.000
6	0 °	23 ′	33 ″	0 °	6 ′	2 ″	0.000
Mean	0 °	17 ′	30 ″	0 °	18 ′	22 ″	Std Dev

Table C.4(b): Vertical pretesting – average rotation angle.

+25° Rotation Angle Accuracy			
Set	Difference	Residuals	Dist Error
1	0 ° 10 ′ 1 ″	-0 ° 14 ′ 2 ″	0.000
2	0 ° 31 ′ 6 ″	0 ° 7 ′ 2 ″	0.000
3	0 ° 29 ′ 57 ″	0 ° 5 ′ 53 ″	0.000
4	0 ° 7 ′ 43 ″	-0 ° 16 ′ 20 ″	0.000
5	0 ° 29 ′ 59 ″	0 ° 5 ′ 55 ″	0.000
6	0 ° 35 ′ 35 ″	0 ° 11 ′ 31 ″	0.000
Mean	0 ° 24 ′ 3 ″	0 ° 11 ′ 58 ″	Std Dev
+20° Rotation Angle Accuracy			
Set	Difference	Residuals	Dist Error
1	0 ° 41 ′ 9 ″	0 ° 2 ′ 43 ″	0.000
2	0 ° 35 ′ 43 ″	-0 ° 2 ′ 42 ″	0.001
3	0 ° 37 ′ 32 ″	-0 ° 0 ′ 53 ″	0.000
4	0 ° 38 ′ 25 ″	-0 ° 0 ′ 0 ″	0.000
5	0 ° 36 ′ 39 ″	-0 ° 1 ′ 46 ″	0.000
6	0 ° 41 ′ 7 ″	0 ° 2 ′ 41 ″	0.000
Mean	0 ° 38 ′ 25 ″	0 ° 2 ′ 16 ″	Std Dev
+15° Rotation Angle Accuracy			
Set	Difference	Residuals	Dist Error
1	0 ° 6 ′ 5 ″	-0 ° 4 ′ 21 ″	0.000
2	0 ° 30 ′ 39 ″	0 ° 20 ′ 13 ″	0.000
3	0 ° 5 ′ 23 ″	-0 ° 5 ′ 3 ″	0.000
4	0 ° 7 ′ 28 ″	-0 ° 2 ′ 58 ″	0.000
5	0 ° 2 ′ 35 ″	-0 ° 7 ′ 51 ″	0.000
6	1 ° 3 ′ 23 ″	0 ° 52 ′ 57 ″	0.000
Mean	0 ° 10 ′ 26 ″	0 ° 11 ′ 26 ″	Std Dev
+10° Rotation Angle Accuracy			
Set	Difference	Residuals	Dist Error
1	0 ° 24 ′ 0 ″	0 ° 17 ′ 32 ″	0.000
2	0 ° 19 ′ 53 ″	0 ° 13 ′ 25 ″	0.000
3	-0 ° 9 ′ 6 ″	-0 ° 15 ′ 33 ″	0.000
4	-0 ° 5 ′ 39 ″	-0 ° 12 ′ 6 ″	0.000
5	-0 ° 10 ′ 0 ″	-0 ° 16 ′ 27 ″	0.000
6	0 ° 19 ′ 36 ″	0 ° 13 ′ 8 ″	0.000
Mean	0 ° 6 ′ 27 ″	0 ° 16 ′ 14 ″	Std Dev

Table C.4(c): Vertical pretesting – average rotation angle.

+5° Rotation Angle Accuracy								
Set	Difference			Residuals			Dist Error	
1	0 °	7 ′	45 ″	0 °	15 ′	6 ″	0.000	
2	-0 °	22 ′	48 ″	-0 °	15 ′	25 ″	0.000	
3	0 °	6 ′	51 ″	0 °	14 ′	12 ″	0.000	
4	-0 °	20 ′	47 ″	-0 °	13 ′	25 ″	0.000	
5	-0 °	22 ′	16 ″	-0 °	14 ′	53 ″	0.000	
6	0 °	7 ′	3 ″	0 °	14 ′	25 ″	0.000	
Mean	-0 °	7 ′	21 ″	0 °	15 ′	59 ″	Std Dev	
+0° Rotation Angle Accuracy								
Set	Difference			Residuals			Dist Error	
1	-0 °	10 ′	25 ″	0 °	0 ′	1 ″	0.000	
2	-0 °	10 ′	28 ″	-0 °	0 ′	1 ″	0.000	
3	-0 °	10 ′	26 ″	0 °	0 ′	0 ″	0.000	
4	-0 °	10 ′	26 ″	0 °	0 ′	0 ″	0.000	
5	-0 °	10 ′	27 ″	-0 °	0 ′	0 ″	0.000	
6	-0 °	10 ′	28 ″	-0 °	0 ′	1 ″	0.000	
Mean	-0 °	10 ′	26 ″	0 °	0 ′	1 ″	Std Dev	
-5° Rotation Angle Accuracy								
Set	Difference			Residuals			Dist Error	
1	-0 °	27 ′	26 ″	-0 °	9 ′	31 ″	0.000	
2	-0 °	26 ′	33 ″	-0 °	8 ′	38 ″	0.000	
3	-0 °	27 ′	39 ″	-0 °	9 ′	44 ″	0.000	
4	0 °	0 ′	29 ″	0 °	18 ′	23 ″	0.000	
5	-0 °	26 ′	32 ″	-0 °	8 ′	37 ″	0.000	
6	0 °	0 ′	13 ″	0 °	18 ′	7 ″	0.000	
Mean	-0 °	17 ′	54 ″	0 °	14 ′	9 ″	Std Dev	
-10° Rotation Angle Accuracy								
Set	Difference			Residuals			Dist Error	
1	-0 °	44 ′	6 ″	-0 °	20 ′	39 ″	0.000	
2	-0 °	40 ′	33 ″	-0 °	17 ′	6 ″	0.000	
3	-0 °	14 ′	28 ″	0 °	8 ′	58 ″	0.000	
4	-0 °	15 ′	24 ″	0 °	8 ′	2 ″	0.000	
5	-0 °	11 ′	38 ″	0 °	11 ′	48 ″	0.000	
6	-0 °	14 ′	30 ″	0 °	8 ′	56 ″	0.000	
Mean	-0 °	23 ′	26 ″	0 °	14 ′	43 ″	Std Dev	

Table C.4(d): Vertical pretesting – average rotation angle.

-15° Rotation Angle Accuracy			
Set	Difference	Residuals	Dist Error
1	0 ° 4 ′ 30 ″	0 ° 0 ′ 49 ″	0.000
2	-0 ° 19 ′ 22 ″	-0 ° 23 ′ 2 ″	0.000
3	-0 ° 3 ′ 47 ″	-0 ° 7 ′ 27 ″	0.000
4	0 ° 2 ′ 21 ″	-0 ° 1 ′ 19 ″	0.000
5	0 ° 6 ′ 40 ″	0 ° 2 ′ 59 ″	0.000
6	0 ° 31 ′ 42 ″	0 ° 28 ′ 1 ″	0.000
Mean	0 ° 3 ′ 40 ″	0 ° 16 ′ 37 ″	Std Dev
-20° Rotation Angle Accuracy			
Set	Difference	Residuals	Dist Error
1	-0 ° 30 ′ 47 ″	-0 ° 3 ′ 19 ″	0.000
2	-0 ° 23 ′ 25 ″	0 ° 4 ′ 2 ″	0.000
3	-0 ° 28 ′ 2 ″	-0 ° 0 ′ 34 ″	0.000
4	-0 ° 30 ′ 48 ″	-0 ° 3 ′ 20 ″	0.000
5	-0 ° 51 ′ 8 ″	-0 ° 23 ′ 40 ″	0.000
6	-0 ° 0 ′ 33 ″	0 ° 26 ′ 54 ″	0.000
Mean	-0 ° 27 ′ 27 ″	0 ° 16 ′ 16 ″	Std Dev
-25° Rotation Angle Accuracy			
Set	Difference	Residuals	Dist Error
1	-0 ° 22 ′ 36 ″	-0 ° 1 ′ 20 ″	0.000
2	-0 ° 18 ′ 0 ″	0 ° 3 ′ 15 ″	0.000
3	-0 ° 22 ′ 36 ″	-0 ° 1 ′ 20 ″	0.000
4	-0 ° 22 ′ 37 ″	-0 ° 1 ′ 21 ″	0.000
5	-0 ° 20 ′ 17 ″	0 ° 0 ′ 58 ″	0.000
6	-0 ° 21 ′ 29 ″	-0 ° 0 ′ 13 ″	0.000
Mean	-0 ° 21 ′ 15 ″	0 ° 1 ′ 50 ″	Std Dev
-30° Rotation Angle Accuracy			
Set	Difference	Residuals	Dist Error
1	-0 ° 34 ′ 40 ″	-0 ° 2 ′ 9 ″	0.000
2	-0 ° 30 ′ 36 ″	0 ° 1 ′ 54 ″	0.000
3	-0 ° 33 ′ 19 ″	-0 ° 0 ′ 48 ″	0.000
4	-0 ° 8 ′ 46 ″	0 ° 23 ′ 44 ″	0.000
5	-0 ° 31 ′ 56 ″	0 ° 0 ′ 34 ″	0.000
6	-0 ° 32 ′ 0 ″	0 ° 0 ′ 30 ″	0.000
Mean	-0 ° 32 ′ 30 ″	0 ° 1 ′ 32 ″	Std Dev

Table C.4(e): Vertical pretesting – average rotation angle.

-35° Rotation Angle Accuracy			
Set	Difference	Residuals	Dist Error
1	-0 ° 32 ′ 46 ″	-0 ° 3 ′ 7 ″	0.000
2	-0 ° 23 ′ 25 ″	0 ° 6 ′ 13 ″	0.000
3	-0 ° 29 ′ 40 ″	-0 ° 0 ′ 1 ″	0.000
4	-0 ° 37 ′ 26 ″	-0 ° 7 ′ 47 ″	0.000
5	-0 ° 24 ′ 57 ″	0 ° 4 ′ 41 ″	0.000
6	-0 ° 3 ′ 19 ″	0 ° 26 ′ 19 ″	0.000
Mean	-0 ° 29 ′ 38 ″	0 ° 5 ′ 43 ″	Std Dev
-40° Rotation Angle Accuracy			
Set	Difference	Residuals	Dist Error
1	-0 ° 13 ′ 45 ″	-0 ° 21 ′ 10 ″	0.000
2	-0 ° 4 ′ 57 ″	-0 ° 12 ′ 22 ″	0.000
3	0 ° 14 ′ 55 ″	0 ° 7 ′ 29 ″	0.000
4	0 ° 6 ′ 6 ″	-0 ° 1 ′ 19 ″	0.000
5	0 ° 25 ′ 35 ″	0 ° 18 ′ 9 ″	0.000
6	0 ° 16 ′ 39 ″	0 ° 9 ′ 13 ″	0.000
Mean	0 ° 7 ′ 25 ″	0 ° 14 ′ 39 ″	Std Dev
0° Rotation Angle Accuracy			
Set	Difference	Residuals	Dist Error
1	-0 ° 10 ′ 26 ″	0 ° 0 ′ 1 ″	0.000
2	-0 ° 10 ′ 28 ″	-0 ° 0 ′ 0 ″	0.000
3	-0 ° 10 ′ 27 ″	0 ° 0 ′ 0 ″	0.000
4	-0 ° 10 ′ 25 ″	0 ° 0 ′ 2 ″	0.000
5	-0 ° 10 ′ 28 ″	-0 ° 0 ′ 0 ″	0.000
6	-0 ° 10 ′ 28 ″	-0 ° 0 ′ 0 ″	0.000
Mean	-0 ° 10 ′ 27 ″	0 ° 0 ′ 1 ″	Std Dev
0°(+45°) Rotation Angle Accuracy			
Set	Difference	Residuals	Dist Error
1	-0 ° 10 ′ 25 ″	0 ° 0 ′ 1 ″	0.000
2	-0 ° 10 ′ 28 ″	-0 ° 0 ′ 1 ″	0.000
3	-0 ° 10 ′ 25 ″	0 ° 0 ′ 1 ″	0.000
4	-0 ° 10 ′ 25 ″	0 ° 0 ′ 1 ″	0.000
5	-0 ° 10 ′ 29 ″	-0 ° 0 ′ 2 ″	0.000
6	-0 ° 10 ′ 28 ″	-0 ° 0 ′ 1 ″	0.000
Mean	-0 ° 10 ′ 26 ″	0 ° 0 ′ 1 ″	Std Dev

Table C.4(f): Vertical pretesting – average rotation angle.

-5°(+40°) Rotation Angle Accuracy							
Set	Difference			Residuals			Dist Error
1	0 °	0 ′	15 ″	-0 °	0 ′	40 ″	0.000
2	0 °	1 ′	42 ″	0 °	0 ′	46 ″	0.000
3	0 °	0 ′	44 ″	-0 °	0 ′	11 ″	0.000
4	0 °	0 ′	14 ″	-0 °	0 ′	41 ″	0.000
5	0 °	2 ′	41 ″	0 °	1 ′	45 ″	0.000
6	-0 °	0 ′	1 ″	-0 °	0 ′	56 ″	0.000
Mean	0 °	0 ′	55 ″	0 °	1 ′	3 ″	Std Dev
-10°(+35°) Rotation Angle Accuracy							
Set	Difference			Residuals			Dist Error
1	-0 °	14 ′	56 ″	-0 °	1 ′	24 ″	0.000
2	-0 °	12 ′	35 ″	0 °	0 ′	56 ″	0.000
3	-0 °	14 ′	28 ″	-0 °	0 ′	56 ″	0.000
4	-0 °	16 ′	20 ″	-0 °	2 ′	48 ″	0.000
5	-0 °	9 ′	17 ″	0 °	4 ′	14 ″	0.000
6	-0 °	13 ′	34 ″	-0 °	0 ′	2 ″	0.000
Mean	-0 °	13 ′	31 ″	0 °	2 ′	26 ″	Std Dev
0°(+45°) Rotation Angle Accuracy							
Set	Difference			Residuals			Dist Error
1	-0 °	10 ′	27 ″	0 °	0 ′	0 ″	0.000
2	-0 °	10 ′	29 ″	-0 °	0 ′	1 ″	0.000
3	-0 °	10 ′	26 ″	0 °	0 ′	1 ″	0.000
4	-0 °	10 ′	27 ″	0 °	0 ′	0 ″	0.000
5	-0 °	10 ′	28 ″	-0 °	0 ′	0 ″	0.000
6	-0 °	10 ′	30 ″	-0 °	0 ′	2 ″	0.000
Mean	-0 °	10 ′	27 ″	0 °	0 ′	1 ″	Std Dev
0°(-45°) Rotation Angle Accuracy							
Set	Difference			Residuals			Dist Error
1	-0 °	10 ′	25 ″	0 °	0 ′	1 ″	0.000
2	-0 °	10 ′	28 ″	-0 °	0 ′	1 ″	0.000
3	-0 °	10 ′	26 ″	0 °	0 ′	0 ″	0.000
4	-0 °	10 ′	26 ″	0 °	0 ′	0 ″	0.000
5	-0 °	10 ′	28 ″	-0 °	0 ′	1 ″	0.000
6	-0 °	10 ′	28 ″	-0 °	0 ′	1 ″	0.000
Mean	-0 °	10 ′	26 ″	0 °	0 ′	1 ″	Std Dev

Table C.4(g): Vertical pretesting – average rotation angle.

+5°(-40°) Rotation Angle Accuracy												
Set	Difference						Residuals					Dist Error
1	0	°	7	′	18	″	0	°	0	′	42 ″	0.000
2	1	°	2	′	27	″	0	°	55	′	51 ″	0.000
3	0	°	7	′	18	″	0	°	0	′	42 ″	0.000
4	0	°	6	′	50	″	0	°	0	′	14 ″	0.000
5	-0	°	23	′	33	″	-0	°	30	′	8 ″	0.000
6	-0	°	20	′	48	″	-0	°	27	′	23 ″	0.000
Mean	0	°	6	′	35	″	0	°	30	′	55 ″	Std Dev
+0°(-45°) Rotation Angle Accuracy												
Set	Difference						Residuals					Dist Error
1	-0	°	10	′	24	″	0	°	0	′	2 ″	0.000
2	-0	°	10	′	27	″	-0	°	0	′	0 ″	0.000
3	-0	°	10	′	26	″	0	°	0	′	0 ″	0.000
4	-0	°	10	′	26	″	0	°	0	′	0 ″	0.000
5	-0	°	10	′	29	″	-0	°	0	′	2 ″	0.000
6	-0	°	10	′	27	″	-0	°	0	′	0 ″	0.000
Mean	-0	°	10	′	26	″	0	°	0	′	1 ″	Std Dev

Appendix D

Sample Horizontal Testing Reductions

Sokkia SRX5 using ATP1 prism

Table D.1: Sokkia 20m horizontal testing 1-3 reductions.

Sokkia 20m Measurement Data 360 Degree Prism				Sighter Target Residuals				Initial Reading Residuals	
				Overall Mean		20.009 m			
Rotation	East	North	RL	Offset	Dist	Offset	Dist	Offset	Dist
0	1000.000	5020.010	11.195	0.000	20.010	0.000	0.001	0.000	0.000
7.5	1000.000	5020.010	11.195	0.000	20.010	0.000	0.001	0.000	0.000
15	1000.000	5020.009	11.195	0.000	20.009	0.000	0.000	0.000	-0.001
22.5	1000.001	5020.009	11.195	0.001	20.009	0.001	0.000	0.001	-0.001
30	1000.000	5020.008	11.195	0.000	20.008	0.000	-0.001	0.000	-0.002
37.5	999.999	5020.009	11.195	-0.001	20.009	-0.001	0.000	-0.001	-0.001
45	999.998	5020.009	11.195	-0.002	20.009	-0.002	0.000	-0.002	-0.001
52.5	1000.000	5020.010	11.196	0.000	20.010	0.000	0.001	0.000	0.000
60	1000.000	5020.010	11.196	0.000	20.010	0.000	0.001	0.000	0.000
60	1000.000	5020.009	11.196	0.000	20.009	0.000	0.000	0.000	0.000
67.5	1000.000	5020.009	11.196	0.000	20.009	0.000	0.000	0.000	0.000
75	1000.001	5020.009	11.196	0.001	20.009	0.001	0.000	0.001	0.000
82.5	1000.001	5020.009	11.196	0.001	20.009	0.001	0.000	0.001	0.000
90	1000.000	5020.008	11.195	0.000	20.008	0.000	-0.001	0.000	-0.001
97.5	999.999	5020.008	11.196	-0.001	20.008	-0.001	-0.001	-0.001	-0.001
105	999.998	5020.009	11.196	-0.002	20.009	-0.002	0.000	-0.002	0.000
112.5	999.999	5020.010	11.195	-0.001	20.010	-0.001	0.001	-0.001	0.001
120	999.999	5020.010	11.195	-0.001	20.010	-0.001	0.001	-0.001	0.001
120	999.999	5020.010	11.195	-0.001	20.010	-0.001	0.001	0.000	0.000
127.5	1000.000	5020.010	11.195	0.000	20.010	0.000	0.001	0.001	0.000
135	1000.000	5020.010	11.195	0.000	20.010	0.000	0.001	0.001	0.000
142.5	1000.001	5020.009	11.195	0.001	20.009	0.001	0.000	0.002	-0.001
150	1000.000	5020.009	11.195	0.000	20.009	0.000	0.000	0.001	-0.001
157.5	1000.000	5020.009	11.195	0.000	20.009	0.000	0.000	0.001	-0.001
165	999.998	5020.009	11.196	-0.002	20.009	-0.002	0.000	-0.001	-0.001
172.5	999.999	5020.009	11.195	-0.001	20.009	-0.001	0.000	0.000	-0.001
180	1000.000	5020.010	11.196	0.000	20.010	0.000	0.001	0.001	0.000

Table D.2: Sokkia 20m horizontal testing sets 4-6 reductions.

Sokkia 20m Measurement Data 360 Degree Prism				Sighter Target Residuals				Initial Reading Residuals	
				Overall Mean		20.009 m			
Rotation	East	North	RL	Offset	Dist	Offset	Dist	Offset	Dist
180	1000.000	5020.010	11.196	0.000	20.010	0.000	0.001	0.000	0.000
187.5	1000.000	5020.010	11.196	0.000	20.010	0.000	0.001	0.000	0.000
195	1000.001	5020.010	11.196	0.001	20.010	0.001	0.001	0.001	0.000
202.5	1000.002	5020.009	11.197	0.002	20.009	0.002	0.000	0.002	-0.001
210	1000.000	5020.009	11.196	0.000	20.009	0.000	0.000	0.000	-0.001
217.5	999.999	5020.009	11.196	-0.001	20.009	-0.001	0.000	-0.001	-0.001
225	999.998	5020.009	11.196	-0.002	20.009	-0.002	0.000	-0.002	-0.001
232.5	999.999	5020.010	11.196	-0.001	20.010	-0.001	0.001	-0.001	0.000
240	1000.000	5020.010	11.196	0.000	20.010	0.000	0.001	0.000	0.000
240	1000.000	5020.010	11.196	0.000	20.010	0.000	0.001	0.000	0.000
247.5	1000.001	5020.010	11.195	0.001	20.010	0.001	0.001	0.001	0.000
255	1000.000	5020.010	11.195	0.000	20.010	0.000	0.001	0.000	0.000
262.5	1000.002	5020.009	11.196	0.002	20.009	0.002	0.000	0.002	-0.001
270	1000.000	5020.009	11.196	0.000	20.009	0.000	0.000	0.000	-0.001
277.5	1000.000	5020.009	11.196	0.000	20.009	0.000	0.000	0.000	-0.001
285	999.999	5020.009	11.196	-0.001	20.009	-0.001	0.000	-0.001	-0.001
292.5	1000.000	5020.009	11.196	0.000	20.009	0.000	0.000	0.000	-0.001
300	1000.001	5020.010	11.196	0.001	20.010	0.001	0.001	0.001	0.000
300	1000.001	5020.010	11.196	0.001	20.010	0.001	0.001	0.000	0.000
307.5	1000.001	5020.009	11.195	0.001	20.009	0.001	0.000	0.000	-0.001
315	1000.002	5020.009	11.195	0.002	20.009	0.002	0.000	0.001	-0.001
322.5	1000.001	5020.009	11.195	0.001	20.009	0.001	0.000	0.000	-0.001
330	1000.000	5020.008	11.196	0.000	20.008	0.000	-0.001	-0.001	-0.002
337.5	999.999	5020.008	11.195	-0.001	20.008	-0.001	-0.001	-0.002	-0.002
345	999.999	5020.009	11.196	-0.001	20.009	-0.001	0.000	-0.002	-0.001
352.5	999.999	5020.010	11.195	-0.001	20.010	-0.001	0.001	-0.002	0.000
360	1000.000	5020.010	11.195	0.000	20.010	0.000	0.001	-0.001	0.000

Table D.3: Sokkia 20m horizontal testing distance averages.

	20m Distance Deviation from Initial Reading						
	Set 1	Set 2	Set 3	Set 4	Set 5	Set 6	Avg
X axis	Meas	Meas	Meas	Meas	Meas	Meas	Meas
0	0.000	0.000	0.000	0.000	0.000	0.000	0.000
7.5	0.000	0.000	0.000	0.000	0.000	-0.001	0.000
15	-0.001	0.000	0.000	0.000	0.000	-0.001	0.000
22.5	-0.001	0.000	-0.001	-0.001	-0.001	-0.001	-0.001
30	-0.002	-0.001	-0.001	-0.001	-0.001	-0.002	-0.001
37.5	-0.001	-0.001	-0.001	-0.001	-0.001	-0.002	-0.001
45	-0.001	0.000	-0.001	-0.001	-0.001	-0.001	-0.001
52.5	0.000	0.001	-0.001	0.000	-0.001	0.000	0.000
60	0.000	0.001	0.000	0.000	0.000	0.000	0.000

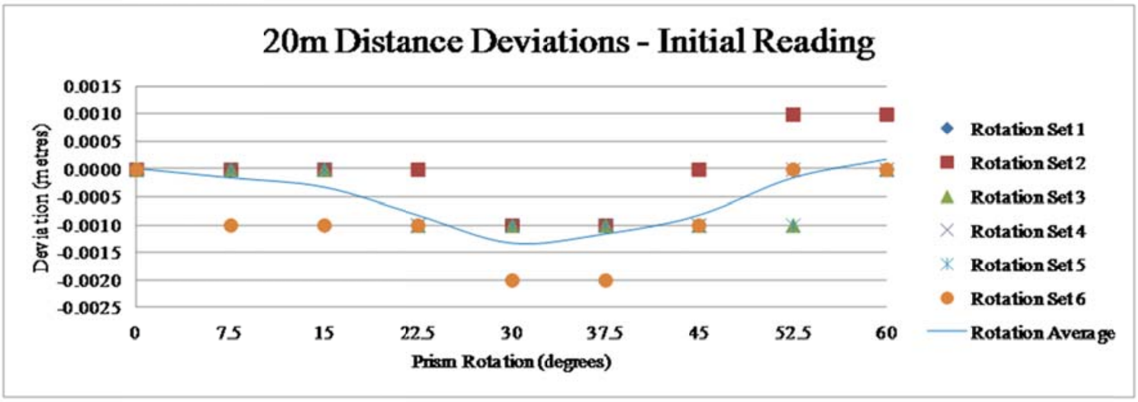

Figure D.1: Sokkia 20m horizontal testing distance results.

Table D.4: Sokkia 20m horizontal testing offset averages.

	20m Horizontal Deviations from Initial Reading								
X axis	Set 1 Meas	Set 2 Meas	Set 3 Meas	Set 4 Meas	Set 5 Meas	Set 6 Meas	Avg Mes	Predic	Res
0	0.000	0.000	0.000	0.000	0.000	0.000	0.000	0.000	0.000
7.5	0.000	0.000	0.001	0.000	0.001	0.000	0.000	0.001	0.001
15	0.000	0.001	0.001	0.001	0.000	0.001	0.001	0.001	0.001
22.5	0.001	0.001	0.002	0.002	0.002	0.000	0.001	0.001	0.000
30	0.000	0.000	0.001	0.000	0.000	-0.001	0.000	0.000	0.000
37.5	-0.001	-0.001	0.001	-0.001	0.000	-0.002	-0.001	-0.001	0.000
45	-0.002	-0.002	-0.001	-0.002	-0.001	-0.002	-0.002	-0.001	0.000
52.5	0.000	-0.001	0.000	-0.001	0.000	-0.002	-0.001	-0.001	0.000
60	0.000	-0.001	0.001	0.000	0.001	-0.001	0.000	0.000	0.000
							Std Dev of Obs		0.000

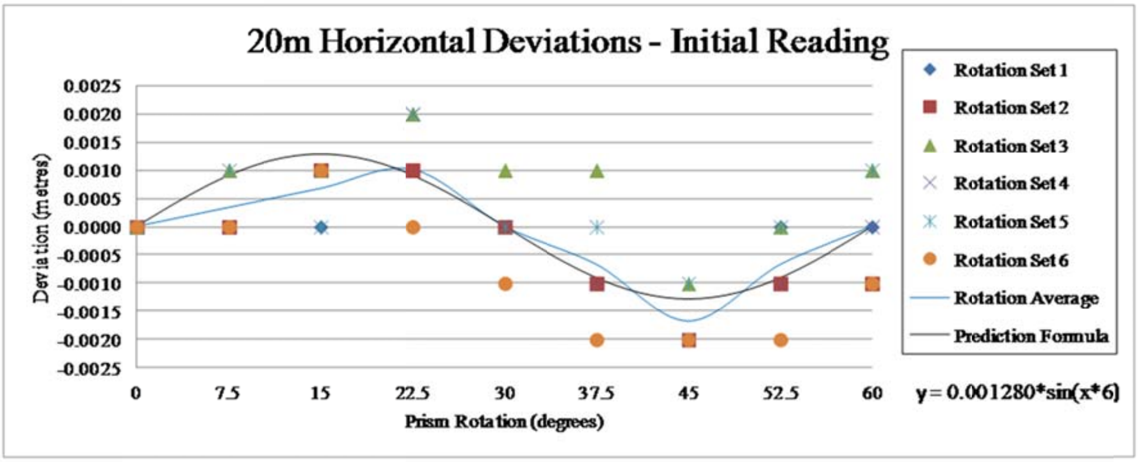

Figure D.2: Sokkia 20m horizontal testing offset results.

Appendix E

Sample Vertical Testing Reductions

Trimble S6 DR 300+ using robotic target kit prism

Table E.1: Trimble vertical testing set 1 – average origin position.

Set 1									
Rotation Origin									
	Bearing						Res	Distance (m)	Res
1	0	°	0	′	7	″	0.3 ″	20.000	0.000
2	0	°	0	′	7	″	0.3 ″	20.000	0.000
3	0	°	0	′	7	″	0.3 ″	20.001	0.001
4	0	°	0	′	6	″	-0.7 ″	20.000	0.000
5	0	°	0	′	7	″	0.3 ″	20.000	0.000
6	0	°	0	′	6	″	-0.7 ″	20.000	0.000
Mean	0	°	0	′	7	″		20.000	

Table E.2: Trimble vertical testing set 1 – 0° check readings.

Check Readings							Diff	Distance (m)
0°	359	°	46	′	59	″		20.000
0°	359	°	47	′	3	″	-4 ″	20.000
0°	359	°	47	′	4	″	-5 ″	20.000

Table E.3(a): Trimble vertical testing set 1 – calculate errors.

0° Tribrach Rotation								Distance (m)		
Reading	359	°	46	′	59	″		20.000		
Calc	89	°	46	′	59	″		0.076	Offset	0.000
Angle	0	°	0	′	0	″	Error	0.000	MC	0.000
+40° Tribrach Rotation								Distance (m)		
Reading	359	°	47	′	53	″		20.053		
Calc	129	°	16	′	59	″		0.089	Offset	0.004
Angle	0	°	0	′	54	″	Error	0.013	MC	0.000
+35° Tribrach Rotation								Distance (m)		
Reading	359	°	47	′	31	″		20.046		
Calc	124	°	16	′	59	″		0.087	Offset	0.003
Angle	0	°	0	′	32	″	Error	0.011	MC	0.000

Table E.3(b): Trimble vertical testing set 1 – calculate errors.

+30° Tribrach Rotation			Distance (m)		
Reading	359 ° 47 ′ 10 ″		20.041		
Calc	119 ° 16 ′ 59 ″		0.086	Offset	0.001
Angle	0 ° 0 ′ 11 ″	Error	0.010	MC	0.000
+25° Tribrach Rotation			Distance (m)		
Reading	359 ° 46 ′ 54 ″		20.033		
Calc	114 ° 16 ′ 59 ″		0.084	Offset	0.002
Angle	-0 ° 0 ′ 5 ″	Error	0.008	MC	0.000
+20° Tribrach Rotation			Distance (m)		
Reading	359 ° 46 ′ 45 ″		20.027		
Calc	109 ° 16 ′ 59 ″		0.082	Offset	0.000
Angle	-0 ° 0 ′ 14 ″	Error	0.006	MC	0.000
+15° Tribrach Rotation			Distance (m)		
Reading	359 ° 46 ′ 42 ″		20.020		
Calc	104 ° 46 ′ 59 ″		0.081	Offset	0.001
Angle	-0 ° 0 ′ 17 ″	Error	0.005	MC	0.000
+10° Tribrach Rotation			Distance (m)		
Reading	359 ° 46 ′ 43 ″		20.014		
Calc	99 ° 46 ′ 59 ″		0.079	Offset	0.000
Angle	-0 ° 0 ′ 16 ″	Error	0.003	MC	0.000
+5° Tribrach Rotation			Distance (m)		
Reading	359 ° 46 ′ 49 ″		20.007		
Calc	94 ° 46 ′ 59 ″		0.078	Offset	0.000
Angle	-0 ° 0 ′ 10 ″	Error	0.002	MC	0.000
0° Tribrach Rotation			Distance (m)		
Reading	359 ° 47 ′ 3 ″		20.000		
Calc	89 ° 46 ′ 59 ″		0.076	Offset	0.000
Angle	0 ° 0 ′ 4 ″	Error	0.000	MC	0.000
-5° Tribrach Rotation			Distance (m)		
Reading	359 ° 47 ′ 22 ″		19.993		
Calc	84 ° 16 ′ 59 ″		0.074	Offset	0.000
Angle	0 ° 0 ′ 23 ″	Error	-0.002	MC	0.000
-10° Tribrach Rotation			Distance (m)		
Reading	359 ° 47 ′ 46 ″		19.987		
Calc	79 ° 16 ′ 59 ″		0.073	Offset	0.000
Angle	0 ° 0 ′ 47 ″	Error	-0.003	MC	0.000

Table E.3(c): Trimble vertical testing set 1 – calculate errors.

-15° Tribrach Rotation									Distance (m)		
Reading	359	°	48	′	20	″			19.981		
Calc	74	°	46	′	59	″			0.071	Offset	0.000
Angle	0	°	1	′	21	″	Error		-0.005	MC	0.000
-20° Tribrach Rotation									Distance (m)		
Reading	359	°	48	′	54	″			19.975		
Calc	69	°	16	′	59	″			0.070	Offset	0.000
Angle	0	°	1	′	55	″	Error		-0.006	MC	0.000
-25° Tribrach Rotation									Distance (m)		
Reading	359	°	49	′	39	″			19.970		
Calc	64	°	16	′	59	″			0.068	Offset	0.001
Angle	0	°	2	′	40	″	Error		-0.008	MC	0.000
-30° Tribrach Rotation									Distance (m)		
Reading	359	°	50	′	27	″			19.965		
Calc	59	°	16	′	59	″			0.066	Offset	0.001
Angle	0	°	3	′	28	″	Error		-0.010	MC	0.000
-35° Tribrach Rotation									Distance (m)		
Reading	359	°	51	′	19	″			19.959		
Calc	54	°	16	′	59	″			0.065	Offset	0.004
Angle	0	°	4	′	20	″	Error		-0.011	MC	0.000
-40° Tribrach Rotation									Distance (m)		
Reading	359	°	52	′	19	″			19.957		
Calc	49	°	16	′	59	″			0.062	Offset	0.003
Angle	0	°	5	′	20	″	Error		-0.014	MC	0.000
0° Tribrach Rotation									Distance (m)		
Reading	359	°	47	′	4	″			20.000		
Calc	89	°	46	′	59	″			0.076	Offset	0.000
Angle	0	°	0	′	5	″	Error		0.000	MC	0.000
Max Tribrach Rotation									Distance (m)		
Reading	359	°	48	′	52	″			20.053		
Calc	132	°	27	′	25	″			0.084	Offset	0.005
Angle	0	°	1	′	53	″	Error		0.008	MC	0.000
Min Tribrach Rotation									Distance (m)		
Reading	359	°	52	′	4	″			19.954		
Calc	48	°	18	′	11	″			0.066	Offset	0.003
Angle	0	°	5	′	5	″	Error		-0.010	MC	0.000

Table E.3(d): Trimble vertical testing set 1 – calculate errors.

0° Tribrach Rotation								Distance (m)		
Reading	359	°	47	′	5	″		20.000		
Calc	89	°	46	′	59	″		0.076	Offset	0.000
Angle	0	°	0	′	6	″	Error	0.000	MC	0.000

Table E.4(a): Trimble vertical testing – average errors per rotation.

Average +0° Angle Deviation & Vertical Error													
Set	Angle Deviation						Residuals						Vert Error	Res
1	0	°	0	′	0	″	0	°	0	′	0	″	0.000	0.000
2	0	°	0	′	0	″	0	°	0	′	0	″	0.000	0.000
3	0	°	0	′	0	″	0	°	0	′	0	″	0.000	0.000
4	0	°	0	′	0	″	0	°	0	′	0	″	0.000	0.000
5	0	°	0	′	0	″	0	°	0	′	0	″	0.000	0.000
6	0	°	0	′	0	″	0	°	0	′	0	″	0.000	0.000
Mean	0	°	0	′	0	″				Mean			0.000	
			Std Dev				0	°	0	′	0	″	Std Dev	0.000
Average +40° Angle Deviation & Vertical Error														
Set	Angle Deviation						Residuals						Vert Error	Res
1	0	°	0	′	54	″	0	°	0	′	1	″	0.013	0.001
2	0	°	0	′	53	″	-0	°	0	′	0	″	0.012	0.000
3	0	°	0	′	51	″	-0	°	0	′	2	″	0.012	0.000
4	0	°	0	′	57	″	0	°	0	′	4	″	0.012	0.000
5	0	°	0	′	54	″	0	°	0	′	1	″	0.013	0.001
6	0	°	0	′	50	″	-0	°	0	′	3	″	0.012	0.000
Mean	0	°	0	′	53	″				Mean			0.012	
			Std Dev				0	°	0	′	2.5	″	Std Dev	0.001
Average +35° Angle Deviation & Vertical Error														
Set	Angle Deviation						Residuals						Vert Error	Res
1	0	°	0	′	32	″	0	°	0	′	2	″	0.011	0.000
2	0	°	0	′	31	″	0	°	0	′	1	″	0.011	0.000
3	0	°	0	′	27	″	-0	°	0	′	3	″	0.011	0.000
4	0	°	0	′	33	″	0	°	0	′	3	″	0.011	0.000
5	0	°	0	′	29	″	-0	°	0	′	1	″	0.011	0.000
6	0	°	0	′	27	″	-0	°	0	′	3	″	0.011	0.000
Mean	0	°	0	′	30	″				Mean			0.011	
			Std Dev				0	°	0	′	2.6	″	Std Dev	0.000

Table E.4(b): Trimble vertical testing – average errors per rotation.

Average +30° Angle Deviation & Vertical Error				
Set	Angle Deviation	Residuals	Vert Error	Res
1	0 ° 0 ′ 11 ″	0 ° 0 ′ 1 ″	0.010	0.001
2	0 ° 0 ′ 12 ″	0 ° 0 ′ 2 ″	0.009	-0.001
3	0 ° 0 ′ 9 ″	-0 ° 0 ′ 1 ″	0.009	-0.001
4	0 ° 0 ′ 13 ″	0 ° 0 ′ 3 ″	0.010	0.001
5	0 ° 0 ′ 9 ″	-0 ° 0 ′ 1 ″	0.010	0.001
6	0 ° 0 ′ 7 ″	-0 ° 0 ′ 3 ″	0.009	-0.001
Mean	0 ° 0 ′ 10 ″	Mean	0.009	
	Std Dev	0 ° 0 ′ 2.2 ″	Std Dev	0.001

Average +25° Angle Deviation & Vertical Error				
Set	Angle Deviation	Residuals	Vert Error	Res
1	-0 ° 0 ′ 5 ″	0 ° 0 ′ 1 ″	0.008	0.000
2	-0 ° 0 ′ 7 ″	-0 ° 0 ′ 1 ″	0.008	0.000
3	-0 ° 0 ′ 7 ″	-0 ° 0 ′ 1 ″	0.008	0.000
4	-0 ° 0 ′ 2 ″	0 ° 0 ′ 4 ″	0.008	0.000
5	-0 ° 0 ′ 5 ″	0 ° 0 ′ 1 ″	0.007	-0.001
6	-0 ° 0 ′ 8 ″	-0 ° 0 ′ 2 ″	0.008	0.000
Mean	-0 ° 0 ′ 5.7 ″	Mean	0.008	
	Std Dev	0 ° 0 ′ 2.2 ″	Std Dev	0.000

Average +20° Angle Deviation & Vertical Error				
Set	Angle Deviation	Residuals	Vert Error	Res
1	-0 ° 0 ′ 14 ″	0 ° 0 ′ 1 ″	0.006	0.000
2	-0 ° 0 ′ 17 ″	-0 ° 0 ′ 2 ″	0.006	0.000
3	-0 ° 0 ′ 16 ″	-0 ° 0 ′ 1 ″	0.006	0.000
4	-0 ° 0 ′ 13 ″	0 ° 0 ′ 2 ″	0.006	0.000
5	-0 ° 0 ′ 15 ″	0 ° 0 ′ 0 ″	0.006	0.000
6	-0 ° 0 ′ 17 ″	-0 ° 0 ′ 2 ″	0.006	0.000
Mean	-0 ° 0 ′ 15 ″	Mean	0.006	
	Std Dev	0 ° 0 ′ 1.6 ″	Std Dev	0.000

Average +15° Angle Deviation & Vertical Error				
Set	Angle Deviation	Residuals	Vert Error	Res
1	-0 ° 0 ′ 17 ″	0 ° 0 ′ 1 ″	0.005	0.001
2	-0 ° 0 ′ 19 ″	-0 ° 0 ′ 1 ″	0.004	0.000
3	-0 ° 0 ′ 19 ″	-0 ° 0 ′ 1 ″	0.004	0.000
4	-0 ° 0 ′ 16 ″	0 ° 0 ′ 2 ″	0.004	0.000
5	-0 ° 0 ′ 19 ″	-0 ° 0 ′ 1 ″	0.004	0.000
6	-0 ° 0 ′ 20 ″	-0 ° 0 ′ 2 ″	0.004	0.000
Mean	-0 ° 0 ′ 18 ″	Mean	0.004	
	Std Dev	0 ° 0 ′ 1.5 ″	Std Dev	0.000

Table E.4(c): Trimble vertical testing – average errors per rotation.

Average +10° Angle Deviation & Vertical Error				
Set	Angle Deviation	Residuals	Vert Error	Res
1	-0° 0′ 16″	0° 0′ 2″	0.003	0.000
2	-0° 0′ 18″	-0° 0′ 0″	0.003	0.000
3	-0° 0′ 19″	-0° 0′ 1″	0.003	0.000
4	-0° 0′ 15″	0° 0′ 3″	0.003	0.000
5	-0° 0′ 19″	-0° 0′ 1″	0.003	0.000
6	-0° 0′ 19″	-0° 0′ 1″	0.003	0.000
Mean	-0° 0′ 18″	Mean	0.003	
	Std Dev	0° 0′ 1.8″	Std Dev	0.000

Average +5° Angle Deviation & Vertical Error				
Set	Angle Deviation	Residuals	Vert Error	Res
1	-0° 0′ 10″	0° 0′ 2″	0.002	0.001
2	-0° 0′ 12″	-0° 0′ 1″	0.001	0.000
3	-0° 0′ 12″	-0° 0′ 1″	0.001	0.000
4	-0° 0′ 9″	0° 0′ 3″	0.001	0.000
5	-0° 0′ 13″	-0° 0′ 2″	0.001	0.000
6	-0° 0′ 13″	-0° 0′ 2″	0.001	0.000
Mean	-0° 0′ 12″	Mean	0.001	
	Std Dev	0° 0′ 1.6″	Std Dev	0.000

Average 0° Angle Deviation & Vertical Error				
Set	Angle Deviation	Residuals	Vert Error	Res
1	0° 0′ 4″	0° 0′ 4″	0.000	0.000
2	0° 0′ 0″	-0° 0′ 0″	0.000	0.000
3	-0° 0′ 1″	-0° 0′ 1″	0.000	0.000
4	0° 0′ 2″	0° 0′ 2″	0.000	0.000
5	-0° 0′ 1″	-0° 0′ 1″	0.000	0.000
6	-0° 0′ 2″	-0° 0′ 2″	0.000	0.000
Mean	0° 0′ 0.3″	Mean	0.000	
	Std Dev	0° 0′ 2.3″	Std Dev	0.000

Average -5° Angle Deviation & Vertical Error				
Set	Angle Deviation	Residuals	Vert Error	Res
1	0° 0′ 23″	0° 0′ 4″	-0.002	0.000
2	0° 0′ 18″	-0° 0′ 1″	-0.002	0.000
3	0° 0′ 18″	-0° 0′ 1″	-0.002	0.000
4	0° 0′ 20″	0° 0′ 1″	-0.002	0.000
5	0° 0′ 16″	-0° 0′ 3″	-0.002	0.000
6	0° 0′ 17″	-0° 0′ 2″	-0.002	0.000
Mean	0° 0′ 19″	Mean	-0.002	
	Std Dev	0° 0′ 2.5″	Std Dev	0.000

Table E.4(d): Trimble vertical testing – average errors per rotation.

Average -10° Angle Deviation & Vertical Error				
Set	Angle Deviation	Residuals	Vert Error	Res
1	0 ° 0 ′ 47 ″	0 ° 0 ′ 4 ″	-0.003	0.000
2	0 ° 0 ′ 44 ″	0 ° 0 ′ 1 ″	-0.004	-0.001
3	0 ° 0 ′ 42 ″	-0 ° 0 ′ 1 ″	-0.003	0.000
4	0 ° 0 ′ 45 ″	0 ° 0 ′ 2 ″	-0.003	0.000
5	0 ° 0 ′ 40 ″	-0 ° 0 ′ 3 ″	-0.003	0.000
6	0 ° 0 ′ 42 ″	-0 ° 0 ′ 1 ″	-0.003	0.000
Mean	0 ° 0 ′ 43 ″	Mean	-0.003	
	Std Dev	0 ° 0 ′ 2.5 ″	Std Dev	0.000
Average -15° Angle Deviation & Vertical Error				
Set	Angle Deviation	Residuals	Vert Error	Res
1	0 ° 1 ′ 21 ″	0 ° 0 ′ 5 ″	-0.005	0.000
2	0 ° 1 ′ 16 ″	0 ° 0 ′ 0 ″	-0.005	0.000
3	0 ° 1 ′ 15 ″	-0 ° 0 ′ 1 ″	-0.005	0.000
4	0 ° 1 ′ 16 ″	0 ° 0 ′ 0 ″	-0.005	0.000
5	0 ° 1 ′ 13 ″	-0 ° 0 ′ 3 ″	-0.005	0.000
6	0 ° 1 ′ 14 ″	-0 ° 0 ′ 2 ″	-0.005	0.000
Mean	0 ° 1 ′ 16 ″	Mean	-0.005	
	Std Dev	0 ° 0 ′ 2.8 ″	Std Dev	0.000
Average -20° Angle Deviation & Vertical Error				
Set	Angle Deviation	Residuals	Vert Error	Res
1	0 ° 1 ′ 55 ″	0 ° 0 ′ 6 ″	-0.006	0.000
2	0 ° 1 ′ 48 ″	-0 ° 0 ′ 1 ″	-0.007	-0.001
3	0 ° 1 ′ 50 ″	0 ° 0 ′ 1 ″	-0.007	-0.001
4	0 ° 1 ′ 48 ″	-0 ° 0 ′ 1 ″	-0.006	0.000
5	0 ° 1 ′ 45 ″	-0 ° 0 ′ 4 ″	-0.006	0.000
6	0 ° 1 ′ 46 ″	-0 ° 0 ′ 3 ″	-0.006	0.000
Mean	0 ° 1 ′ 49 ″	Mean	-0.006	
	Std Dev	0 ° 0 ′ 3.6 ″	Std Dev	0.001
Average -25° Angle Deviation & Vertical Error				
Set	Angle Deviation	Residuals	Vert Error	Res
1	0 ° 2 ′ 40 ″	0 ° 0 ′ 10 ″	-0.008	0.000
2	0 ° 2 ′ 30 ″	-0 ° 0 ′ 1 ″	-0.008	0.000
3	0 ° 2 ′ 31 ″	0 ° 0 ′ 1 ″	-0.008	0.000
4	0 ° 2 ′ 30 ″	-0 ° 0 ′ 1 ″	-0.008	0.000
5	0 ° 2 ′ 26 ″	-0 ° 0 ′ 5 ″	-0.008	0.000
6	0 ° 2 ′ 26 ″	-0 ° 0 ′ 5 ″	-0.008	0.000
Mean	0 ° 2 ′ 31 ″	Mean	-0.008	
	Std Dev	0 ° 0 ′ 5.1 ″	Std Dev	0.000

Table E.4(e): Trimble vertical testing – average errors per rotation.

Average -30° Angle Deviation & Vertical Error				
Set	Angle Deviation	Residuals	Vert Error	Res
1	0 ° 3 ′ 28 ″	0 ° 0 ′ 12 ″	-0.010	0.000
2	0 ° 3 ′ 19 ″	0 ° 0 ′ 3 ″	-0.010	0.000
3	0 ° 3 ′ 16 ″	-0 ° 0 ′ 1 ″	-0.010	0.000
4	0 ° 3 ′ 13 ″	-0 ° 0 ′ 4 ″	-0.009	0.001
5	0 ° 3 ′ 11 ″	-0 ° 0 ′ 6 ″	-0.009	0.001
6	0 ° 3 ′ 12 ″	-0 ° 0 ′ 5 ″	-0.011	-0.001
Mean	0 ° 3 ′ 17 ″	Mean	-0.010	
	Std Dev	0 ° 0 ′ 6.3 ″	Std Dev	0.001

Average -35° Angle Deviation & Vertical Error				
Set	Angle Deviation	Residuals	Vert Error	Res
1	0 ° 4 ′ 20 ″	0 ° 0 ′ 10 ″	-0.011	0.000
2	0 ° 4 ′ 11 ″	0 ° 0 ′ 1 ″	-0.011	0.000
3	0 ° 4 ′ 11 ″	0 ° 0 ′ 1 ″	-0.012	-0.001
4	0 ° 4 ′ 8 ″	-0 ° 0 ′ 2 ″	-0.011	0.000
5	0 ° 4 ′ 5 ″	-0 ° 0 ′ 5 ″	-0.011	0.000
6	0 ° 4 ′ 4 ″	-0 ° 0 ′ 6 ″	-0.011	0.000
Mean	0 ° 4 ′ 9.8 ″	Mean	-0.011	
	Std Dev	0 ° 0 ′ 5.8 ″	Std Dev	0.000

Average -40° Angle Deviation & Vertical Error				
Set	Angle Deviation	Residuals	Vert Error	Res
1	0 ° 5 ′ 20 ″	0 ° 0 ′ 10 ″	-0.014	-0.001
2	0 ° 5 ′ 11 ″	0 ° 0 ′ 1 ″	-0.013	0.000
3	0 ° 5 ′ 10 ″	-0 ° 0 ′ 0 ″	-0.013	0.000
4	0 ° 5 ′ 11 ″	0 ° 0 ′ 1 ″	-0.013	0.000
5	0 ° 5 ′ 5 ″	-0 ° 0 ′ 5 ″	-0.013	0.000
6	0 ° 5 ′ 5 ″	-0 ° 0 ′ 5 ″	-0.013	0.000
Mean	0 ° 5 ′ 10 ″	Mean	-0.013	
	Std Dev	0 ° 0 ′ 5.5 ″	Std Dev	0.000

Average 0° Angle Deviation & Vertical Error				
Set	Angle Deviation	Residuals	Vert Error	Res
1	0 ° 0 ′ 5 ″	0 ° 0 ′ 4 ″	0.000	0.000
2	0 ° 0 ′ 1 ″	0 ° 0 ′ 0 ″	0.000	0.000
3	0 ° 0 ′ 1 ″	0 ° 0 ′ 0 ″	-0.001	-0.001
4	0 ° 0 ′ 2 ″	0 ° 0 ′ 1 ″	0.000	0.000
5	-0 ° 0 ′ 2 ″	-0 ° 0 ′ 3 ″	0.000	0.000
6	-0 ° 0 ′ 1 ″	-0 ° 0 ′ 2 ″	0.000	0.000
Mean	0 ° 0 ′ 1 ″	Mean	0.000	
	Std Dev	0 ° 0 ′ 2.4 ″	Std Dev	0.000

Table E.4(f): Trimble vertical testing – average errors per rotation.

Average Maximum Angle Deviation & Vertical Error				
Set	Angle Deviation	Residuals	Vert Error	Res
1	0 ° 1 ′ 53 ″	0 ° 0 ′ 20 ″	0.008	-0.001
2	0 ° 1 ′ 43 ″	0 ° 0 ′ 10 ″	0.008	-0.001
3	0 ° 1 ′ 23 ″	-0 ° 0 ′ 10 ″	0.010	0.001
4	0 ° 1 ′ 34 ″	0 ° 0 ′ 1 ″	0.010	0.001
5	0 ° 1 ′ 23 ″	-0 ° 0 ′ 10 ″	0.010	0.001
6	0 ° 1 ′ 22 ″	-0 ° 0 ′ 11 ″	0.010	0.001
Mean	0 ° 1 ′ 33 ″	Mean	0.009	
	Std Dev	0 ° 0 ′ 13 ″	Std Dev	0.001
Average Minimum Angle Deviation & Vertical Error				
Set	Angle Deviation	Residuals	Vert Error	Res
1	0 ° 5 ′ 5 ″	0 ° 0 ′ 6 ″	-0.010	0.001
2	0 ° 5 ′ 5 ″	0 ° 0 ′ 6 ″	-0.012	-0.001
3	0 ° 4 ′ 45 ″	-0 ° 0 ′ 14 ″	-0.011	0.000
4	0 ° 4 ′ 55 ″	-0 ° 0 ′ 4 ″	-0.010	0.001
5	0 ° 5 ′ 1 ″	0 ° 0 ′ 2 ″	-0.011	0.000
6	0 ° 5 ′ 2 ″	0 ° 0 ′ 3 ″	-0.011	0.000
Mean	0 ° 4 ′ 59 ″	Mean	-0.011	
	Std Dev	0 ° 0 ′ 7.7 ″	Std Dev	0.001
Average 0° Angle Deviation & Vertical Error				
Set	Angle Deviation	Residuals	Vert Error	Res
1	0 ° 0 ′ 6 ″	0 ° 0 ′ 5 ″	0.000	0.000
2	0 ° 0 ′ 1 ″	0 ° 0 ′ 0 ″	0.000	0.000
3	-0 ° 0 ′ 1 ″	-0 ° 0 ′ 2 ″	0.000	0.000
4	0 ° 0 ′ 2 ″	0 ° 0 ′ 1 ″	0.000	0.000
5	-0 ° 0 ′ 1 ″	-0 ° 0 ′ 2 ″	0.000	0.000
6	-0 ° 0 ′ 2 ″	-0 ° 0 ′ 3 ″	0.000	0.000
Mean	0 ° 0 ′ 0.8 ″	Mean	0.000	
	Std Dev	0 ° 0 ′ 2.9 ″	Std Dev	0.000

Table E.5: Trimble vertical testing – maximum & minimum average rotation angle.

Average Maximum Tribrach Rotation Angle												
Set	Rotation Angle						Residuals					
1	42	°	40	′	26	″	0	°	38	′	11	″
2	41	°	53	′	13	″	-0	°	9	′	2	″
3	41	°	53	′	13	″	-0	°	9	′	2	″
4	42	°	0	′	13	″	-0	°	2	′	2	″
5	41	°	53	′	13	″	-0	°	9	′	2	″
6	41	°	53	′	13	″	-0	°	9	′	2	″
Mean	42	°	2	′	15	″						
			Std Dev				0	°	18	′	55	″

Average Minimum Tribrach Rotation Angle												
Set	Rotation Angle						Residuals					
1	-41	°	28	′	48	″	0	°	8	′	9	″
2	-41	°	28	′	48	″	0	°	8	′	9	″
3	-41	°	28	′	48	″	0	°	8	′	9	″
4	-41	°	56	′	43	″	-0	°	19	′	47	″
5	-41	°	39	′	16	″	-0	°	2	′	20	″
6	-41	°	39	′	16	″	-0	°	2	′	20	″
Mean	-41	°	36	′	57	″						
			Std Dev				0	°	10	′	58	″

Table E.6: Trimble vertical testing results.

TrimbleS6 DR 300+ using robotic target kit prism							
Vertical Angle						Vertical Height Error	Horizontal Distance Error
90	°	0	′	0	″	0.000	0.000
50	°	30	′	53	″	0.012	0.005
55	°	30	′	30	″	0.011	0.003
60	°	30	′	10	″	0.009	0.001
65	°	30	′	6	″	0.008	0.001
70	°	30	′	15	″	0.006	0.001
75	°	0	′	18	″	0.004	0.001
80	°	0	′	18	″	0.003	0.000
85	°	0	′	12	″	0.001	0.001
90	°	0	′	0	″	0.000	0.000
95	°	30	′	19	″	-0.002	0.000
100	°	30	′	43	″	-0.003	-0.001
105	°	1	′	16	″	-0.005	0.000
110	°	31	′	49	″	-0.006	0.000
115	°	32	′	31	″	-0.008	0.000
120	°	33	′	17	″	-0.010	0.001
125	°	34	′	10	″	-0.011	0.002
130	°	35	′	10	″	-0.013	0.003
90	°	0	′	1	″	0.000	0.000
47	°	59	′	18	″	0.009	0.005
131	°	41	′	55	″	-0.011	0.002
90	°	0	′	1	″	0.000	0.000